SIGNAL PROCESSING BY OCTOPUS CELLS FOR ACOUSTIC AND ELECTRICAL HEARING: A MODELLING STUDY

by

Gertruida Elizabeth Blignaut

Submitted in partial fulfilment of the requirements for the degree
Master of Engineering (Bioengineering)

in the

Department of Electrical, Electronic and Computer Engineering
Faculty of Engineering, Built Environment and Information Technology

UNIVERSITY OF PRETORIA

July 2016

SUMMARY

SIGNAL PROCESSING BY OCTOPUS CELLS FOR ACOUSTIC AND ELECTRICAL HEARING: A MODELLING STUDY

by

Gertruida Elizabeth Blignaut

Supervisor: Prof J.J. Hanekom

Department: Electrical, Electronic and Computer Engineering

University: University of Pretoria

Degree: Master of Engineering (Bioengineering)

Keywords: Octopus cell, cochlear nucleus, cochlear implant, coincidence detector, dendritic delay, travelling wave, travelling wave delay, temporal pitch, rate pitch, pulse rate difference limens.

A computational model of a single octopus cell as well as a population of octopus cells was developed. The models were used to investigate the ability of octopus cells to compensate for the travelling wave delay, remove jitter from the neural activity and encode pitch for normal hearing. Furthermore the response of octopus cells to cochlear implant (CI) stimulation with the ACE strategy was investigated to determine whether pitch can be extracted from CI stimulation in the same way as from acoustic stimulation. Their ability to extract the pulse rate from single-electrode stimulation was also investigated. The response of the octopus cells to single-electrode stimulation at different pulse rates was used to predict pulse rate difference limens, which were compared to psychoacoustic measurements found in literature.

It was found that octopus cells are sensitive to the delay of synaptic inputs on their dendrites but are broadly tuned to this delay. By evaluating the jitter together with the travelling wave delay present in the activity of auditory nerve fibres (ANFs), it was determined that octopus cells may rather act as coincidence detectors, which extract common interspike intervals (ISIs) from many ANFs. The octopus cell model was found to encode the frequency of pure tones in their ISIs for pure tone acoustic stimulation. They were also found to encode the pitch of a vowel in their ISIs, which was the same as the fundamental frequency extracted from the vowel with a speech processing algorithm. The octopus cell model responded to the pulse rate of the CI stimulation and could therefore not extract the frequency of pure tones from CI stimulation in the same way as from acoustic stimulation. The entrainment of the modelled octopus cell population decreased when the pulse rate of a single electrode increased beyond 300 pps. Pulse rate difference limens were predicted from the standard deviation of the ISIs of the octopus cell population response to single electrode stimulation. The predicted difference limens were in the same range as measured values, which suggests that octopus cells may play a role in the measured perceptual limit at 300 pps. From the findings of this study it is suggested that CI stimulation strategies should be developed to encode pitch in the periodicity of their stimulation to enable octopus cells to extract pitch information from CI stimulation.

OPSOMMING

SEINVERWERKING DEUR SEEKATSELLE *(OCTOPUS CELLS)* VIR AKOESTIESE EN ELEKTRIESE GEHOOR: ŉ MODELLERINGSTUDIE

deur

Gertruida Elizabeth Blignaut

Studieleier: Prof J.J. Hanekom

Departement: Elektriese, Elektroniese en Rekenaaringenieurswese

Universiteit: Universiteit van Pretoria

Graad: Magister in Ingenieurswese (Bio-ingenieurswese)

Sleutelwoorde: Seekatsel, kogleêre nukleus, kogleêre inplanting, saamvaldeteksie, dendrietvertraging, loopgolf, loopgolfvertraging, temporale toonhoogte, kleinste waarneembare verskil in pulstempo

ŉ Model van ŉ enkelseekatsel (*octopus cell*) sowel as ŉ populasie van seekatselle is ontwikkel. Die modelle is gebruik om die vermoë van seekatselle te ondersoek om te kompenseer vir die loopgolfvertraging, om bibber te verwyder uit die neurale kode en om toonhoogte te enkodeer vir normale gehoor. Verder is die respons van seekatselle vir kogleêre inplantingstimulasie met die ACE-strategie ondersoek om te bepaal of toonhoogte op dieselfde manier vanuit kogleêre inplantingstimulasie onttrek kan word as vanuit akoestiese stimulasie. Hulle vermoë om pulstempo van enkel-elektrodestimulasie te onttrek is ook ondersoek. Die respons van seekatselle op enkel-elektrodestimulasie is gebruik om die kleinste waarneembare verskil in pulstempo te voorspel, wat vergelyk is met psigoakoestiese metings vanuit die literatuur.

Een bevinding is dat seekatselle sensitief is vir die vertraging van sinapsinsette op hul dendriete, maar hulle is wyd ingestem vir hierdie vertraging. Deur die bibber op die gehoorsenuwee-aktiwiteit saam met die loopgolfvertraging in hul aktiwiteit te evalueer, is bevind dat seekatselle waarskynlik eerder saamvaldeteksie doen, wat gemeenskaplike interpulsintervalle vanaf die gehoorsenuwee onttrek. Daar is bevind dat die seekatselmodel die frekwensie van suiwer tone in hul gemeenskaplike interpulsintervalle enkodeer vir akoestiese stimulasie met suiwer tone. Verder is bevind dat seekatselle die toonhoogte van ’n vokaal in hul gemeenskaplike interpulsintervalle enkodeer, wat dieselfde is as die grondtoon wat vanaf die vokaal onttrek is deur ’n spraakverwerkingsalgoritme. Die seekatselmodel reageer op die pulstempo van kogleêre inplantingstimulasie en kan daarom nie die frekwensie van suiwer tone op dieselfde manier vanuit kogleêre inplantingstimulasie as vanuit akoestiese stimulasie onttrek nie. Die sinchronisasie van die stimulus van die gemodelleerde seekatselpopulasie neem af wanneer die pulstempo van ’n enkel-elektrode toeneem bo 300 pps. Die kleinste waarneembare verskil in pulstempo is voorspel vanuit die standaardafwyking van die gemeenskaplike interpulsintervalle van die seekatselpopulasie se respons op enkel-elektrodestimulasie teen verskillende pulstempo’s. Die voorspelde kleinste waarneembare verskille is in dieselfde bereik as gemete waardes, wat aandui dat seekatselle moontlik ’n rol speel in die gemete persepsielimiet by 300 pps. Op grond van die bevindinge van hierdie studie word voorgestel dat kogleêre inplantingstimulasiestrategieë ontwikkel word wat toonhoogte enkodeer in die periodisiteit van hul stimulasie om dit moontlik te maak vir seekatselle om toonhoogte-inligting vanuit kogleêre inplantingstimulasie te onttrek.

LIST OF ABBREVIATIONS

ACE	Advanced combination encoder
AN	Auditory nerve
ANF	Auditory nerve fibre
AP	Action potential
BM	Basilar membrane
CF	Characteristic frequency
CI	Cochlear implant
CIS	Continuous interleaved sampling
CN	Cochlear nucleus
DC	Direct current
DL	Difference limen
I_h	Hyperpolarisation activated mixed-cation current
ISI	Interspike interval
ISIH	Interspike interval histogram
K^+_{HT}	High-threshold potassium ion
K^+_{LT}	Low-threshold potassium ion
Na^+	Sodium ion
PRDL	Pulse rate difference limen
PSP	Post-synaptic potential
PSTH	Post-stimulus time histogram
VCN	Ventral cochlear nucleus

ACKNOWLEDGEMENTS

The financial assistance of the National Research Foundation (NRF) of South Africa towards this research is hereby acknowledged.

I would like to thank all my friends and family for their continuous love and support.

I would also like to thank the Bioengineering research group for their support and interest in my research. A special thanks to Miss Johanie Roux for her friendship and support.

Most of all I want to thank my Heavenly Father who has been with me every step of the way.

“I can do all things through Christ who strengthens me” – Phil 4:13

TABLE OF CONTENTS

CHAPTER 1 INTRODUCTION

1.1 CONTEXT OF THE PROBLEM

Two of the most prominent theories of pitch perception are the place model and the timing model (Hartmann, 1996). The place model is related to the tonotopic organisation in the cochlea where high frequencies cause maximum basilar membrane (BM) motion near the base and low frequencies at the apex. The maximum BM displacement at these positions cause maximum activation of auditory nerve fibres (ANFs) from the base for high frequencies moving toward the apex for low frequencies. The frequency of a stimulus is then encoded in the positions of maximum ANF activity in the cochlea. The timing, or temporal, model is based on neural synchrony where the frequency of a stimulus is encoded in the period of the ANF activity. It has been shown that the place model holds at higher frequencies while the timing model dominates at low frequencies (Hartmann, 1996; Cedolin and Delgutte, 2005; Larsen *et al.*, 2008; Clark, 1996; Moore, 2003; Zeng, 2002). Experiments with multi-electrode stimulation (Eddington *et al.*, 1978) showed that the pitch associated with the place of the electrode that is stimulated follows the tonotopic arrangement but the pitch perceived on a single electrode also increased when the pulse rate on a single electrode increased between 60 pps and 400 pps. This provides evidence of both place pitch and temporal pitch.

It has been suggested (Rhode, 1995; Cai *et al.*, 2001) that cochlear nucleus (CN) cells, including octopus cells may provide an estimate of periodicity or temporal pitch in the interspike intervals (ISIs) of their response. Onset units in the CN, which include octopus cells (Britt and Starr, 1975; Ostapoff *et al.*, 1994), have been shown to entrain to low frequency stimuli (Rhode *et al.*, 2010; Babalian *et al.*, 2003; Ostapoff *et al.*, 1994). This entrainment of octopus cells to low frequencies may therefore provide an estimate of temporal pitch to the higher levels of auditory processing. For an understanding of the temporal pitch encoding mechanisms of the auditory nerve it is therefore suggested that octopus cells and their role in pitch encoding should be investigated.

Octopus cells are found in the most caudal and dorsal extremes of the ventral cochlear nucleus (VCN) where the ANFs are closely bundled as they cross from the ventral to the dorsal CN (Osen, 1969). They are limited to a single area in the CN called the octopus cell area. The tonotopic arrangement of ANFs is maintained as they enter the CN (Gelfand, 2010;

Mcginley *et al.*, 2012) and octopus cells are usually oriented perpendicularly to the ANFs (Bal and Baydas, 2009; Osen, 1969). ANFs encoding high frequencies arriving in the CN from the cochlear base terminate rostrally while those with low frequency information from the apex terminate caudally in the CN. With this arrangement the ANFs from the base terminate distally on the octopus cell dendrites and ANFs from the apex terminate proximally. It is estimated that octopus cells receive input from ANFs spanning between 1/5 and 2/3 of the tonotopic range (Mcginley *et al.*, 2012) although there is insufficient proof that this is indeed the range from which they receive input. In mice there are about 200 octopus cells receiving input from 12000 ANFs which suggest that each octopus cell receives input from about 60 ANFs if it is assumed that each ANF terminates on only one octopus cell (Oertel *et al.*, 2000).

For an octopus cell to generate an action potential (AP), it must be depolarised at a rate between 5 mV/ms and 15 mV/ms (Ferragamo and Oertel, 2002; Golding *et al.*, 1995). Therefore, they need coincident inputs, of which the post synaptic potentials (PSPs) can be added to allow the cell to be depolarised at the desired rate (Mcginley and Oertel, 2006). For this reason octopus cells are classified as coincidence detectors (Golding *et al.*, 1995) that reduce the jitter of the neural firing (Rhode and Smith, 1986). The convergence of many ANFs on an octopus cell provides a structural basis for the temporal coding of frequency information through the coincident arrival of APs during a specific time window (Clark, 2003; Ferragamo and Oertel, 2002).

In normal hearing there is a delay between the firing of basal and apical ANFs because of the time taken by the travelling wave on the BM to propagate from the base to the apex (Goldstein *et al.*, 1971; Greenberg, 1997; Ruggero and Rich, 1987). The tonotopic arrangement of ANF synapses on the octopus cell dendrites suggests that these cells may compensate for the travelling wave delay with the dendritic delay (Spencer *et al.*, 2012; Mcginley *et al.*, 2012; Oertel, 1997). The PSPs from synapses on the dendrites need a finite time to reach the soma, where they are summed. The PSPs from synapses closer to the soma will reach the soma in less time than those from distal synapses, which creates a dendritic delay in the octopus cell. If this time difference is the same as the time difference between the inputs from the ANFs, the PSPs should be added more efficiently in the soma to reach the threshold. Therefore the dendritic delay of octopus cells may possibly compensate for the travelling wave delay (Mcginley *et al.*, 2012; Spencer *et al.*, 2012; Oertel, 1997). Although it was shown with models that octopus cells may compensate for the travelling wave delay in this manner (Mcginley *et al.*, 2012; Spencer *et al.*, 2012), the approaches that

were followed may provide unreliable results and therefore the same investigation should be undertaken using a different approach where the input delay is adjusted directly to test the effect of this delay.

In cochlear implants (CI) the input signal is filtered into various frequency bands and the electrodes from each band are stimulated with current proportional to the energy in the band (Loizou, 1999a; Loizou, 1999b; Choi and Lee, 2012; Clark, 2003; Kiefer *et al.*, 2001). The number of electrodes, the sequence of activation and pulse rate differ between CI stimulation strategies. Most of the present stimulation strategies use high pulse rates on the electrodes (Choi and Lee, 2012; Kiefer *et al.*, 2001). Because only the spectrum of the signal is used to determine the place of electrode stimulation, the place coding mechanism is mostly used in CIs (Rubinstein, 2004), with some temporal information available in the amplitude modulation of the pulse trains (Vandali *et al.*, 2005; Mckay *et al.*, 1995). The temporal information in the ANF activity and the phase differences between different positions in the cochlea are therefore not accurately conveyed by CI stimulation (Moore, 2003). The lack of temporal information may lead to difficulty in pitch perception by CI users.

While the position of the electrodes that are stimulated provides place information in a CI, the pulse rate may provide temporal information. The pulse rate on a single electrode has been shown to convey pitch up to around 300 pps after which the pulse rate difference limens (PRDLs) increase greatly (Kong and Carlyon, 2010; Tong and Clark, 1985; Townshend *et al.*, 1987; Vandali and Van Hoesel, 2011; Venter and Hanekom, 2014; Zeng, 2002). This suggests that there is an upper limit for temporal pitch perception from the CI pulse rate at 300 pps.

Research gaps

Although it is known that octopus cells are involved in the processing of temporal information, it is not clear how they process this information and how they present it to the next level of the auditory system. Better understanding of the temporal processing by octopus cells is therefore needed. The response of octopus cells to acoustic stimulation was investigated mostly for pure tone inputs. The response of octopus cells to speech has not been investigated before. The way in which they respond to speech may provide insight into the processing of voice pitch.

Literature does not indicate from which range of ANFs octopus cells receive input. Many different ranges of input to octopus cells have been used in previous studies. Therefore a

range should be found that is optimal for octopus cells to function, which may suggest a range from which they may typically receive input.

Although it has been suggested that octopus cells compensate for the travelling wave delay, this mechanism can be investigated further with different methods from what has been reported to gain better understanding of it.

The response of octopus cells to electrical stimulation of the auditory nerve (AN) by a CI has not been determined before. By comparing the responses of octopus cells for acoustic and electrical stimulation, some reasons for perceptual differences between these stimuli may be determined. On the basis of these results, suggestions can be made on temporal encoding by CIs in future stimulation strategies.

The origin of the 300 pps limit in single-electrode PRDLs is unknown. It was therefore investigated whether it may be related to octopus cells and whether these perceptual data can be predicted from the response of octopus cells.

1.2 RESEARCH QUESTIONS AND HYPOTHESIS

The hypothesis that was investigated is that octopus cells respond differently to acoustic and electrical stimulation of the AN for the same input. The second hypothesis is that octopus cells are sensitive to the delay of an input sweep on its dendrites and therefore compensate for the travelling wave delay. Another hypothesis is that octopus cells encode pitch in the ISIs of their response to acoustic stimulation of the auditory nerve. The last hypothesis is that octopus cells are responsible for the 300 Hz perceptual limit in pulse rate discrimination for single-electrode CI stimulation.

The following research questions were investigated:

- Are octopus cells sensitive to the delay of a sweep of synaptic inputs from ANFs terminating on their dendrites? Previous research has proposed that octopus cells compensate for the travelling wave delay by a delay on their dendrites (Mcginley *et al.*, 2012; Spencer *et al.*, 2012). This study investigates this further, using a different method.
- What is the optimal range of input from the cochlea to octopus cells? Research has suggested that octopus cells receive input from a third of the tonotopic range. Assuming that octopus cells reduce jitter (Golding *et al.*, 1995) as well as compensate for the travelling wave delay (Mcginley *et al.*, 2012; Oertel, 1997; Spencer *et al.*, 2012), an optimal range can potentially be found where these functions are performed optimally.

- How do octopus cells respond to acoustic stimulation of the AN? The response to pure tone acoustic stimulation as well as stimulation with complex signals, may give insight into the temporal processing mechanisms of octopus cells (Bal and Oertel, 2000; Clark, 2003; Gelfand, 2010; Greenberg, 1997; Ferragamo and Oertel, 2002; Golding *et al.*, 1995; Levy and Kipke, 1997; Oertel, 1997).
- What is the function of octopus cells in the processing of information from ANFs? Octopus cells are known to be involved in the processing of temporal information (Bal and Oertel, 2000; Clark, 2003; Gelfand, 2010; Greenberg, 1997; Ferragamo and Oertel, 2002; Golding *et al.*, 1995; Levy and Kipke, 1997; Oertel, 1997). It has been suggested that they compensate for the travelling wave delay (Mcginley *et al.*, 2012; Spencer *et al.*, 2012) and function as coincidence detectors (Golding *et al.*, 1995). Therefore it has to be investigated which function they have in the processing of temporal information.
- How do octopus cells respond to electrical stimulation of the AN by a CI? Octopus cells are expected to respond differently to CI stimulation from acoustic stimulation and this may have an influence on the listening performance of CI users.
- What are the differences between the octopus cell response to acoustic and electrical stimulation of the AN? The differences may explain the differences in perception between electrical and acoustic stimulation.
- Can PRDLs be predicted from the octopus cell model? Prediction of perceptual data from a model may be useful in understanding the origin of the perceptual measurements.

1.3 APPROACH

The approach that was followed is illustrated in Figure 1.1. This is a model-based study. The squares show what was used, the circles what was done and the diamonds outcomes or results that were expected.

First a Hodgkin-Huxley type model of a single octopus cell was developed based on an existing model from literature (Spencer *et al.*, 2012). The model was used as a single octopus cell to investigate the sensitivity of the model to changing parameters to obtain an indication of the function of the different parameters and ion channels used in the model. The outputs from existing models of acoustic stimulation of the AN, as well as electrical stimulation, were used as inputs to the octopus cell model. The single octopus cell model was used to investigate the effect of the delay of an input sweep on a single dendrite to test the sensitivity to the travelling wave delay and the hypothesis that octopus cells may compensate for the

travelling wave delay in normal hearing by a dendritic delay. Different input ranges from the cochlea with pure tone acoustic stimulation were also investigated to investigate the effect of the range and the corresponding theoretical travelling wave delay on the output of the single octopus cell. This process is shown in Figure 1.1 and will be described in more detail below.

The approach was as follows with regard to the numbers in the blocks of Figure 1.1:

1. A single octopus cell model was created based on an existing model found in literature. This model was used as a single octopus cell to determine the following:
    1a. Whether the model is valid by verifying the model simulation results with measurements found in literature.
    1b. The effects of changing certain model parameters. This was done to determine the importance of the parameters on the functionality of the octopus cell model.
    1c. How the model responds to synaptic input sweeps with different delays on a single dendrite. This was used to determine a possible optimal sweep delay as well as whether octopus cells may compensate for the travelling wave delay with their dendritic delay.
2. Existing models of the travelling wave for acoustic stimulation and a CI with the Advanced Combination Encoder (ACE) strategy for electrical stimulation, each connected to ANF models, were used to provide input to the octopus cell model. The discharge times from the ANF models were used to create synaptic input events on the octopus cell model.
    2a. The single octopus cell model was then simulated for inputs from the AN for acoustic stimulation. This was repeated for different ranges of BM positions for the ANFs terminating on the octopus cell. This was used to determine whether there is an optimal range of ANF input to an octopus cell which results in the best entrainment to low frequencies. The theoretical travelling wave delay of the ranges was also used to determine if the travelling wave delay of a range of input to an octopus cell has an influence on the response of the octopus cell. This was again used to determine whether there may be an optimal input delay to octopus cells.
3. A population of octopus cells was created by arranging octopus cells to receive input from ANFs arranged linearly from the base to the apex to receive inputs from the whole cochlea. The octopus cell population model again received input from the travelling wave and ANF model for acoustic stimulation.

3a. Different input ranges from the cochlea were tested with acoustic pure tone stimulation on the population to find the optimal range in the cochlea of ANFs terminating on octopus cells. The optimal range was assumed to be the range with minimum jitter and potentially the best compensation for travelling wave delay on the population output.

3b. The population response was simulated for acoustic pure tone stimulation. This was used to

- Determine how octopus cells may encode pitch; and
- Compare the octopus cell population response for CI stimulation with pure tone inputs.

3c. The octopus cell population's response to a complex acoustic signal in the form of a recording of a spoken vowel was also investigated. A vowel was used for the stimulation because the pitch of a vowel is not represented in the frequency spectrum as for pure tones and also because the pitch of a vowel changes over time which allowed the ability of octopus cells to follow changing pitch to be investigated.

- This result was used together with the pure tone acoustic stimulation results to determine the temporal coding mechanisms of especially pitch by octopus cells.

4. The octopus cell population model was simulated for inputs from the CI and ANF model to predict the response of octopus cells to CI stimulation with the ACE strategy.

4a. The response to pure tone inputs with different frequencies was simulated.

- This was compared to the responses of the octopus cells to acoustic stimulation at the same frequencies. The differences between their responses may give information about the ability of octopus cells to extract information from CI stimulation compared to normal hearing.

4b. The octopus cell population response was simulated for CI stimulation on a single electrode at different pulse rates. This was done because of the apparent ability of octopus cells to extract temporal information, which should be present in the pulse rate of a CI.

- The single-electrode pulse rate difference limens were predicted from the data and compared to measured psychoacoustic data.

The octopus cell model was simulated from code written in Matlab[1]. The models of acoustic and electrical stimulation of the AN were also implemented in Matlab.

All the simulations were performed at a sound intensity of 80 dB SPL (Sound Pressure Level).

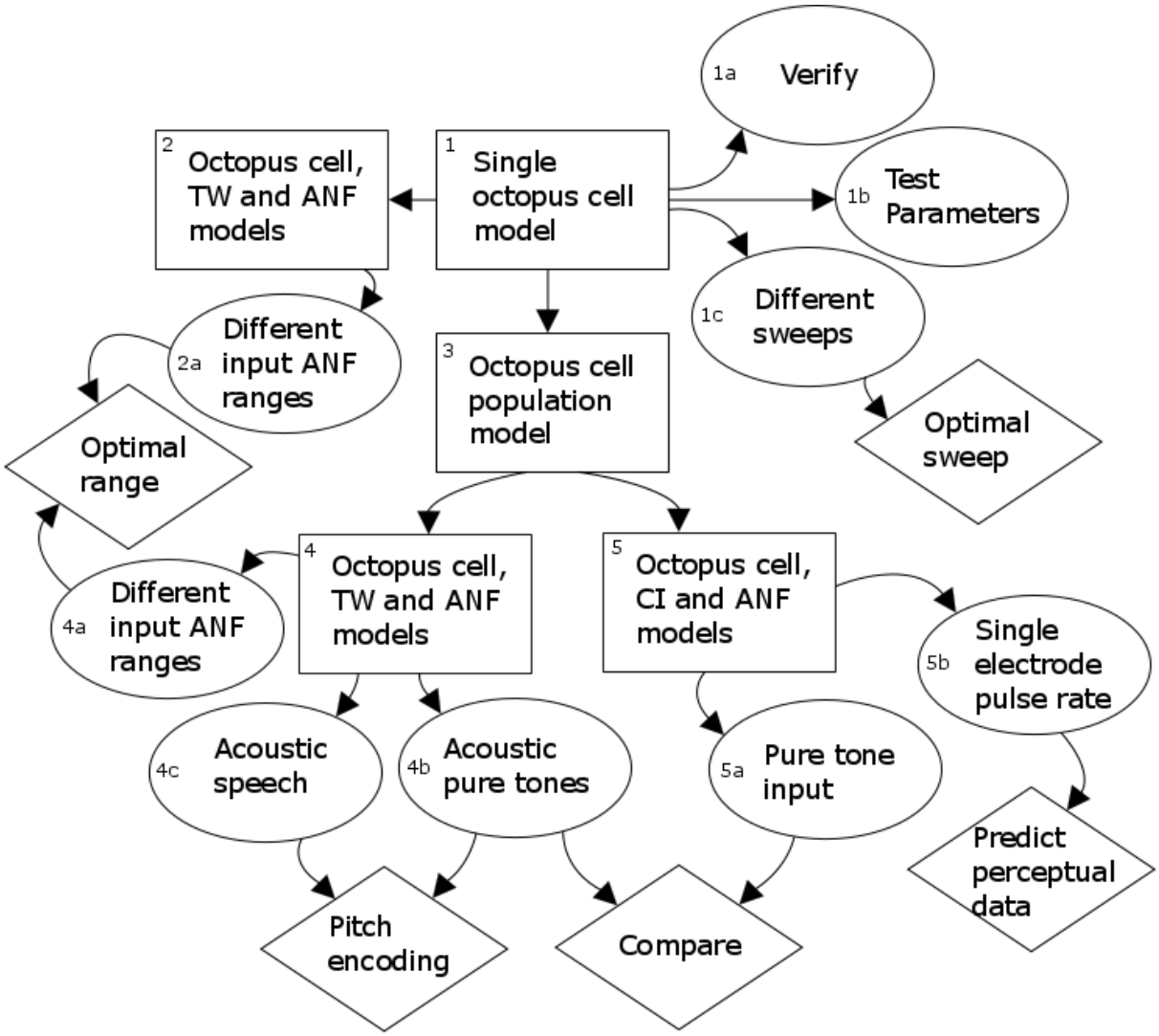

Figure 1.1. Research approach. The square blocks indicate what was used, the circles what was done and the diamonds indicate the outcomes or results. First a single octopus cell model was developed and tested, followed by an octopus cell population model. Both these models used other models as inputs to test the response of the octopus cells to acoustic and electrical CI stimulation of the AN. TW = Travelling wave.

[1] www.mathworks.com

1.4 CONTRIBUTION

The most significant anticipated contribution of the current study is a characterisation of the response of octopus cells to acoustic and electrical stimulation of the AN through model simulations. The differences in the octopus cell model response to acoustic and electrical stimulation of the AN by pure tones was determined to determine the pitch encoding mechanisms of octopus cells and if the same is achieved for acoustic and electrical stimulation. The response of octopus cells to electrical stimulation of the AN by a CI is a significant contribution since it may give insight into the extraction of information from CIs by octopus cells, which has not been determined before. This information can be used in later studies aimed at the development of CI stimulation strategies to encode temporal information that can be extracted by higher order processing of which the octopus cells form a part. In this study only suggestions are made regarding CI stimulation strategies to encode information that may be extracted by octopus cells. The suggestions are based on the simulation results of the study. Pulse rate difference limens for single electrode CI stimulation were also predicted from the octopus cell model output. This may provide more information about the origin of perceptual limitations of temporal pitch in CI users.

Other contributions of the study are the possible optimal delay of an input sweep on octopus cell dendrites and the extent to which the dendritic delay may compensate for the travelling wave delay. A possible optimal range of ANFs providing input from the cochlea to octopus cells was also determined. The population of octopus cells that was developed is another contribution of the study that has not been reported before in literature.

1.5 OVERVIEW OF STUDY

Chapter 2 contains a study on the available literature on octopus cell anatomy and physiology, octopus cell models, pitch, temporal processing in the auditory system and the current state of CIs. This will provide the context of the present study.

Chapter 3 is a detailed description of the development of the single octopus cell model. It also describes the connection between the octopus cell model and models of acoustic and electrical stimulation of the AN. The development of a model of a population of octopus cells is also described.

Chapter 4 gives the results of the verification of the octopus cell model by comparison with measured results and the sensitivity of the model to changing model parameters.

Chapter 5 describes the study on the sensitivity of the octopus cell model to input delays on its dendrites. The investigation of different input ranges to a population of octopus cells to determine a possible optimal range is also discussed in this chapter.

In Chapter 6 the octopus cell population model's response to pure tone acoustic and electrical stimulation, as well as acoustic stimulation with a complex signal, are investigated and discussed. The effect of CI stimulation on temporal coding that can be extracted by octopus cells is discussed. A model is developed to predict PSDLs from the octopus cell population's response.

In Chapter 7 the results from Chapters 4, 5 and 6 are discussed especially in terms of the impact of the results on the development of CI stimulation strategies for temporal coding. Possible shortcomings in the present model are also discussed.

Chapter 8 is the conclusion of the study, summarising the most important findings and the contributions made to the field of study related to this work. Possible future work that may build on the present study is also presented in this chapter.

CHAPTER 2 LITERATURE STUDY

2.1 ACOUSTIC AND ELECTRICAL STIMULATION OF THE AUDITORY NERVE

2.1.1 Acoustic stimulation of the auditory nerve by the travelling wave

In normal hearing, sound waves in the air are collected by the outer ear and directed to the middle ear via the tympanic membrane, which vibrates in response to these sound waves. The vibrations on the tympanic membrane are transmitted via the middle ear ossicles, acting as an impedance matching network, to the oval window, which is a small opening at the base of the cochlea. The vibrations on the oval window, where the incus is attached, are transmitted to the perilymph inside the cochlear duct where the pressure differences in the fluids cause displacements on the BM, which are transduced to electrical signals by the hair cells of the organ of Corti (Clark, 2003; Gelfand, 2010).

There are different views on how energy is transmitted from the stapes to the hair cells and how the BM displacements activates the hair-cells. Some of the theories that have been investigated are the resonance, telephone, place-volley, travelling wave and standing wave theories. Although research on the resonance theory continues (Bell, 2012), there is sufficient proof that a travelling wave exists inside the cochlea, which is responsible for the stimulation of the hair cells and that it carries information (Gelfand, 2010; Clark, 2003). According to the travelling wave theory the vibrations from the oval window are transmitted to the hair cells by the BM as a wave of BM motion propagating from the cochlear base to the apex, known as the travelling wave.

The cochlear travelling wave was first observed by Georg von Békésy (Von Békésy, 1956) in the early 1900s (Olson *et al.*, 2012) in studies on cadaver cochleae with a strobe light under a microscope. He observed a wave travelling on the BM from the base to the apex of the cochlea after stimulation. He determined that the hair cells on the organ of Corti are activated by the movement of the BM caused by the travelling wave.

The frequency with the lowest threshold, called the characteristic frequency (CF), of the BM changes with position in the cochlea. The highest CF is located at the base and it decreases towards the apex, where the lowest CF position is located. As the travelling wave propagates from the base to the apex there are phase changes on the BM, causing the displacement

pattern to reach maxima at the CF positions corresponding to the frequencies in the input signal. The travelling wave caused by a stimulus builds up to the CF position of the stimulus and then quickly dies away. The BM therefore acts as a series of lowpass filters from the base to the apex and only the frequencies lower than the CF are propagated further from each position on the membrane while higher frequencies are quickly attenuated after the CF position. The CF as a function of position along the organ of Corti was determined by Greenwood (1990) and it gives an estimation of where the travelling wave amplitude will reach a maximum for a certain frequency. One of the encoding mechanisms of the travelling wave is therefore hypothesised to be in the maximum place of activation, which is at the CF positions of the frequencies in the input signal. The same observations were made with regard to the changes in the travelling wave for different frequencies and stimulus levels with direct measurements (Olson *et al.*, 2012), hydrodynamic modelling (Ren *et al.*, 2013) and modelling of the fluid mechanics and physics in the cochlea (Reichenbach and Hudspeth, 2014).

Timing characteristics exist in the firing of the ANFs, which cannot be accounted for by the place of maximum activation in the cochlea. One of these characteristics is the finite delay in the activation of the ANFs as the travelling wave propagates from the base to the apex along the BM (Clark, 2003). For wideband stimuli there will be maxima in the travelling wave pattern at various positions along the BM, corresponding to the positions of all the frequency components in the signal. There will be a time delay between the ANF discharge times of the nerves in the base of the cochlea and those in the apex because the travelling wave takes time to travel from the base to the apex. The total delay was measured and calculated to be up to 8-10 ms in humans (Goldstein *et al.*, 1971; Oertel *et al.*, 2000; Ruggero and Rich, 1987). There might be some information in this delay that may be utilised by some cells, especially octopus cells (Mcginley *et al.*, 2012; Spencer *et al.*, 2012; Oertel, 1997) in the CN that may be sensitive to the delay between their inputs. The consonants and glottal pulses in speech are wideband signals and therefore the processing of the travelling wave delay may possibly be used in speech processing at higher levels such as the CN, inferior colliculus, thalamus and cortex (Spencer *et al.*, 2012). Low frequency spectral information can also be encoded in the latency of the travelling wave, which remains constant for changes in sound pressure level (Greenberg, 1997).

ANFs entrain to the frequency of a pure tone acoustic stimulus with the upper limit for neural phase locking at 4-5 kHz (Javel and Mott, 1988). Although the neurons do not all lock on to the stimulus frequency, a population of neurons can provide periodicity information, known

as the volley theory (Wever and Bray, 1930). The frequency of the pure tone is therefore encoded by the periodicity of the travelling wave motion for low frequencies. This encoding mechanism is known as temporal coding and will be discussed in more detail in Section 2.4.

2.1.2 Electrical stimulation of the auditory nerve by cochlear implants

CIs have been developed to restore hearing for profoundly deaf individuals by electrical stimulation of the AN. A CI consists of a speech processor, usually worn behind the ear, a transcutaneous radio frequency link and an electrode array implanted into the cochlea (Clark, 2003; Loizou, 1999a). CIs use multi-electrode stimulation and therefore have many electrodes, up to 22, on the single electrode array (Loizou, 1999b; Wilson and Dorman, 2008; Rubinstein, 2004).

2.1.2.1 Stimulation strategies

The place-pitch mechanism, where each position in the cochlea has a certain CF, is typically exploited in CIs (Clark, 2003; Clark, 1996; Loizou, 1999a; Loizou, 1999b; Rubinstein, 2004). The input signal is therefore filtered into several frequency bands, usually one for each electrode. The energy in each filter band is then used to determine which electrodes to switch on and at which stimulation pulse amplitude. The amplitude of the current pulses is determined by the amount of energy in each frequency band.

There are different stimulation strategies, which differ in their frequency bands used, number of electrodes activated, type of stimulation pulse, pulse rate and sequence of activation of electrodes. Three of the most common strategies currently used are the Continuous Interleaved Strategy (CIS), ACE and HiRes120 (Choi and Lee, 2012; Wilson and Dorman, 2008). These strategies all encode the spectrum of the input signal in the electrical stimulation pattern on the electrodes using high stimulation rates. Some of the older strategies used feature extraction techniques in an attempt to provide specific features, of especially speech, through the CI stimulation. These techniques used different pulse rates and not all were as high as the pulse rates most commonly used in modern CIs.

The ACE, CIS and HiRes120 strategies are most commonly used in present cochlear implants, with ACE being the default in the Cochlear[2] CI, CIS in Med-El[3] implants and HiRes120 in Advanced Bionics[4] CIs (Wilson and Dorman, 2008; Choi and Lee, 2012; Kiefer

[2]www.cochlear.com
[3] www.medel.com
[4] www.advancedbionics.com

et al., 2001). The ACE strategy uses 22 implanted electrode channels and HiRes120 uses 15 channels. Both the ACE and CIS strategy activate the electrodes with the highest energy in their filter bands at a fixed pulse rate of 600-1800 pps. With the CIS strategy the stimulation order of the electrodes can be varied to minimise interaction between the channels. The HiRes120 strategy uses virtual channels by varying current levels on neighbouring electrodes to steer the locus of the stimulation to a position different from that of the electrodes. The FineHearing strategy from Med-El is said to encode the fine structure of sounds, which improves pitch and sound quality to the user.

The SPEAK strategy (Skinner *et al.*, 1994), also known as the Spectral Peak strategy, is similar to the ACE strategy, with the signal being filtered into 16 frequency bands. The six filters with the highest energy are stimulated at a pulse rate between 180 and 300 pps, differing between users. For broad spectra more channels are stimulated at a lower rate and narrow-spectrum signals are stimulated on fewer electrodes at a higher rate.

Some of the feature extraction strategies are F0/F2, which was one of the earliest of these strategies, F0/F1/F2 and the MPEAK (or MULTIPEAK) strategy, which was an improvement on the F0/F1/F2 strategy. In the F0/F2 strategy the frequency of the second formant (F2) is conveyed by stimulating the electrode at the position corresponding to the F2 frequency and the fundamental frequency (F0) is conveyed by the pulse rate of the electrode. In the F0/F1/F2 strategy another electrode is stimulated at the place corresponding to the frequency of the first formant (F1), again at a pulse rate equal to F0 for voiced sections and 100 pps for unvoiced sections. With the MPEAK strategy, two more high-frequency electrodes were added to the F1 and F2 electrodes to stimulate four electrodes. The MPEAK strategy stimulates at a pulse rate equal to F0 for voiced and 250 pps for unvoiced sections.

The feature extraction strategies tend to yield poor performance in noisy conditions because of difficulty with extracting the features from the noise (Loizou, 1999b). The strategies that present the whole spectrum to the user by the use of many frequency bands were found to yield better speech perception results (Manrique *et al.*, 2005) and are therefore used in CIs, rather than the older feature extraction strategies.

2.1.2.2 Emulating mechanisms of normal hearing in cochlear implants

For most CI stimulation strategies the place-pitch mechanism is used to deliver frequency information to the user (Loizou, 1999a; Choi and Lee, 2012; Clark, 2003; Clark, 1996; Kiefer *et al.*, 2001). The stimulation is therefore mostly only according to the frequency spectrum and the signal envelope, while the fine structure of the signal and most of its

temporal information is lost to the CI user for some strategies. It has been shown that the amplitude modulations of the pulse trains may contain some temporal information (Vandali *et al.*, 2005; Mckay *et al.*, 1995). Furthermore, delivering fine structure in CIs may improve speech perception for especially lexical languages such as Mandarin (Xu and Pfingst, 2003), proving that the encoding of temporal fine structure in CIs is important.

In normal hearing, the cochlear travelling wave encodes information in both place codes according to the frequency spectrum by means of maxima on the BM, and temporal codes in the form of periodicity in the BM motion which results in temporal information in the ANF firing patterns. A large amount of this information may be lost to CI users because of the way in which a CI extracts information from a signal and delivers it in the cochlea. It is especially the temporal information that is lost to CI users, which may be a reason for poor pitch perception by these users (Sucher and Mcdermott, 2007; Gfeller *et al.*, 2007). If this information can be delivered to a CI user, it may improve the hearing performance and speech perception of CI users (Clark, 2003). Therefore stimulation strategies that provide more information contained in the travelling wave may potentially improve CI performance.

It has been shown that different filter banks used in CIs may improve F0 coding through place pitch cues (Laneau and Wouters, 2004), although temporal pitch cues improve pitch discrimination. The same study found that pitch discrimination is improved when the filter bank outputs beat at the fundamental frequency and these beats are in phase, which emphasises the importance of temporal coding in CIs.

2.1.2.3 New experimental stimulation strategies

There have been some, but not many, attempts to emulate the travelling wave in CIs. In one attempt to encode speech by including some travelling wave information (Taft *et al.*, 2009; Taft *et al.*, 2010), the travelling wave delay was used to desynchronise the frequency bands before stimulation by the electrodes. The travelling wave delay was calculated as a function of frequency and used in the signal processing and stimulation. The strategy was based on the ACE strategy, in which the incoming signal is filtered into 22 bands from which the eight maxima are selected to be mapped to stimulation of the electrodes. In the new strategy the filter banks were delayed according to the travelling wave delay of their CFs before the selection of the maxima for stimulation. The speech processing strategy was tested with standard test protocols and it was found that stimulation with the delays resulted in better speech perception and also reduced noise thresholds, although pitch ranking did not improve. With another analysis it was also found that speech perception improved most when the

delay that was implemented was about 6.6 ms, which corresponds to the travelling wave delay over the range of the electrode array; however, the results varied widely among subjects.

Other strategies to encode the fundamental frequency as temporal information were developed and tested (Vandali *et al.*, 2005; Vandali and Van Hoesel, 2011; Vandali and Van Hoesel, 2012). These strategies were all based on the ACE strategy but they encoded F0 by using different amplitude modulation schemes on the electrode pulse trains. One strategy, named Multi-channel Envelope Modulation, which provides F0 periodicity information, extracted from the envelope of the broadband signal, across all activated channels, seemed to result in better pitch perception in quiet and noise in different speech perception tests. F0mod, another strategy based on the ACE strategy with pulse train modulations, also improved pitch perception in CI users (Francart *et al.*, 2015). The encoding of the fundamental frequency by modulating the pulse trains was also investigated for the CIS strategy (Green *et al.*, 2004) and it showed some small advantages in pitch perception.

2.2 COCHLEAR NUCLEUS AND OCTOPUS CELLS

2.2.1 Anatomy and physiology

The CN is a part of the brainstem situated between the pons and the medulla in the region where the AN, which comes from the cochlea, penetrates the brainstem (Bal *et al.*, 2009). The CN is the first part of the auditory pathway after the cochlea (Gelfand, 2010). There are various cells in the CN with unique functions. These include spherical bushy, globular bushy, multipolar, octopus, stellate, cartwheel, pyramidal, giant and granule cells (Bal *et al.*, 2009; Gelfand, 2010; Godfrey *et al.*, 1975; Hackney *et al.*, 1990; Oertel, 1997; Oertel, 1999; Rhode *et al.*, 2010). These cells have various response properties, which are classified as primary-like, onset, chopper, pauser and build-up. Because of their responses, which are time dependent, these cells are mostly involved in processing of temporal information from signals (Bal and Oertel, 2000; Clark, 2003; Gelfand, 2010; Greenberg, 1997; Ferragamo and Oertel, 2002; Golding *et al.*, 1995; Levy and Kipke, 1997; Oertel, 1997).

Octopus cells are found in the most caudal and dorsal extreme of the VCN where the ANFs are closely bundled as they cross from the VCN to the dorsal CN (Bal and Baydas, 2009; Golding *et al.*, 1995; Kane, 1977; Schwartz and Kane, 1977). They are found only in this one area of the CN, called the octopus cell area. They have large somas with a few thick dendrites emerging from only one side of the soma and extending across and perpendicular

to the ANFs (Golding *et al.*, 1999; Osen, 1969). Each octopus cell receives inputs from a large number of ANFs and fires with exceptional temporal precision (Mcginley *et al.*, 2012). These cells are involved in extraction of temporal information from the firing of ANFs from the cochlea (Oertel, 2005; Golding *et al.*, 1995; Oertel, 1997; Oertel, 1999).

Octopus cells are classified as onset units (Britt and Starr, 1975; Ostapoff *et al.*, 1994) because of the onset response to sustained electrical stimulation and high-frequency acoustic stimulation (Bal and Baydas, 2009). Onset units exhibit only one spike at the onset of the stimulation with a short first-spike latency and entrain to low-frequency stimuli (Rhode and Smith, 1986) up to around 400 Hz – 1 kHz, with variation between individual cells.

Octopus cells have fast responses to synaptic inputs or transmembrane current stimulation. They have been shown to have voltage-dependent K^+ channels, which are responsible for short PSPs in these cells (Golding *et al.*, 1995; Bal and Oertel, 2001). Their response is further regulated by the presence of hyperpolarisation activated mixed cation current (I_h), which is responsible for a large portion of the resting potential as well as the low input resistance of the cell (Bal and Oertel, 2000).

Measurements of the anatomy of octopus cells from literature are given in Table 2.1 and physiological measurements are summarised in Table 2.2.

Table 2.1. Anatomical measurements of octopus cells from literature

Animal	Cell body diameter (µm)	#Dendrites	Dendrite diameter (µm)	Dendrite length (µm)	Resting potential (mV)	Input resistance (MΩ)	#ANFs terminating on cell	Reference
15-and-16-day-old cats	3-5	Up to 9	-	-	-59.4 ± 0.4	15.8 ± 1.5	>60	(Bal and Baydas, 2009)
7-day-old cats	-	-	-	-	-59.2 ± 0.9	24.1 ± 5.7	>60	(Bal and Baydas, 2009)
17-26-day-old mice	-	-	-	-	-	10	>50	(Golding *et al.*, 1995)
17-26-day-old mice	-	-	2-4	-	-60.6 ± 5.8	3.2 ± 1.5	-	(Ferragamo and Oertel, 2002)
2-week-old-dogs	-	-	-	-	-60.5 ± 0.7	17.58 ± 1.3	-	(Bal *et al.*, 2009)
Guinea pigs	25	-	-	200-300	-	-	-	(Hackney *et al.*, 1990)
Mice	25	-	-	-	-63 ± 3	17.58 ± 1.3	-	(Golding *et al.*, 1999)

Table 2.2. Physiological measurements of octopus cells from literature

Animal	Time constant for hyperpolarizing responses (ms)	Amplitude of AP (mV)	Duration of AP (ms)	Latency (Current pulse to peak of AP) (ms)	Reference
15-and-16 day-old cats	1.28 ± 0.3	43.1 ± 3	0.32 ± 0.03	0.62 ± 0.03 (4 nA)	(Bal and Baydas, 2009)
7-day-old cats	3.6 ± 1.5	56.3 ± 6.6	0.5 ± 0.07	0.74 ± 0.05 (4 nA)	(Bal and Baydas, 2009)
17-26-day-old mice	-	5-10	-	1.14 ± 0.04 (weak) 1.02 ± 0.02 (strong)	(Golding *et al.*, 1995)
2-week-old dogs	1.34 ± 0.13	51.6 ± 2.16	0.36 ± 0.02	0.54 ± 0.04	(Bal *et al.*, 2009)
Mice	0.21 ± 0.06	15.15 ± 6.9	-	-	(Golding *et al.*, 1999)

2.2.2 Possible functions of octopus cells

Compensation for travelling wave delay

The tonotopic arrangement of ANFs is retained as they enter the CN (Gelfand, 2010; Mcginley *et al.*, 2012). Nerves encoding high frequencies, coming from the base of the cochlea, terminate rostrally in the octopus cell area, while those encoding low frequencies, coming from the apex, terminate caudally. The octopus cells are arranged in such a manner that the synapses from high-frequency ANFs are furthest away from the soma and the low-frequency ANF synapses closest to the soma (Oertel *et al.*, 2000). In cats each octopus cell has synapses from about 60 ANFs arranged in this fashion (Bal and Baydas, 2009; Golding *et al.*, 1995). Because of the dendritic delays, potentials from synapses further from the soma take a longer time to reach the soma than those closer to the soma. Octopus cells require the summation of multiple synaptic inputs to reach threshold (Oertel *et al.*, 2000). For the cell to generate an AP, it must be depolarised at a rate of around 10 mV/ms (Ferragamo and Oertel, 2002; Golding *et al.*, 1995) and this depolarisation only occurs when the inputs from the synapses are in such an order that they all reach the soma at approximately the same time to be summed efficiently. The inputs from the distal synapses must therefore occur before those from the proximal synapses. Because of the tonotopic arrangement of the nerves in the CN and the delay between the ANF firings caused by the travelling wave delay, this may be possible in octopus cells. The arrangement of the ANF synapses on the octopus cell dendrites therefore suggest the possibility that these cells compensate for the travelling wave delay in the ANF firing (Mcginley *et al.*, 2012; Spencer *et al.*, 2012; Oertel, 1997). Acoustic stimulation with chirps with the same delay as the travelling wave delay lead to stronger auditory brainstem responses than clicks at the same loudness level (Elberling *et al.*, 2007). This also suggests a sensitivity of the auditory brainstem to the travelling wave delay.

Broadband transient sounds should activate an octopus cell with a sweep of excitation from the distal tips of its dendrites towards the soma. A modelling study to test this hypothesis (Mcginley *et al.*, 2012) found that the PSPs in octopus cells was largest when the sweep duration corresponded to the travelling wave delay of the inputs to the cell, which spans about a third of the tonotopic range. For inputs that are randomised and therefore do not have a sweep from the distal tips to the soma, the PSPs was much smaller and APs could not be generated by the octopus cells.

Coincidence detection

Octopus cells have been found to be coincidence detectors (Golding *et al.*, 1995), which need coincident inputs from many ANFs to reach threshold and generate an AP. This sensitivity is achieved by the rate of depolarisation threshold (Ferragamo and Oertel, 2002; Golding *et al.*, 1995) present in octopus cells. The PSPs from many ANFs therefore have to arrive in a time short enough for sufficient summation of the potentials in the soma to reach threshold. This mechanism causes octopus cells to be coincidence detectors. By the summation of many inputs over time a single, precise AP is produced by an octopus cell. There is jitter present on the firing of ANFs and producing a single AP from many random inputs over time leads to a reduction in jitter of the neural firing pattern in the auditory system (Rhode and Smith, 1986), which may enhance the temporal representation of information for the next level of the auditory pathway.

Speech perception

The synchrony in the firing of groups of ANFs is a pattern that is important for the understanding of speech, since broadband transients and gaps are critical features of consonants (Oertel *et al.*, 2000). The phase locking of octopus cells to low frequencies could play a role in pitch encoding in the auditory system, while the onset response may be used in sound localisation (Rhode and Smith, 1986). Octopus cells can encode the temporal features of acoustic stimulation with greater precision than ANF inputs and those of other neurons in the CN. The time over which temporal summation of excitation from ANFs can occur is limited and thus provides temporal precision (Golding *et al.*, 1995). Of all the cells in the CN, octopus cells synchronise strongest to the fundamental frequency of speech-like sounds. Because of all these characteristics of the octopus cells, they may play an important role in speech recognition (Ferragamo and Oertel, 2002). In humans the information from the octopus cells may be used in higher levels such as the inferior colliculus, thalamus and cortex to increase the reliability of the classification of sounds in speech (Spencer *et al.*, 2012).

2.2.3 Application to cochlear implants

CIs encode frequency information by exploiting the place-pitch mechanism and therefore they mostly use place codes in their encoding of information, as discussed in Section 2.1.2. The time domain information and the rich encoding by the cochlear travelling wave may therefore be lost to CI users. This may be a cause of the difficulties in pitch and speech

perception that CI users experience (Gfeller *et al.*, 2007). Since the cells in the CN, especially octopus cells, respond to temporal information in the ANF firing patterns, the encoding mechanisms used in CIs may influence the response of octopus cells for CI users.

2.3 MODELLING OCTOPUS CELLS

Octopus cells have been modelled with compartmental Hodgkin-Huxley type (Hodgkin and Huxley, 1952) models (Cai *et al.*, 2000; Mcginley *et al.*, 2012; Cai *et al.*, 1997a; Levy and Kipke, 1997; Spencer *et al.*, 2012) as well as an integrate-and-fire point model (Kalluri and Delgutte, 2003). The models were developed to represent the anatomy of octopus cells and also to behave similarly to experimental measurements to be used to investigate the characteristics and responses of these cells. The number of dendrites, their diameters and the number and arrangement of the synapses varied between the models.

2.3.1 Octopus cell models and the modelling results

The models that were found in literature will be discussed below.

Cai et al. (1997) and Cai et al. (2000)

The model was developed to determine the mechanisms responsible for the onset response of octopus cells. It was a compartmental Hodgkin-Huxley model based on available measured anatomical and physiological data. The model had passive dendrites but the soma contained active channels of which the contribution of the low-threshold potassium (K^+_{LT}) and hyperpolarization activated mixed-cation (I_h) channels to the onset response was evaluated.

In the 1997 model only the responses to electrical current stimulation were investigated by injecting a transmembrane direct current (DC) or half-wave rectified sine wave stimulation current. The model was solved numerically by using the Crank-Nicolson method at a time resolution of 10 µs.

In the 2000 model synapses were added to the model as a battery-conductance branch, which is the same as an ion channel in the model. The conductance of the channel was modelled with an alpha-function

$$g(t) = G\left(\frac{\frac{t-t_0}{t_p}}{e^{\frac{t-t_0}{t_p}}}\right), \tag{2.1}$$

with t_0 the time of stimulation. The function reaches a maximum at $t = t_0 + t_p$, therefore t_p is the peak time. The value of t_p was set to 0.12 ms to generate brief synaptic events. G is the synaptic conductance, which can vary over a wide range and was chosen as 3.68 nS because octopus cells usually receive many small synaptic inputs. Spike trains measured on six ANFs were used as the model inputs to investigate the model response to 1 kHz tone bursts. The inputs of the six ANFs were repeated to give a total of 120 inputs to the model in no specific arrangement according to the position of the ANFs in the cochlea.

It was found that the low input impedance of the octopus cell, partly caused by the presence of I_h, played a major role in the onset response. The K^+_{LT} conductance was also found to play a major role, while Na^+ played a lesser role in the response. The sensitivity to the rate of depolarisation was found to be caused by the presence of K^+_{LT} channels.

One problem with the model is that it contains passive dendrites, while there is sufficient proof that octopus cells have active dendrites with K^+_{LT} and I_h channels (Bal and Oertel, 2000; Bal and Oertel, 2001; Golding *et al.*, 1995). Another problem is that the model received input from only six ANFs with no tonotopic arrangement on the dendrites, while the functionality of octopus cells is believed to be caused by the input from many ANFs, which are tonotopically arranged on the dendrites (Mcginley *et al.*, 2012).

Levy and Kipke (1997)

The model was created with the aim of developing a biologically plausible model of the octopus cell that can be used as a tool for investigating underlying octopus cell mechanisms and describing octopus cell processing. It was a compartmental Hodgkin-Huxley model. The four dendrites were represented by a single equivalent cylinder and the active axon was lumped into the soma resulting in 15 dendrite compartments and two soma compartments.

The input to the model was from a separate model of the auditory periphery, which simulated the ANF spike trains for certain stimuli. The responses to stimulation current on the soma as well as short tone bursts with input from the auditory periphery model were evaluated. Synapses were implemented as a variable conductance in the membrane. With an input at time $t = 0$ the synaptic conductance change occurred as described by the alpha-function

$$g_{syn}(t) = A_c \overline{g_{syn}}^{\,t/t_p} e^{-t/t_p} \quad , \tag{2.2}$$

where $\overline{g_{syn}}$ is the maximum synaptic conductance and t_p is the time to the peak of the function. A_c is the membrane surface area of the compartment in cm^2. This was implemented as the second-order differential equation

$$g''_{syn}(t) + \frac{2g'_{syn}}{t_p} + \frac{g_{syn}}{t_p^2} = \frac{e}{t_p}s(t) \quad , \tag{2.3}$$

where $s(t)$ is the input spiketrain given by

$$s(t) = \delta(t - t_n) \quad , \tag{2.4}$$

with $t_n, n = 1, \ldots N$ representing the spike times of N spikes.

The model did not have any K^+_{LT} or I_h channels, which have been found to play a crucial role in the response characteristics of octopus cells. Therefore it is not a biologically accurate model, although it did produce the desired responses. Lumping the dendrites into a single dendrite with 15 compartments also reduced the number of possible synapses on the dendrites, which may reduce the ability of the model to predict responses to many synaptic inputs.

McGinley et al. (2012)

The model was developed to test the hypothesis that the arrangement of ANF inputs on the dendrites of octopus cells compensates for the travelling wave delay.

A passive and an active model were developed. The parameters of the passive model were optimised to match in vivo recordings. The active model contained K^+_{LT} and I_h active ion channels. The implementation of the geometry of the octopus cell was not described clearly.

The synapses were modelled as a conductance changing as the sum of two exponentials. The activation times of the synapses were increased linearly with distance from the soma to model the dendritic delay. Each synaptic conductance was implemented as

$$g_{syn}(t) = g_{max}\frac{1}{\eta}\left(-e^{-t/\tau_r} + e^{-t/\tau_d}\right) \quad , \tag{2.5}$$

where g_{max} is the maximum conductance, η is a normalisation factor, τ_r is the rise time and τ_d is the decay time. The normalisation factor was

$$\eta = -e^{t_p/\tau_r} + e^{t_p/\tau_d} \quad , \tag{2.6}$$

where

$$t_p = \log\left(\frac{\tau_d}{\tau_r}\right) \cdot \frac{(\tau_d \cdot \tau_r)}{(\tau_d - \tau_r)} \tag{2.7}$$

is the time corresponding to the peak synaptic conductance.

It was found that input soma-directed sweeps with the appropriate delay generate the largest and sharpest PSPs in the soma. The fastest rate of rise in the active dendritic models was achieved for sweep durations smaller than 1 ms. Randomised activation of synapses resulted in the smallest rate of rise in the resultant PSP. The optimal sweep duration for the maximum PSP peak was measured as 0.4 ms, which is close to a third of the cochlear travelling wave delay in mice.

The geometry of the model is not clear from the description and therefore it will be difficult to reproduce the model. The differences between the active and passive models were also not described clearly; neither the implementation of the synapses.

Spencer et al. (2012)

The model was developed to test whether the dendritic delay of octopus cells compensate for the travelling wave delay to improve coincidence detection. It was a compartmental Hodgkin-Huxley model. The model contained K^+_{LT} and I_h channels in its dendrites and soma and was therefore the only existing model with active dendrites.

The input to the model was from a published model of the auditory periphery (Zilany *et al.*, 2009). With this model the travelling wave delay was recreated by superimposing its output with the travelling wave delay equation

$$t_{delay} = \left(\frac{1000}{f_{cf}}\right) + t_{offset} \quad , \tag{2.8}$$

where f_{cf} is the CF of the ANF to where the delay is measured (Greenberg, 1997).

Synapses were implemented as a conductance with the double exponential function

$$G_{syn}(t) = W\left(e^{-t/\tau_{decay}} - e^{-t/\tau_{rise}}\right) \quad , \tag{2.9}$$

where W is a constant used to adjust the strength of the synapses such that they had the same influence on the soma. The rise and decay time constants were used as $\tau_{rise} = 70\ \mu s$ and $\tau_{decay} = 340\ \mu s$.

The model generated the same output for a transmembrane electrical stimulus as measured data. The results showed that octopus cells were more likely to receive input from high frequency ANFs. It was also concluded that the dendritic delay compensated for the travelling wave delay by producing a better response when the travelling wave delay of the input was the same as the dendritic delay of the octopus cell.

The model had active dendrites, which are the same as physiological measurements. It also received input from many ANFs, which were arranged tonotopically on the dendrites. The implementation of the model is clearly described, which makes this model the best to be reproduced.

Summary of Hodgkin-Huxley type models

The geometry, constants, active channels and number of inputs for all the models discussed are summarised in Table 2.3.

All the models of this type were implemented as compartmental models. Some of the models do not contain the active ion channels that have been measured and may therefore not be an accurate representation of reality. Although the model from McGinley et al (2012) produced responses that are similar to measurements, the implementation of the model is not described clearly and the model cannot be reproduced easily. The model that was described most clearly and that would be the easiest to reproduce is the model from Spencer *et al.* (2012).

Kalluri and Delgutte (2003)

A model of neurons with an onset-response was developed to investigate the mechanisms underlying this response. Octopus cells are known to be onset-units, therefore this model may be used to model octopus cells. It was implemented as an integrate-to-threshold point model with a large number of weak synaptic inputs.

Discharge patterns on the ANFs were generated with a computational model (Carney, 1993). The onset-neuron (octopus cell) model was implemented with a leaky-integrator model to describe the synaptic integration and spike generation. The model operation was determined by an intracellular voltage and a threshold. The flow of synaptic current through the neural

membrane was represented by a resistor-capacitor (RC) circuit. The change in synaptic conductance was modelled with an alpha-function

$$g_s(t) = G_s \frac{1}{\tau_s} e^{\left(-\frac{1}{\tau_s}+1\right)} \quad , \tag{2.10}$$

with G_s the maximum synaptic conductance and τ_s the synaptic time constant, which was set to 100 μs for all synapses. The model received input from between 1 and 2000 ANFs from a 1 octave CF range.

The model behaved like a coincidence detector which needed many inputs with a low membrane time constant to reach threshold. The model was however most appropriate for onset-chopper (On-C) units, which discharge at a certain rate following the onset response. Octopus cells are not On-C units and are classified as Onset-I units, therefore the model cannot be used for sufficient modelling of octopus cells without modification.

From the models described above the model from Spencer *et al*. (2012) seems to be the best one to be reproduced to study octopus cells with a model.

2.4 PITCH PERCEPTION WITH ACOUSTIC AND ELECTRICAL HEARING

2.4.1 Definition of pitch and models of pitch perception

Pitch is the ordering of sound from low to high on the scale that is used for melody in music. Pitch depends mostly on the frequency content of a stimulus but also on the sound pressure and waveform (Hartmann, 1996).

There are several models of pitch perception. They fit into three categories: place models, timing models and template models. It has been shown that place models hold at higher frequencies while timing models dominate at low frequencies (Hartmann, 1996; Cedolin and Delgutte, 2005; Larsen *et al.*, 2008; Clark, 1996; Moore, 2003; Zeng, 2002; Javel and Mott, 1988).

The place theory is based on the tonotopic organisation of the neurons in the cochlea. This tonotopic organisation is said to be retained in the higher levels of auditory processing up to the auditory cortex (Clark, 2003). The cochlear travelling wave causes maximum displacement of the BM at the place corresponding to the frequency in a signal, which causes a maximum in the neural activity for the neurons at that place. One phenomenon that can be explained by the place model is diplacusis, which is when a person hears the same sound

differently in the two ears. This is thought to be because of irregularities between individual cochleae. The shift of pitch as the intensity of a tone is changed can also be explained by the place of the maximum peak of the BM displacement because of the travelling wave, which shifts basally as intensity increases, which will lead to a higher perceived pitch (Hartmann, 1996).

The timing theory, also known as the temporal theory, assumes that pitch is determined by neural synchrony, periodicity and other temporal patterns. The synchrony of ANF firing at lower frequencies, especially up to 2000 Hz, supports the timing model and suggests that pitch may be related to the synchrony of ANFs to complex tones (Javel and Mott, 1988). Broadband sounds that have no clear spectral maxima have perceived pitch for listeners. This supports the idea that pitch is not only a place code, but also a temporal code, which is in the timing of the neural firing (Hartmann, 1996). Pitch of complex tones and the perception of the missing fundamental can also be explained by the extraction of the periodicity of the stimulus (Horst *et al.*, 1986). Amplitude modulated noise can elicit pitch, which indicates that temporal regularities in certain waveforms can convey pitch (Burns and Viemeister, 1976).

According to the template model there will be a template to which each input signal is matched (Hartmann, 1996). The fundamental frequency of the template with the best fit corresponds to the perceived pitch of the tone. Evidence for this theory is the pitch that can be perceived by playing the different frequency components into the two ears, called dichotic hearing. Even though dichotic hearing is seen as evidence for place coding, the temporal processing from the CN may be used higher in the auditory processing for perception of this pitch (Rhode, 1995).

Temporal coding of pitch has been suggested to be present in the ISIs of the firing of certain CN units (Rhode, 1995). Onset-I units, which include octopus cells, may provide a robust estimate of pitch to the higher levels of auditory processing in its ISIs.

Table 2.3. Summary of octopus cell parameters used in previous Hodgkin-Huxley computational models.

		Cai et al (1997, 2000)	Levy and Kipke (1997)	McGinley *et al.* (2012)	Spencer *et al.* (2012)
Geometry	**Number of dendrites**	4	4	-	4
	Dendrite diameter (µm)	5	7	-	3
	Dendrite length (µm)	200	150	-	280
	Number of dendrite compartments	20	15	-	20
	Soma diameter (µm)	32	25	-	25
	Soma length (µm)		25	-	25
	Axon diameter (µm)	3	3	-	3
	Axon length (µm)	70	300	-	2
	Axon hillock diameter (µm)	-	5	-	3
	Axon hillock length (µm)	-	15	-	30
Constants	**Membrane capacitance, Cm (µF/cm^2)**	1	1	2.1 ± 0.9	0.9
	Internal resistance, Ri (Ω·cm)	100	150	195 ± 88	100
	Resting potential (mV)	-62	-	-73	-62
Active channels	**Dendrites**	None	-	K^+_{LT} I_h	K^+_{LT} I_h
	Soma	Na^+ K^+ K^+_{LT} I_h	-	K^+_{LT} I_h	K^+_{LT} K^+_{HT} I_h
	Axon	Na^+ K^+	-	-	Na^+
Input	**Number of ANFs terminating on cell**	20 x 6	60	-	60

2.4.2 Pitch in cochlear implants

In CIs the input signal is filtered into frequency bands and the electrodes are activated according to the energy in each electrode's filter band (Clark, 2003; Loizou, 1999a; Loizou, 1999b). Therefore mostly the place coding mechanism from normal hearing is implemented in CIs, while most temporal information is lost to the CI user.

The effective number of independent channels with a CI is around eight (Friesen *et al.*, 2001), while in normal hearing there are many more channels which can provide a place code with a higher resolution. The place resolution of CIs is therefore much lower than in normal hearing which may be one factor decreasing the performance of CI listeners (Strydom and Hanekom, 2011).

CIs do not convey most of the temporal information in the firing of the ANFs or the phase differences between different positions in the cochlea as in normal hearing (Moore, 2003). Many CIs also do not attempt to convey fine time structure. The normal hearing mechanisms can therefore possibly not operate optimally with CI stimulation.

The rate of stimulation on a single electrode in a CI has been shown to convey pitch up to a pulse rate of 300 pps, after which the rate discrimination limens increase greatly. This shows that the upper boundary of temporal pitch discrimination in CIs may be around 300 Hz (Kong and Carlyon, 2010; Tong and Clark, 1985; Venter and Hanekom, 2014; Zeng, 2002).

The upper limit of temporal pitch in CIs has been hypothesised to arise at a level of processing central to the AN but common to binaural and pitch processes (Carlyon and Deeks, 2010). It was speculated that this is the inferior colliculus, but it does not exclude the possibility that the CN plays a role in the upper limit of pitch discrimination. It was suggested by Carlyon and Deeks (2010) that the electrical stimulation patterns have to be adjusted to enable higher levels of processing to process temporal information from the ANFs.

The responses of cells in the ventral CN was measured for single-electrode stimulation with an analogue current (Clopton and Glass, 1984). The measurements showed that the units in the CN responded with a small latency to the peaks in the electrode current. The units therefore responded to the periodicities of the stimulation signals. For complex signals the units responded to the envelope of the signal. It was suggested by Clopton and Glass (1984) that stimulating with fixed pulse rates on multiple electrodes will not evoke the pitch percepts related to the periodicity of input waveforms, therefore variable interpulse intervals should be used to provide temporal information in CIs.

Because of the use of temporal pitch at low frequencies the temporal information that is available in normal hearing should be encoded in CIs in addition to the place pitch. Encoding temporal information in CIs may improve pitch perception for CI users, which may improve speaker identification and speech recognition.

2.5 RESEARCH GAPS

Studies on pitch perception should focus more on the temporal properties of activity in the AN and the VCN (Macherey *et al.*, 2011). The development of cochlear implant stimulation strategies that can better utilise coincidence detection and provide stimuli to reproduce the phase delays of the BM travelling wave is likely to lead to better temporal coding of pitch with CIs (Clark, 2003). Emulating the travelling wave with temporal encoding of pitch may lead to better pitch perception and speech perception in noise for CI users (Gfeller *et al.*, 2007).

The extraction of temporal pitch by octopus cells should be investigated for a better understanding of this mechanism. The response of octopus cells to electrical stimulation of the AN should be investigated to determine how octopus cells extract information from CIs and possible reasons for perceptual limitations of CI users and improvements to CI stimulation strategies. It is also necessary to determine the level of sensitivity of octopus cells to the delay of inputs on their dendrites to determine if and how much octopus cells may compensate for the travelling wave delay, since this may influence the methods that should be used to encode information to be extracted by octopus cells.

CHAPTER 3 DEVELOPMENT OF THE OCTOPUS CELL MODEL

3.1 INTRODUCTION

This chapter provides a detailed description of the development of the octopus cell model that was used in the rest of the study. The combination of many single octopus cells to create a population of octopus cells will also be discussed. Providing synaptic inputs to the octopus cell model from ANF models which receive input from a travelling wave and CI model respectively, is also described in this chapter.

3.2 METHOD

The octopus cell model had to be developed to study the response of octopus cells to acoustic and electrical stimulation of the AN in the cochlea. For results that are an accurate prediction of the octopus cell response the anatomy and physiology from measurements on octopus cells had to be represented in the model to be as close to reality as possible. For this reason it was decided to implement a Hodgkin-Huxley model instead of an integrate-and-fire model to include the known ion channels present in octopus cells as accurately as possible. The model was also implemented as a multi-compartmental model to represent the geometry from anatomical measurements of the octopus cell in the model.

3.2.1 Single octopus cell model

Of the models discussed in Section 2.3, the model of Spencer *et al.* (2012) was the closest representation of the anatomy and physiology of octopus cells given in Section 2.2.1. The model used in this study was therefore based on the model given in that article. Some minor changes were made to the model, which will be discussed.

The model geometry consists of four dendrites each with 20 compartments, a single soma compartment and an axon with ten compartments. The first axon compartment represents the axon hillock and was implemented as a passive compartment. The second axon compartment from the soma was the axon initial segment, which is where there is a large concentration of Na^+ channels and APs are generated. The geometry is illustrated in Figure 3.1, with more detail given in Table 3.1. The active channels used for each part of the model were implemented as given in Spencer *et al.* (2012) and are also given in Table 3.1.

Measurements on octopus cells have shown that they have active low threshold potassium ion channels (K^+_{LT}), high-threshold potassium ion (K^+_{HT}) channels and hyperpolarisation activated mixed cation channels (I_h) in their dendrites (Golding *et al.*, 1999; Bal and Oertel, 2000; Bal and Oertel, 2001). In cortical layer 5 pyramidal neurons (Kole *et al.*, 2008), other cortical neurons (Kole and Stuart, 2012), neurons in the avian auditory pathway (Kuba, 2012) and other neurons (Clark *et al.*, 2009), APs were found to be generated at the axon initial segment, where there is a high concentration of sodium ion (Na^+) channels. This same principle was applied to the octopus cell model by adding an axon initial segment with a high concentration of Na^+ channels. Active ion channels were therefore implemented in the model at the same locations as found in literature.

The axial resistivity (R_i) of the model was used as 300 Ω·cm and the membrane capacitance (C_m) was 0.9 µF/cm^2. The axial resistivity value of 300 Ω·cm that was used is higher than the value used by Spencer *et al.* (2012), which was 100 Ω·cm. This was done for stability when solving the model since a smaller value led to instability in the solving algorithm. The value has been used as 100 Ω·cm in many simulations but different values have also been reported (Levy and Kipke, 1997). The axial resistance of myelinated human sensory nerve fibres was calculated as 33 Ω·cm for a propagation velocity which is the same as measured data (Wesselink *et al.*, 1999). The value used in the study is ten times this measured value, which may have an influence on the results and should be considered when evaluating results. However, as will be shown later, the influence was not as large as to lead to an invalid model.

The passive axon was added to the model to increase the resistance between the soma and the last axon compartment at rest. This was done to ensure that there is a large enough membrane voltage at the axon initial segment to reach threshold and generate an AP. Without the long axon, the membrane voltage in the axon initial segment remained too close to rest because of the compartment at rest adjacent to it. The active channels in the axons of octopus cells have not been measured experimentally and were therefore not included in the model. It has been shown that the length of the axon that is preserved in a slice of the CN has no effect on the generated APs when the octopus cell is stimulated from the AN (Golding *et al.*, 1999). Therefore the axon length can be adjusted without compromising the validity of the model. It is important to note that this was only implemented to solve the model and is not a representation of the physiology of an octopus cell axon. The only functional part of the axon is the axon initial segment, which represents physiology.

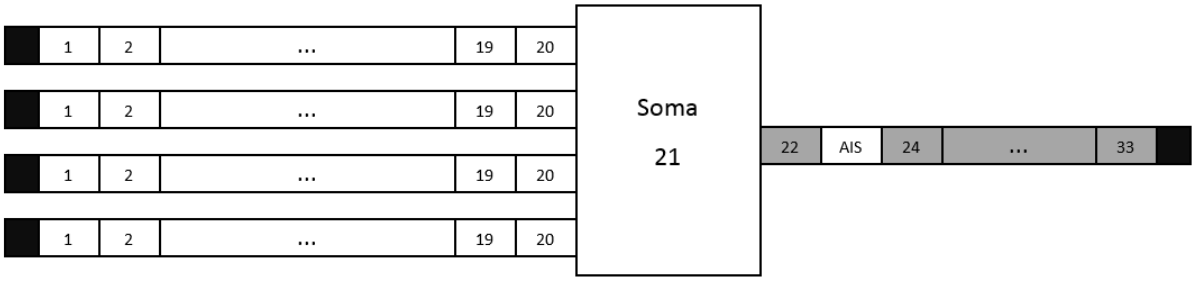

Figure 3.1. Multi-compartmental octopus cell model. There are four dendrites each with 20 compartments, a soma, a passive axon and an active axon initial segment. The compartments indicated in black were kept at rest for the execution of the solving algorithm. The compartments indicated in grey are passive and do not contain any active ion channels. AIS = Axon initial segment.

Table 3.1. Model geometry and active ionic channels. K^+_{LT} = Low threshold potassium. I_h = Hyperpolarisation activated mixed cation channel. K^+_{HT} = High threshold potassium. Na^+ = Sodium.

Part of model	Compartment diameter (µm)	Compartment length (µm)	Number of compartments	Active ion channels
Dendrites	3	12.5	4 x 20	K^+_{LT} I_h
Soma	25	25	1	K^+_{LT} K^+_{HT} I_h
Axon	3	3	1 + 10	-
Axon initial segment	3	3	1	Na^+

Each block in Figure 3.1 is a circuit used to model the ion channels as illustrated in Figure 3.2, which is the circuit representation of the cell membrane as modelled in a Hodgkin-Huxley type model. The different compartments are connected with a series resistance between the compartments, shown as R_i in the figure. This is also called the axial resistance, since it is along the axis of the cell being modelled.

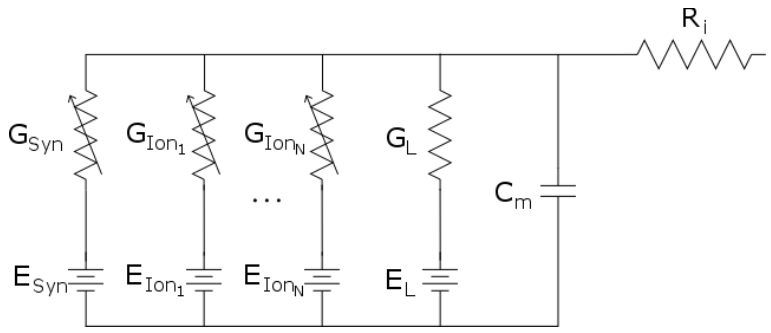

Figure 3.2. Circuit diagram of each compartment of the Hodgkin-Huxley type octopus cell model. Each ion channel is modelled with a voltage dependent variable conductance and a reversal potential. G_{Syn} is the synaptic channel conductance and E_{Syn} the synapse channel reversal potential. G_{Ion1}…G_{IonN} are the ion channel conductances with their reversal potentials E_{Ion1}…E_{IonN}. G_L is the leakage conductance. C_m is the membrane capacitance. The compartments are connected by a series resistor R_i, named the axial resistance.

All the active channels were implemented with Hodgkin-Huxley type equations where the conductance of an ion channel is determined by gating variables. The gating variables are in turn determined by rate constants, which describe the closing and opening rates of the ion channel gates in the membrane (Rattay, 1990).

For each channel the ionic current of that channel is given by the equation

$$I_x = g_x(a)(V - E_x) \quad , \tag{3.1}$$

for the ion x, where g_x is the voltage-dependent conductivity of the channel determined by the gating variable a, V is the membrane voltage and E_x is the reversal potential of the channel.

Each gating variable a can be calculated with the differential equation

$$\frac{da(t)}{dt} = Q\frac{1}{a_\tau(V)}\big(a_\infty(V) - a(t)\big) \quad , \tag{3.2}$$

where the time constant, a_τ, and the steady state value, a_∞, are functions of rate constants, which are functions of the membrane voltage.

Q is a temperature-dependent variable given by

$$Q = Q_{10}^{(T-T_0)/10} \quad , \tag{3.3}$$

where T is the temperature of the model simulation. $Q_{10} = 3$, $T_0 = 22$ ℃ except for the I_h channel where $Q_{10} = 4.5$ and $T_0 = 33$ ℃.

The sodium channel was derived from the bushy cell model in Rothman *et al.* (1993) because of the strong phase-locking of the model to low frequencies and the ability of the model to predict the response of onset units. The channel conductance depends on the gating variables m and h and is calculated with

$$g_{Na}\big(m(t), h(t)\big) = \overline{g_{Na}} m(t)^3 h(t) \quad , \tag{3.4}$$

where $\overline{g_{Na}}$ is the maximum sodium conductance. The gating variables are calculated with

$$m_\tau(V) = \frac{1}{\frac{0.36(V+49)}{1-e^{-\frac{(V+49)}{3}}} - \frac{0.4(V+58)}{1-e^{\frac{(V+58)}{20}}}} \tag{3.5}$$

$$m_\infty(V) = \frac{1}{1 - 1.11\frac{(V+58)\left(1-e^{-\frac{(V+49)}{3}}\right)}{(V+49)\left(1-e^{\frac{(V+58)}{20}}\right)}} \tag{3.6}$$

$$h_\tau(V) = \frac{1}{\frac{2.4}{1+e^{\frac{(V+68)}{3}}} + \frac{0.8}{1+e^{(V+61.3)}} + \frac{3.6}{1+e^{-\frac{(V+21)}{10}}}} \tag{3.7}$$

$$h_\infty(V) = \frac{\frac{2.4}{1+e^{\frac{(V+68)}{3}}} + \frac{0.8}{1+e^{(V+61.3)}}}{\frac{2.4}{1+e^{\frac{(V+68)}{3}}} + \frac{0.8}{1+e^{(V+61.3)}} + \frac{3.6}{1+e^{-\frac{(V+21)}{10}}}} \tag{3.8}$$

The K^+_{LT} channel conductance depends on the gating variables w and z and is calculated with

$$g_{KLT}(w,z) = \overline{g_{KLT}} w(t)^4 z(t) \ , \tag{3.9}$$

where $\overline{g_{KLT}}$ is the maximum low-threshold potassium conductance. The gating variables are calculated with

$$w_\tau(V) = \frac{100}{6e^{\frac{(V+60)}{6}} + 16e^{-\frac{(V+60)}{45}}} + 1.5 \tag{3.10}$$

$$w_\infty(V) = \frac{1}{\left(1 + e^{-\frac{(V+48)}{6}}\right)^{0.25}} \tag{3.11}$$

$$z_\tau(V) = \frac{1000}{e^{\frac{(V+60)}{20}} + e^{-\frac{(V+60)}{8}}} + 50 \tag{3.12}$$

$$z_\infty(V) = \frac{0.5}{1 + e^{\frac{(V+71)}{10}}} + 0.5 \tag{3.13}$$

The K^+_{HT} channel conductance depends on the gating variables n and p and is calculated with

$$g_{KHT}(n,p) = \overline{g_{KHT}}(0.85n(t)^2 + 0.15p(t)) \ , \tag{3.14}$$

where $\overline{g_{KHT}}$ is the maximum high-threshold potassium conductance. The gating variables are calculated with

$$n_\tau(V) = \frac{100}{11e^{\frac{(V+60)}{24}} + 21e^{-\frac{(V+60)}{23}}} + 0.7 \tag{3.15}$$

$$n_\infty(V) = \frac{1}{\left(1 + e^{-\frac{(V+15)}{5}}\right)^{0.5}} \tag{3.16}$$

$$p_\tau(V) = \frac{100}{4e^{\frac{(V+60)}{32}} + 5e^{-\frac{(V+60)}{22}}} + 5 \tag{3.17}$$

$$p_\infty(V) = \frac{1}{1 + e^{-\frac{(V+23)}{6}}} \tag{3.18}$$

The I_h channel conductance depends on the gating variable H and is calculated with

$$g_{I_h}(H) = \overline{g_{I_h}} H(t) \ , \tag{3.19}$$

where $\overline{g_{I_h}}$ is the maximum channel conductance. The gating variable is calculated with

$$H_\tau(V) = \frac{125e^{10.44\frac{(V+50)}{(273.16+T)}}}{1 + e^{34.81\frac{(V+50)}{(273.16+T)}}} \tag{3.20}$$

$$H_\infty(V) = \frac{1}{1 + e^{\frac{(V+66)}{7}}} \tag{3.21}$$

The leakage current is calculated with

$$I_L = g_L(V - E_L). \tag{3.22}$$

The synapses were implemented in the same way as an ion channel. The synaptic conductance was implemented with the equation

$$g_{syn}(t) = W\left(e^{-\frac{t-t_{event}}{\tau_{decay}}} - e^{-\frac{t-t_{event}}{\tau_{rise}}}\right) \ , \ t > t_{event} \ , \tag{3.23}$$

where W is a scaling constant and t_{event} is the arrival time of an AP on the ANF that terminates on the dendrite compartment. The rise and decay time constants were implemented as $\tau_{decay} = 340\ \mu s$ and $\tau_{rise} = 70\ \mu s$. The synaptic current was calculated with

$$I_{syn} = g_{syn}(V - E_{syn}) \ , \tag{3.24}$$

where E_{syn} is the synapse reversal potential which was implemented as 45 mV in the model. The 45 mV is different from the model in Spencer *et al.* (2012), where it is 0 mV, but it was increased to get a larger change in the membrane voltage for a synaptic input. It has also been used as 20 mV (Cai *et al.*, 2000) or 45 mV (Levy and Kipke, 1997) in other models. At the arrival of each AP on the ANF the synaptic conductance will change, causing a synaptic current in the membrane, which will increase the membrane voltage as a PSP. Only excitatory synapses were included in the model, since inhibitory synapses has not been found in octopus cells by measurements (Golding *et al.*, 1995).

The synaptic conductance as a function of time from equation (3.23) for an input arriving at t = 0.2 ms is shown in Figure 3.3. This is the unscaled conductance before it is multiplied with the scaling factor W.

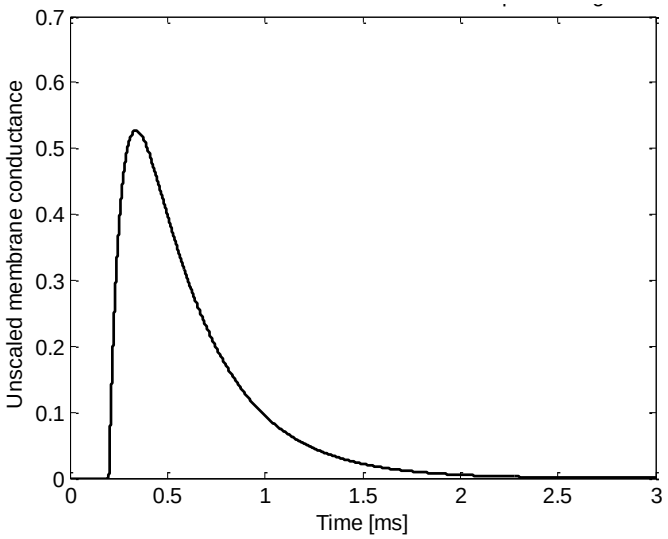

Figure 3.3. Unscaled membrane conductance as a function of time for a synaptic input arriving at t = 0.2 ms. The conductance changes with time from the arrival of the spike with an alpha-function.

The scaling factor was calculated to ensure that every synapse has nearly the same influence on the soma regardless of its position along the dendrite, in the same way as suggested in Gulledge *et al.* (2005) and Williams and Stuart (2003) for CA1 hippocampal pyramidal neurons. The magnitude of the PSP at the site of initiation therefore becomes larger as the distance from the soma increases. This is possibly because of several factors, including smaller effective input capacitance and more receptors (Williams and Stuart, 2003). The scaling was performed in a manner that ensured that the maximum voltage of a PSP in the soma would be around -59 mV for all the synapses regardless of their position on the dendrite. Each synapse therefore leads to a rise of 1.72 mV from the resting potential in the

soma. With the voltage threshold of -39.11 mV, a total of 13 coincident inputs, regardless of their position on the synapse, will be needed to reach threshold and generate an AP.

The values of W were implemented in the model as W = [4000, 1100, 510, 300, 200, 142, 108, 85, 68, 55, 45.5, 38, 32.5, 27.5, 23.5, 20, 17.2, 14.8, 12.65, 11] adjusted manually from the most distal to most proximal synapses. W as a function of distance from the soma is shown in Figure 3.5. W has the form of an exponential function. Using the curve fitting tool in Matlab, an equation for W was derived as

$$W(x) = 2.128e^{0.02296x} + 6.076 \times 10^{-12}e^{0.1358x} \quad , \quad R^2 = 0.9998 \qquad (3.25)$$

where x is the distance from the soma in µm.

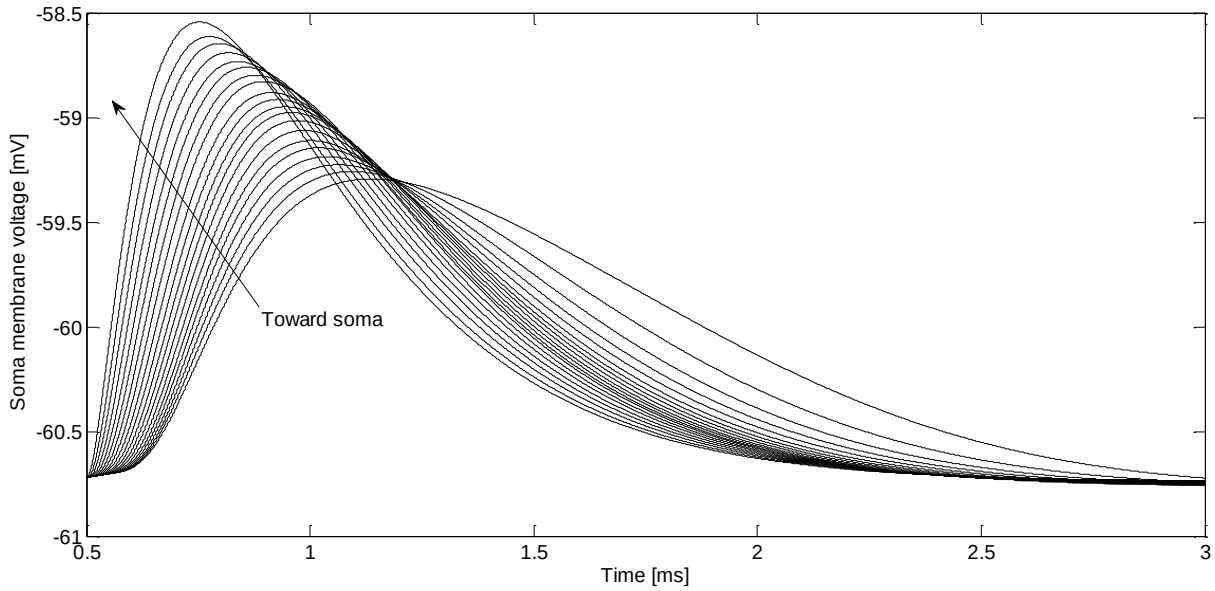

Figure 3.4. PSPs in the soma for synaptic inputs on each compartment of a single dendrite. The arrow indicates the position of the synapse towards the soma. The difference between the PSP amplitude of the most proximal and distal synapses is less than 1 mV. Therefore the position of the synapse on the dendrite does not have a large influence on the effect the synapse has on the soma.

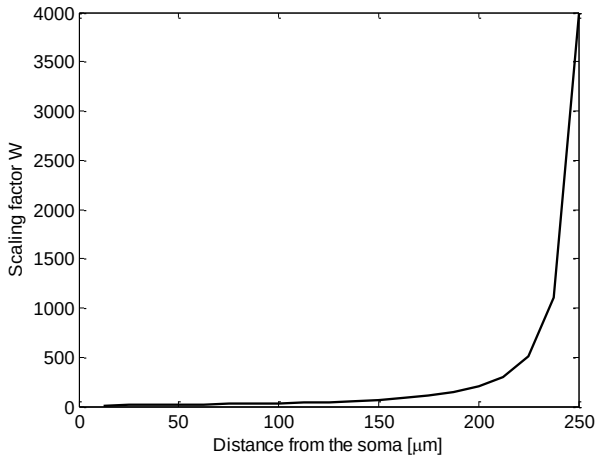

Figure 3.5. Synapse scaling factor W as a function of the distance from the soma. W has the form of an exponential function.

The membrane voltage was calculated with the differential equation

$$\frac{dV}{dt} = \left(-I_{syn} - I_L - I_{KLT} - I_H - I_{Na} - I_{KHT} + I_s + \frac{d}{4R_i dx^2}(V_{x-1} - 2V_x + V_{x+1}) \right) \Big/ C_m \tag{3.26}$$

where I_{syn} is the synaptic current, I_L is the leakage current, I_s is an electrical transmembrane stimulation current, all in µA/cm^2, d is the diameter of the compartment in cm, dx is the compartment length in cm, R_i is the axial resistivity in Ω·cm, C_m is the membrane capacitance in µF/cm^2 and x is the compartment at which the voltage is calculated.

The term $\frac{d}{4R_i dx^2}(V_{x-1} - 2V_x + V_{x+1})$ is a numerical approximation of the term $\frac{d^2V}{dx^2}$, as derived in Plonsey and Barr (2007). This is used to calculate the membrane voltage in the compartment x because of the membrane voltages of the adjacent compartments.

The model was implemented in Matlab and it was solved using the Euler method, which is a simple way of solving differential equations numerically. This method was chosen for its ease of implementation. It however resulted in the model being unstable and it had to be solved for really small time steps of 50 ns to avoid instability. The method was still successful in solving the model, but it is suggested that another method be implemented in future. The algorithm to implement the Euler method will be discussed below.

Starting with the differential equation

$$\frac{dy}{dt} = f(y,t) \ , \tag{3.27}$$

it is rewritten as

$$\frac{\Delta y}{\Delta t} = f(y,t) \ , \tag{3.28}$$

or

$$\Delta y = f(y,t)\Delta t \ . \tag{3.29}$$

The value of Δt is chosen, which is the step size of the solution. At each time t, Δy is calculated from equation (3.29), after which y_{t+1} is calculated with

$$y_{t+1} = y_t + \Delta y \ , \tag{3.30}$$

which is used in the next iteration.

The above method was used in the algorithm to solve the model in Matlab. The algorithm is illustrated in Figure 3.6, indicating the equations used at each step. It starts with calculating the initial values, using the initial membrane voltage as the resting potential of the cell. First the channel conductances are calculated, which are used to calculate the ion currents. After that the change in gating variables and the membrane voltage are calculated, which are used to calculate the gating variables and membrane voltage at the next step. This process is repeated for each compartment at each time step to solve the model.

To use equation (3.26) to solve the membrane voltage, it is necessary to assign values to the first and last compartments of the model to ensure V_{x-1} and V_{x+1} are defined when calculating at the compartments at the ends of the model. These compartments were therefore implemented to remain at rest, indicated by the black blocks in Figure 3.1.

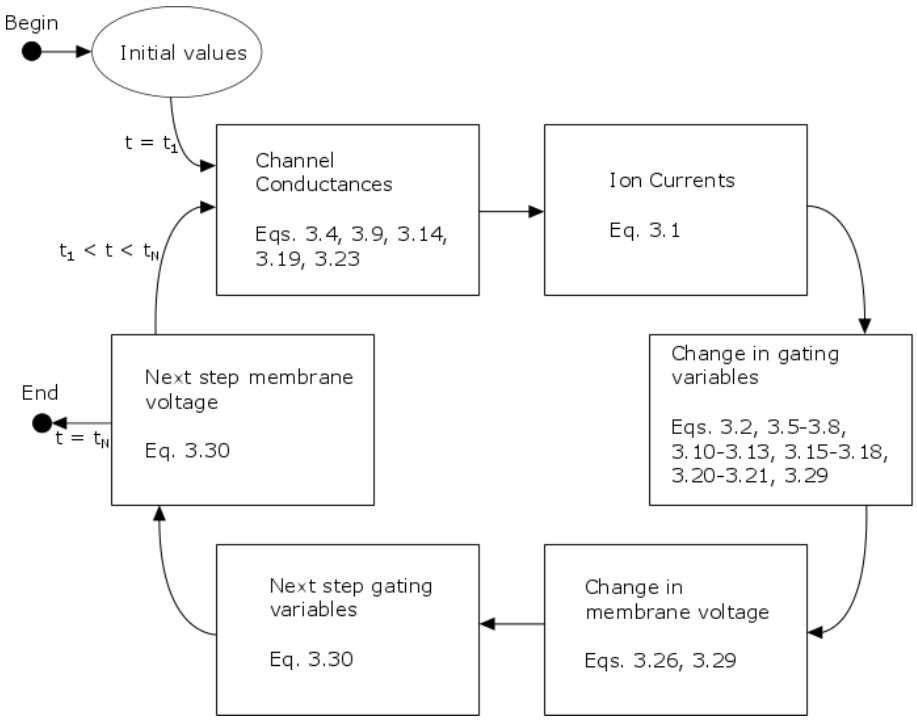

Figure 3.6. Algorithm used to solve the model with the Euler method and the equations used for each step. Time t_1 is the starting time and t_N is the end time for calculation at N time samples.

The model had four dendrites, all connected to a single soma. At this point, the currents from the four dendrites had to be added in the soma. The connection of the dendrite compartments at the soma is shown in Figure 3.7 where only the axial resistances to the compartments connected to the soma are shown. The V_{x-1} term in equation (3.26) therefore had to be changed, since not only one compartment is linked to the soma. For the soma compartment the term $(V_{x-1} - 2V_x + V_{x+1})$ was therefore replaced with

$$(V_{x-1} - 2V_x + V_{x+1}) = \frac{V_{Den1} + V_{Den2} + V_{Den3} + V_{Den4}}{4} - 2V_{Soma} + V_{Axon} \quad , \tag{3.31}$$

where V_{denx} is the membrane voltage of the compartment of dendrite x adjacent to the soma. This equation was derived by applying Kirchoff's Current Law in the soma compartment, as described in Cai *et al.* (1997b).

The constants used in the model are given in Table 3.2. The reference is given for when it was changed from the value given in Spencer *et al.* (2012). The model geometry is given in Table 3.1.

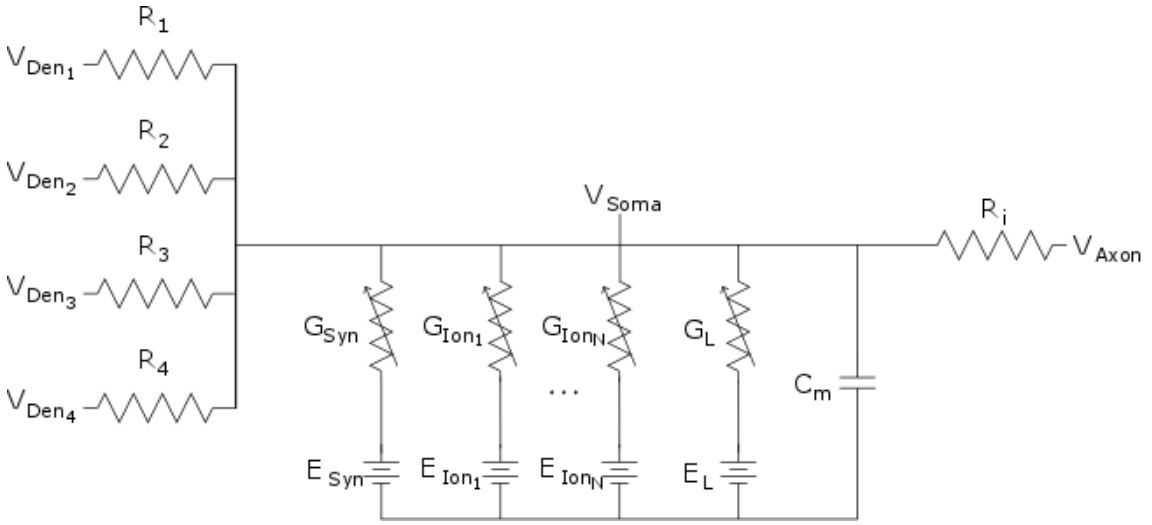

Figure 3.7. Connection of the compartments at the soma of the octopus cell model. Only the axial resistances to the other compartments are shown. All four dendrites terminate on the soma, which will lead to their axial currents being summed in the soma.

3.2.2 Travelling wave and cochlear implant models as input to the octopus cell model

A model of the travelling wave in the cochlea generating inputs to a neural model was used to generate ANF discharge times, which were used as inputs for the octopus cell model for acoustic stimulation (Schmidt, 2016). The travelling wave model was based on an existing model (Duifhuis *et al.*, 1985; Duifhuis, 2012). The neural model that was used to generate the AP discharge times from the BM motion is a phenomenological model of the AN (Zilany *et al.*, 2009). This process is illustrated in Figure 3.8A. The travelling wave model receives an acoustic signal as the input and generates the travelling wave BM motion for the next step. The BM displacements are then used by a model of the hair cells and ANFs to generate the ANF discharge times because of the acoustic stimulation. These discharge times are then used as the spike times at the octopus cell synapses. From the octopus cell model the soma membrane voltage can then be measured in response to the inputs from the ANFs.

To generate inputs to the octopus cells for CI stimulation, a model of the ACE CI speech processing strategy was used, combined with a model of the auditory periphery and a model of the AN for pulse train electrical stimulation (Bruce *et al.*, 1999). The connection between the models is shown in Figure 3.8B. The CI model receives an acoustic input, which is then filtered into the frequency bands of the electrodes, after which the six channels with the highest energy are selected. The amplitudes and activation times of the current pulses are then calculated for stimulation by the CI. From the electrode activation the current spread in the cochlea is calculated to determine the current at all the ANFs in the model. The discharge

times for each ANF because of the current from the electrodes is then calculated by using the neural model. The discharge times from the neural model are again used as the spike input times for the synapses of the octopus cell model, after which the response of the octopus cell is measured as the membrane voltage in its soma.

Table 3.2. Octopus cell model constants. References are given where the constants were changed from that used in Spencer *et al.* (2012).

Constant	**Symbol**	**Value**	**Reference**
Model temperature	T	37 °C	-
Axial resistance	R_i	300 Ω·cm	(Levy and Kipke, 1997)
Membrane capacitance	C_m	0.9 µF/cm^2	-
Resting potential	V_{rest}	-62 mV	-
K^+_{LT} reversal potential	E_{KLT}	-70 mV	-
K^+_{HT} reversal potential	E_{KHT}	-70 mV	-
I_h reversal potential	E_H	-38 mV	-
Na^+ reversal potential	E_{Na}	55 mV	-
Leakage potential	E_L	-62 mV	-
Synaptic potential	E_{syn}	45 mV	(Cai *et al.*, 2000)
Maximum K^+_{LT} conductance – soma	$\overline{g_{KLT}}$	40.7 mS/cm^2	-
Maximum K^+_{LT} conductance – dendrites	$\overline{g_{KLT}}$	2.7	-
Maximum K^+_{HT} conductance	$\overline{g_{KHT}}$	6.1	-
Maximum I_h conductance - soma	$\overline{g_H}$	7.6	-
Maximum I_h conductance – dendrites	$\overline{g_H}$	0.6	-
Maximum Na^+ conductance	$\overline{g_{Na}}$	4244.1	-
Leakage conductance	$\overline{g_L}$	2	-

The outputs from both neural models were the discharge times of a population of ANFs arranged to be spread linearly in position from the base to the apex along the BM in the cochlea. Each octopus cell received input from 80 ANFs, one on each dendrite compartment. The basal ANFs terminated distally on the dendrites and the more apical neurons terminated proximally on the dendrites. This was done to keep the tonotopic arrangement of the ANF termination on octopus cells (Gelfand, 2010; Mcginley *et al.*, 2012; Oertel *et al.*, 2000). The termination of the ANFs was arranged starting from the most distal compartment of one dendrite, followed by the same compartments on the other three dendrites and continuing to the second compartment of the first dendrite, followed by the second compartments of the other dendrites and continuing in this manner. This was repeated up to the 20th compartment of the fourth dendrite. An example of the termination of the ANFs on an octopus cell with ANFs originating between the positions of 5000 Hz and 2500 Hz is shown in Figure 3.9.

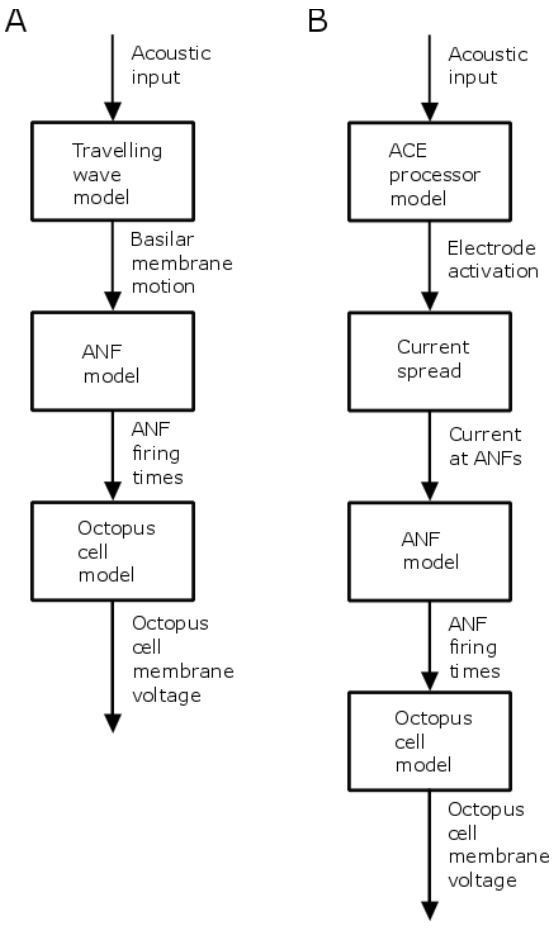

Figure 3.8. Connection between various models used in the simulations. A. Models used for simulation of an acoustic input. B. Models used for simulation of CI stimulation.

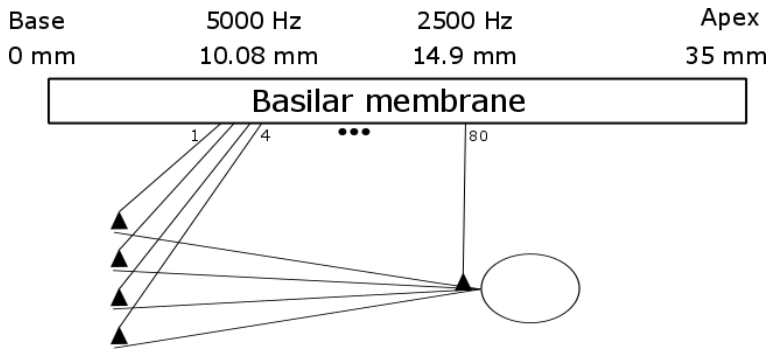

Figure 3.9. Termination of ANFs on the octopus cell shown for ANFs between the positions of 2500 Hz and 5000 Hz on the BM. The neurons terminated with synapses with the high-frequency (basal) ANFs from the most distal positions on the dendrites moving proximally as the ANF positions moved towards the apex.

3.2.3 Population of octopus cells

There are many octopus cells in the CN likely to receive input from different ranges from the cochlea. Therefore the single octopus cell model was extended to a population of octopus cells. The cells were arranged to each receive input from the same distance along the BM in the cochlea. The possible optimal range will be discussed in Chapter 5. If each octopus cell receives input from a third of the cochlea, three octopus cells would span the whole cochlea. Therefore nine octopus cells, namely a multiple of three were implemented to ensure that the whole cochlea and many different positions of input were accounted for. The octopus cells were arranged linearly in position from the base to the apex. The number of ANFs used in the simulation was chosen in a manner to ensure that no two octopus cells received input from the same ANF. The population of nine octopus cells and their arrangement across the BM are illustrated in Figure 3.10. The octopus cell numbers shown in the figure will be used in the rest of this dissertation with octopus cell number 1 receiving input from basal ANFs, moving towards octopus cell number 9, which receives input from the apical ANFs.

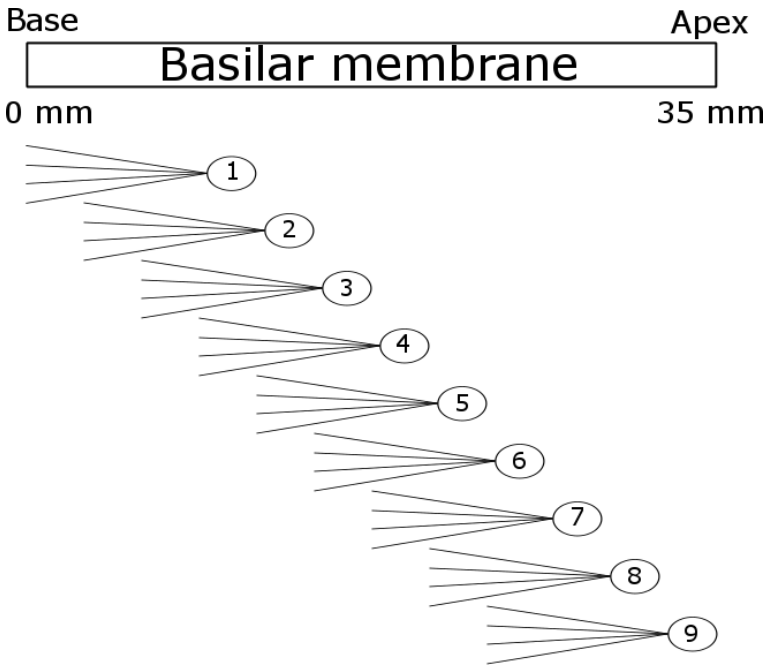

Figure 3.10. Population of nine octopus cells, each receiving input from a third of the cochlea, arranged linearly from the base to the apex. Each cell receives input from ANFs over the range of the BM where the cell is drawn in the figure.

3.3 DISCUSSION

A model of a single CN octopus cell was implemented in Matlab to resemble the measured anatomy and physiology found in literature from measurements on octopus cells. The model was based on a previously published model (Spencer *et al.*, 2012) with some minor adjustments.

The octopus cell model can receive input from a transmembrane current applied at any position on the cell, as well as synaptic inputs on the dendrites. The synapses were implemented in the same way as ion channels, with the synaptic conductance changing as a function of time from the arrival time of an AP at the synapse. Since the synapses are only dependent on the arrival times of APs, only the discharge times of ANFs are needed to simulate the response of the octopus cell to ANF input.

Models of the auditory periphery for both acoustic stimulation in normal hearing and stimulation by a CI were used to generate inputs to the octopus cell model. With these models the octopus cell model's response to acoustic and electrical stimulation of the AN can be simulated. The range on the BM of the ANFs terminating on the octopus cell can be changed to investigate different ranges or randomisation of the ANF inputs.

The single octopus cell model was extended to a population of octopus cells to simulate the response of octopus cells for input from the whole of the cochlea. The range of the BM from which each octopus cell can receive input can be changed to test its effect. The number of octopus cells in the population was limited by simulation time and was therefore not increased beyond nine cells. The number of octopus cells can however be increased in future for a better representation of reality.

The model had to be solved with time steps of 50 ns to obtain stability in the solving algorithm. This small time step led to long simulation times. Another algorithm that may allow larger time steps and faster execution is advisable and should be implemented in future.

CHAPTER 4 OCTOPUS CELL MODEL VERIFICATION AND SENSITIVITY TO CHANGING PARAMETERS

4.1 INTRODUCTION

It should be determined whether a model represents reality accurately before it can be used to predict data from the real world. Therefore the model in Chapter 3 was verified by comparing the model simulation results to published results from experimental measurements. It was assumed that if the octopus cell model could predict data of the same voltages at the same time as in the measured data, the model would be valid and could be used to predict the responses of octopus cells to various inputs that may be encountered in the real world.

The effect that a change in the parameters in the model would have on the response of the model also had to be investigated. When the effects of the various parameters are known the function of these in the model can be determined and it can also be determined which parameters to change to achieve certain outcomes with the model. Therefore the effects of changing the axial resistance, membrane capacitance and maximum ion channel conductances on the model response in terms of thresholds and AP shape were simulated.

4.2 METHOD

4.2.1 Model verification

The model was verified by comparing the model outputs to the published measured results, which are summarised in Table 2.2. The outputs that were measured and the methods used to measure each of them are given below.

Response to electrical stimulus

A transmembrane DC stimulus was introduced in the model by changing I_s, in μA/cm^2, in equation (3.26). This was used to model transmembrane electrical stimulation of the octopus cell, which was used to compare the model output to experimental measurements of electrical stimulation of octopus cells in slices. The following transmembrane electrical stimuli were applied to measure the response:

- DC current pulse
- DC current step with long duration
- DC current step followed by another increasing step
- DC pulse train with 50% duty cycle at different frequencies

Membrane resistance

The membrane resistance was measured by applying a transmembrane current ramp with magnitude small enough not to generate an AP. The membrane voltage was measured for each current value and the resistance was calculated as the gradient of the plot with V as a function of I, therefore applying Ohm's Law. Membrane resistance R_m was therefore measured as

$$R_m[\Omega] = \frac{\Delta V\ [mV]}{\Delta I\ [mA]}\ , \tag{4.1}$$

from a graph of the membrane voltage as a function of stimulus current. The stimulus current first had to be converted to current magnitude in mA which can be used in equation (4.1), from the current density in µA/cm^2, which is used in equation (3.26). This was done with

$$I = I_D \times \frac{\pi \times d \times l}{1000}\ , \tag{4.2}$$

where I is the current magnitude, I_D is the current density, d is the diameter in cm and l is the length of the compartment in cm in the model.

The stimulus current was applied to the compartment of which the resistance had to be measured, which was the soma in most cases.

Minimum current to generate an AP [nA]

A transmembrane stimulus current pulse with a width of 100 µs was applied at the soma. The amplitude of the step was increased until the octopus cell generated an AP. This current value was taken as the minimum needed for an AP, which is the current threshold. At the minimum current, the membrane voltage just before the AP is generated was taken as the voltage threshold of the octopus cell.

Action potential amplitude [mV]

The amplitude was measured as the difference between the peak voltage of the AP in the soma and the resting potential in the soma, as shown in Figure 4.1. This was measured for a transmembrane stimulus current at threshold.

Action potential duration [ms]

The duration was measured as the time between the 10% points of the membrane voltage for the AP. It is therefore the difference between the time when the voltage has increased from the resting potential to 10% of the amplitude of the AP and decreased again to the same voltage value. This is shown in Figure 4.1. This was measured for a transmembrane stimulus current at threshold.

Latency [ms]

Latency is the time from the stimulus onset to the peak of the AP. The latency was therefore measured from the onset of a current pulse at threshold and the time of the peak of the AP, as shown in Figure 4.1.

Rate of depolarisation threshold [mV/ms]

A transmembrane current ramp was applied to the soma with increasing rate of rise until the octopus cell generated an AP. The rate of rise was changed by changing the rise time of the current rising from zero to a maximum, which was the current threshold for an AP. The gradient of the membrane voltage as a function of time was taken as the threshold. The rate of depolarisation threshold was therefore calculated with

$$Rate_{Thres} = \frac{\Delta V}{\Delta t} \quad , \tag{4.3}$$

at the minimum rate which generated an AP by applying a ramped transmembrane current.

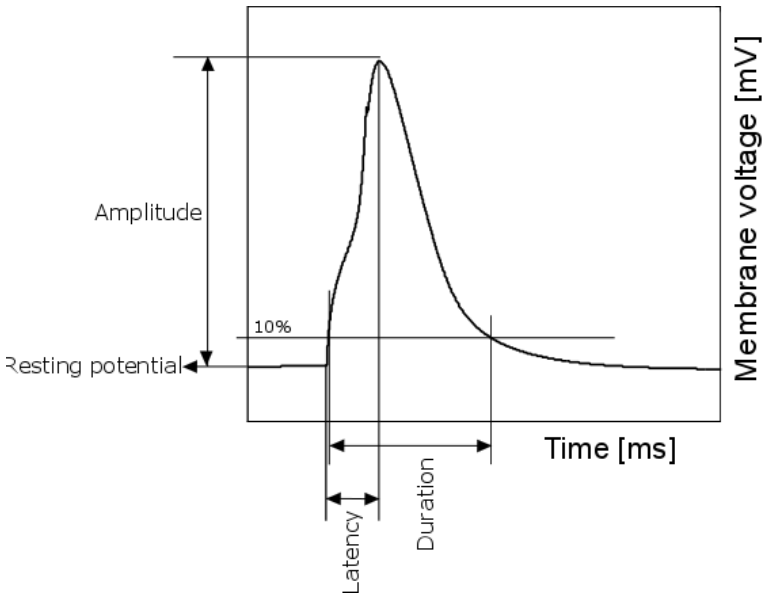

Figure 4.1. Illustration of the measurements taken from an AP.

4.2.2 Parameter sensitivity

The effect of changing the axial resistance, membrane capacitance and maximum ion channel conductances in the model was evaluated. This was done by changing each of the parameters individually while keeping the other parameters constant. The following were measured for changes in all the parameters:

- Soma membrane resistance
- Resting potential
- Minimum transmembrane current needed to generate an AP
- Voltage threshold of the soma for an AP
- AP amplitude
- AP duration
- Latency
- Rate of depolarisation threshold
- Dendritic delay – Time difference between the maxima of PSPs in the soma for a most proximal and most distal synapses.

The outputs that were measured were chosen on the basis of how important they are to the functionality of the octopus cell model as well as measurements that were found in literature to which the model could be compared. The dendritic delay was chosen because the delay may be important in compensating for the travelling wave delay (Spencer *et al.*, 2012;

Mcginley *et al.*, 2012). To compensate for the travelling wave delay the dendritic delay has to be the same as the travelling wave delay over the range from which the octopus cell receives input. Therefore it is important to know which parameters change the dendritic delay and by how much it can be changed.

4.3 RESULTS

4.3.1 Model verification

The model was compared to measured results found in literature, which are summarised in Table 2.1 and Table 2.2 in Section 2.2.1 to determine its validity. All of these results are summarised in the "Original" row in Table 4.1.

Membrane resistance

The soma membrane voltage for a ramped stimulus current is given in Figure 4.2. From this graph the membrane resistance is calculated as $R_m = 636\ 504\ \Omega$.

This is much smaller than experimentally measured resistances, which are a few mega ohms in magnitude.

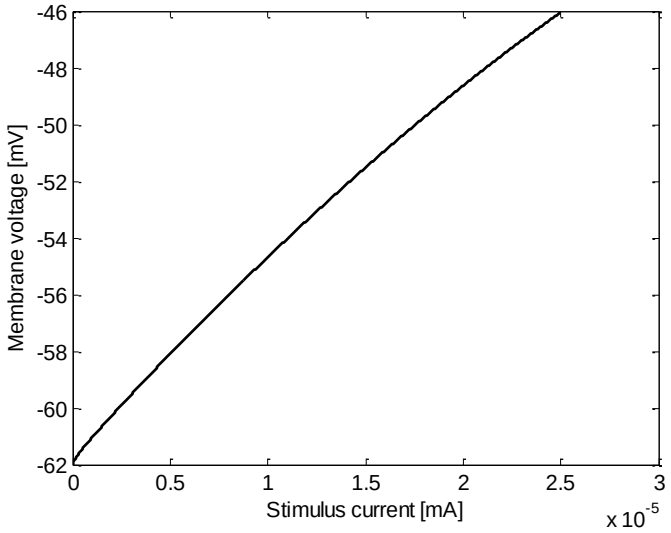

Figure 4.2. Soma membrane voltage for a ramped transmembrane stimulus current in the soma. This was used to calculate the membrane resistance of the soma.

Minimum current to generate an AP

For a pulse of 100 µs width, the minimum current that was needed to generate an AP was measured as 40 nA. The soma membrane voltage for stimulation at this threshold is shown

in Figure 4.3. From this figure the voltage threshold was also measured at the point to which the membrane voltage increased because of the current before the AP was generated. This threshold was -39.5 mV.

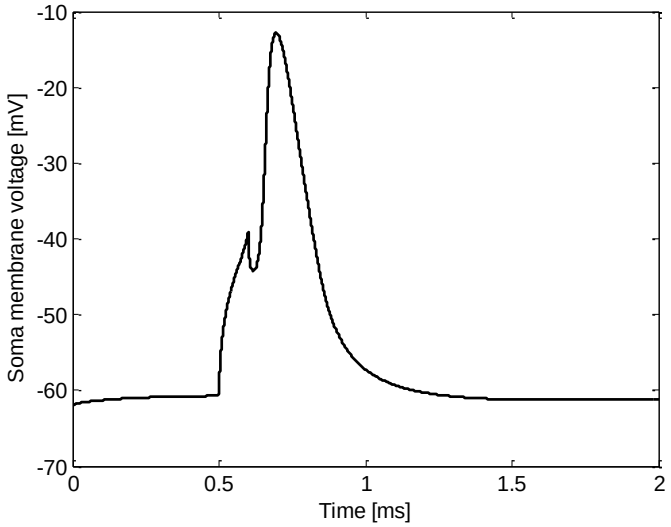

Figure 4.3. Soma membrane voltage for a current pulse at the threshold of 40 nA at a duration of 100 µs.

Response to transmembrane electrical stimulation

The soma membrane voltage for a DC current pulse of 40 nA, which is the threshold of the cell, and 100 µs duration is shown in Figure 4.3. The octopus cell generates a single AP with some latency following the stimulus onset.

The soma membrane voltage for a transmembrane DC current step with amplitude 40 nA and duration 4 ms starting from 0.5 ms is shown in Figure 4.4. The octopus cell does not generate another AP but the membrane stays depolarised for the duration of the current stimulation. The modelled octopus cell therefore has an onset response and is valid to model onset units.

For the sustained depolarisation the model response does not have a hyperpolarising sag as in some measurements. The response resembles the measurement on 7-day-old cats more than that on 15-day-old cats reported in Bal and Baydas (2009).

The soma membrane voltage for a transmembrane DC current step of 40 nA followed by a step of 80 nA is shown in Figure 4.5. The octopus cell only generates an AP at the onset of the first current step, and not again at the second increasing current step. This is different from literature (Bal and Baydas, 2009; Oertel *et al.*, 2000) where a second AP is generated

at the onset of the second step. The difference might be because of the increased current needed by the model to generate an AP.

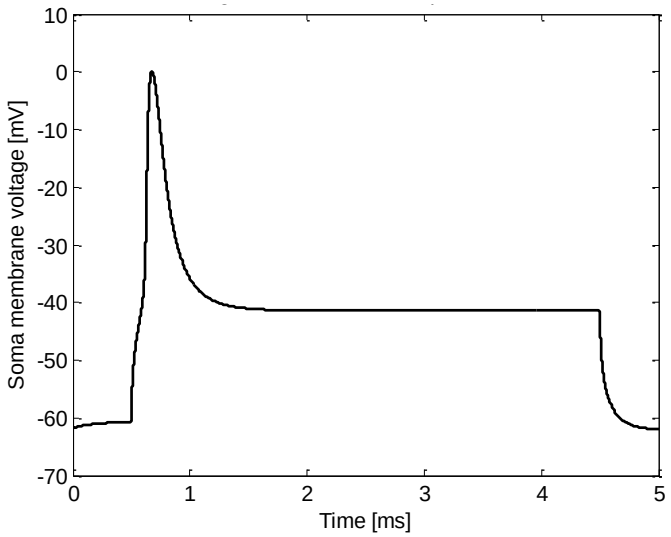

Figure 4.4. Soma membrane voltage for a DC current step of 40 nA and duration of 4 ms.

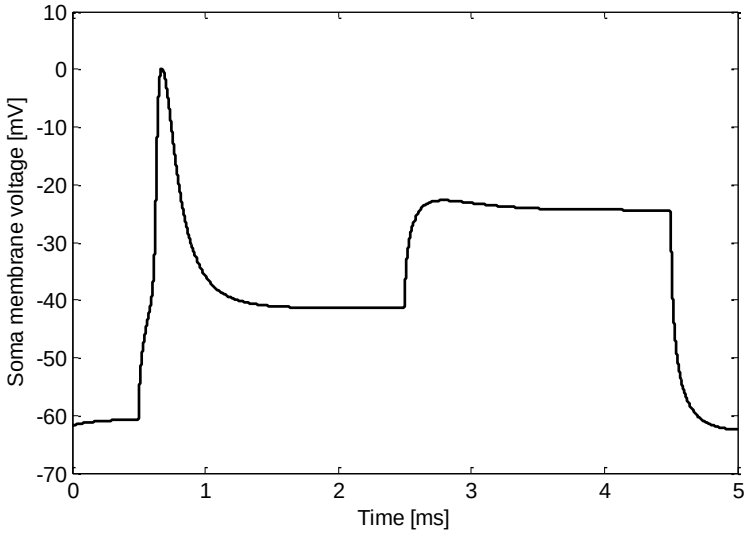

Figure 4.5. Soma membrane voltage for transmembrane current steps of 40 nA and increasing to 80 nA, starting at times 0.5 ms and 2.5 ms respectively. The octopus cell model does not generate a second AP when the current is increased, as it did in experimental measurements.

The soma membrane voltage for a transmembrane current square wave stimulus of 40 nA amplitude and 1100 Hz with a 50% duty cycle is shown in Figure 4.6. 1100 Hz was the maximum frequency to which the octopus cell entrained, which is slightly higher than measured data where the octopus cells entrained up to 780 Hz (Bal and Baydas, 2009) and 1000 Hz (Oertel *et al.*, 2000).

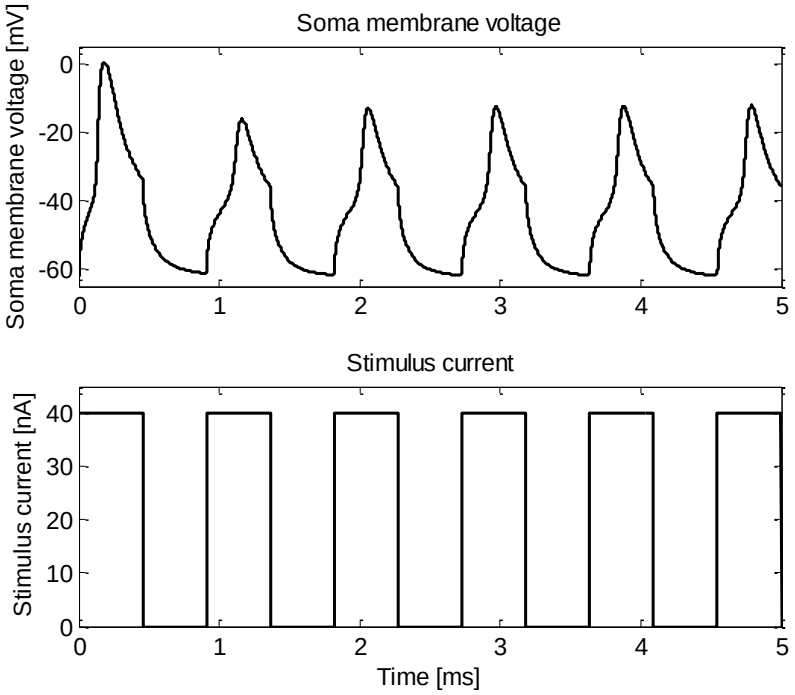

Figure 4.6. Soma membrane voltage for stimulation with a 40 nA transmembrane square wave stimulation current at a frequency of 1100 Hz at 50% duty cycle.

The octopus cell model had the same behaviour for electrical stimulation as found in measurements. The only difference is that the octopus cell model needs more current to reach threshold than what was needed in the measurements. This is because of the low membrane resistance of the model, which is much lower than measured. The lower membrane resistance makes it necessary to stimulate with more current to reach the voltage threshold. The aim of the model was however not to predict the response of octopus cells to transmembrane electrical stimulation and therefore the increased current needed in the cell should not influence the results of the model for stimulation by synaptic input, which is what the model was developed for.

Action potential amplitude

The AP amplitude was measured at threshold, therefore from the AP shown in Figure 4.3. The amplitude was calculated as 47.68 mV. This is in the range of experimental measurements on octopus cells.

Action potential duration

From Figure 4.3 the AP duration was measured as 0.4612 ms, which is in the same range as experimental measurements.

Latency

The latency was measured from Figure 4.3 as 0.19 ms. This measured latency is much smaller than what was measured experimentally and the modelled cell therefore responds more quickly to an electrical pulse than what has been measured. This can be because of the lower membrane resistance which decreases the time constant of the membrane and leads to a quicker response.

Rate of depolarisation threshold

The soma membrane voltage for stimulation with a transmembrane current with a maximum of 40 nA and rate of rise at the minimum that generated an AP is shown in Figure 4.7. It was taken to be an AP when the membrane voltage in the soma exceeded -30 mV. This threshold for an AP was also used in later measurements.

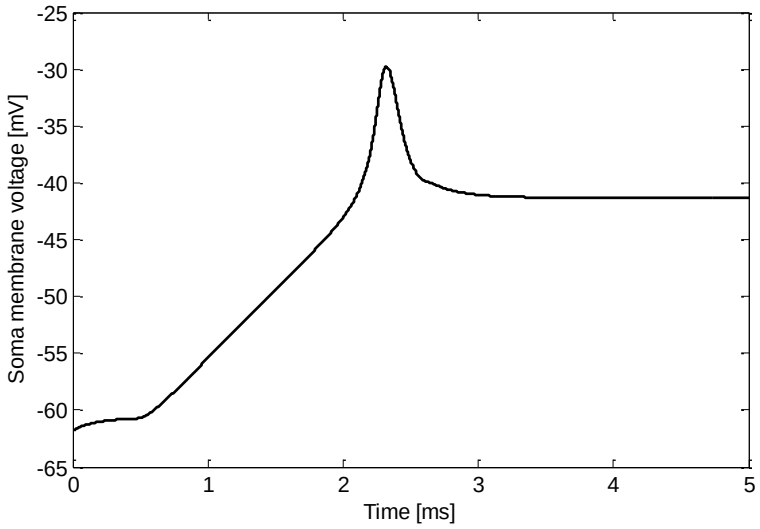

Figure 4.7. Soma membrane voltage for stimulation with a rising transmembrane current at the rate of depolarisation threshold. The maximum stimulation current was 40 nA, which is the threshold for a current pulse.

From Figure 4.7 the rate of depolarisation threshold was calculated as 12.07 mV/ms. The rate of depolarisation threshold measured from the model was in the range of experimental measurements. The sensitivity of octopus cells to the rate of depolarisation plays a big role in their functionality. Therefore the sensitivity of the model to the rate of depolarisation is important for a valid octopus cell model. The model can therefore be used for investigation of octopus cell responses.

Dendritic delay

The soma membrane voltages for a most distal and most proximal synaptic input on a single dendrite are shown in Figure 4.8. The dendritic delay was measured as the time difference between the peaks of the distal and proximal synapses. From the figure the dendritic delay of the modelled octopus cell was measured as 0.3835 ms. The dendritic delay of octopus cells has not been measured experimentally and there are no data with which to compare the model results. The model in Spencer *et al.* (2012) however had a dendritic delay of 0.25 ms, which is different from this model. The main reason for the difference is the change in the axial resistance in the present model from the Spencer model.

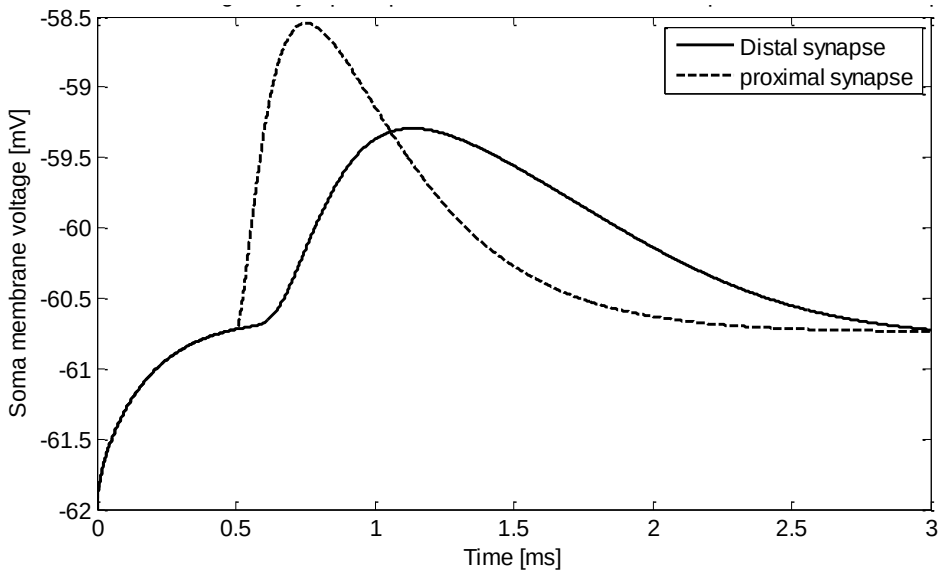

Figure 4.8. Soma membrane voltage for synaptic inputs at the most distal and most proximal dendrite compartments used to measure the dendritic delay. There is a difference in the time it takes each input to reach a maximum in the soma. The differences between the times to these maxima were taken as the dendritic delay of the octopus cell model.

The model response was in the measured ranges except for the membrane resistance and the AP latency. The model membrane resistance is much lower than that given in literature but it does not influence the model behaviour for stimulation with synaptic inputs. It does however have a large effect on the transmembrane stimulation current needed to generate an AP, which was measured as 1.8 nA – 2 nA experimentally (Bal and Baydas, 2009; Golding *et al.*, 1999) but is about 40 nA in the model. As in measurements (Bal and Baydas, 2009; Golding *et al.*, 1995) the model also entrained to stimulation current pulses up to 800 Hz. The model predicts the behaviour of an octopus cell with reasonable accuracy.

4.3.2 Parameter sensitivity

All the results are summarised in Table 4.1 in terms of the effect on the octopus cell response when each of the parameters was changed to half and double the original model value.

4.3.2.1 Simulation 1. Axial resistance

The effect of changing the axial resistance (R_i) was evaluated. The soma membrane voltage for a synaptic input at the most distal synapse with different axial resistances is shown in Figure 4.9. Increasing R_i increases the membrane resistance, which leads to slower responses because of the increase in the time constant of the membrane. Therefore increasing R_i increases the dendritic delay. However, when R_i becomes too large, the membrane resistance between the distal synapses and the soma becomes too large for PSPs to reach the soma. The largest R_i where the distal synapses still had an influence at the soma was 600 Ω·cm, therefore it should not be increased beyond this point. Even when R_i = 600 Ω·cm the PSPs become so small in the soma that many more coincident inputs are needed to reach threshold.

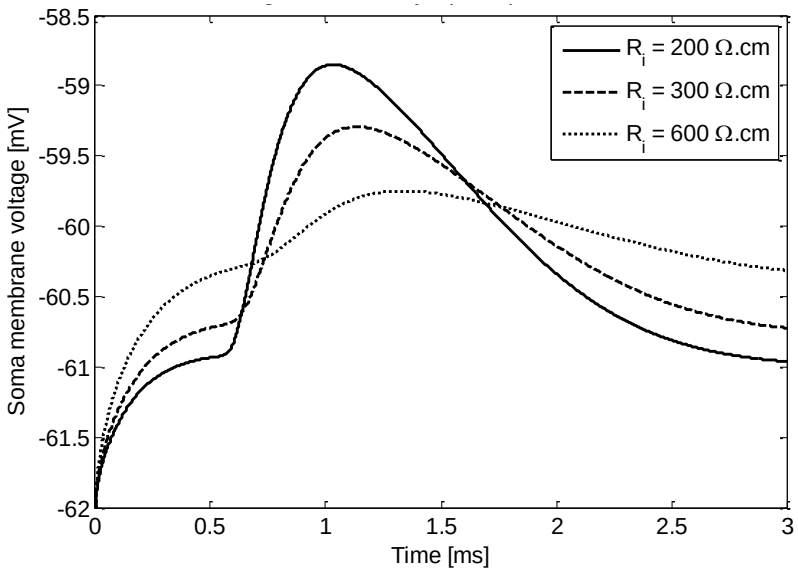

Figure 4.9. Soma membrane voltage for a distal synaptic input at time = 0.3 ms for different axial resistances. When the axial resistance increases the resting potential increases and the amplitude of the PSP in the soma decreases.

4.3.2.2 Simulation 2. Membrane capacitance (C_m)

The membrane voltage at the soma for a distal synaptic input on a single dendrite for different values of C_m is shown in Figure 4.10. The capacitance was increased from 0.6 µF/cm^2 to 3 µF/cm^2 in steps of 0.1 µF/cm^2. When C_m is increased the PSP in the soma becomes wider because of the longer time constant of the membrane, which results in a slower response. The amplitude of the PSP decreases because of an increase in the membrane

resistance, resulting in a larger decrease in the membrane voltage from the distal end of the dendrite to the soma.

Increasing the membrane capacitance increased the AP latency and duration. Octopus cells are known for their exceptional speed. Therefore the membrane capacitance should not be increased because it will compromise the speed of the octopus cell response.

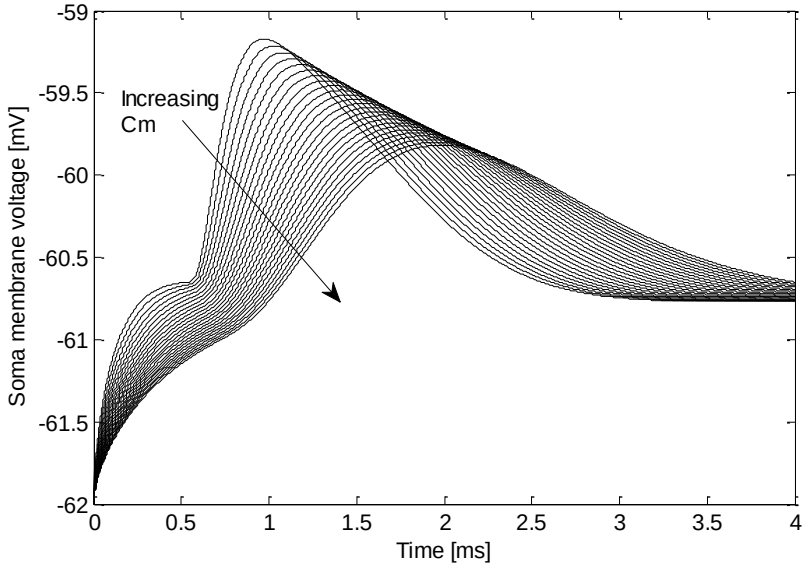

Figure 4.10. The membrane voltage at the soma for synaptic input at the most distal dendrite compartment. The capacitance was increased from 0.6 µF/cm^2 to 3 µF/cm^2 in steps of 0.1 µF/cm^2. As the membrane capacitance increases, the voltage at the soma becomes wider and smaller.

4.3.2.3 Simulation 3. Maximum K^+_{LT} conductance

Dendrites

The membrane voltage in the soma after a distal synaptic input on a single dendrite for different values of the maximum K^+_{LT} conductance in the dendrites is shown in Figure 4.11. When the conductance is decreased, the resting potential as well as the amplitude of the PSP in the soma increase without greatly affecting the duration of the AP. The delay to the maximum in the soma after a most distal synaptic input for different K^+_{LT} conductances in the dendrites is shown in Figure 4.12. The dendritic delay is largest when the K^+_{LT} conductance is zero and decreases as the conductance is increased. Therefore the K^+_{LT} conductance in the dendrites is partially responsible for the speed of the octopus cell response, since increasing the K^+_{LT} conductance increases the speed of the response of the cell. If a larger dendritic delay is needed in an octopus cell model, the conductance of the K^+_{LT} channels should be decreased.

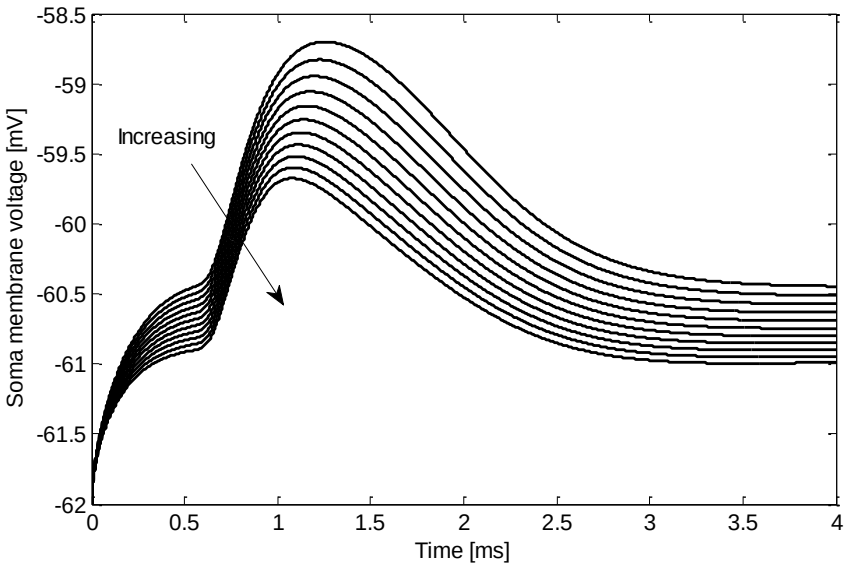

Figure 4.11. The membrane voltage at the soma for synaptic input at the most distal dendrite compartment with different values of the maximum K^+_{LT} conductance in the dendrites. The conductance was increased from 0 mS/cm^2 to 10 mS/cm^2 in steps of 1 mS/cm^2.

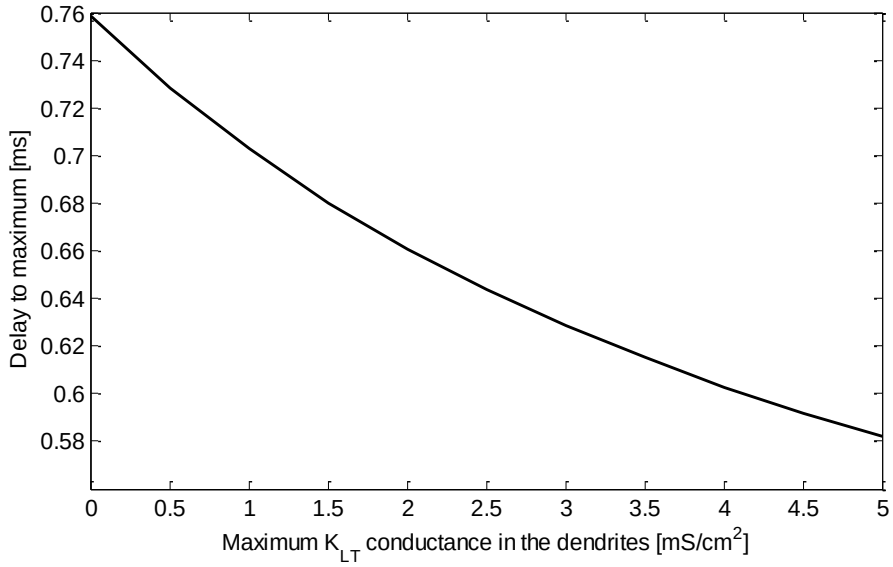

Figure 4.12. Delay to the maximum voltage in the soma for a distal synaptic input on one dendrite of the octopus cell for different values of the maximum K^+_{LT} conductance in the dendrites**.**

Soma

The soma membrane voltage for a synaptic input on the most distal dendrite compartment on a single dendrite is shown in Figure 4.13 for a changing maximum K^+_{LT} conductance in the soma. As the conductance is increased the resting potential of the soma decreases, which leads to a decrease in the maximum voltage in the soma for synaptic input. The rate of depolarisation threshold increases above the measured values when the K^+_{LT} conductance is too large, as shown in Table 4.1.

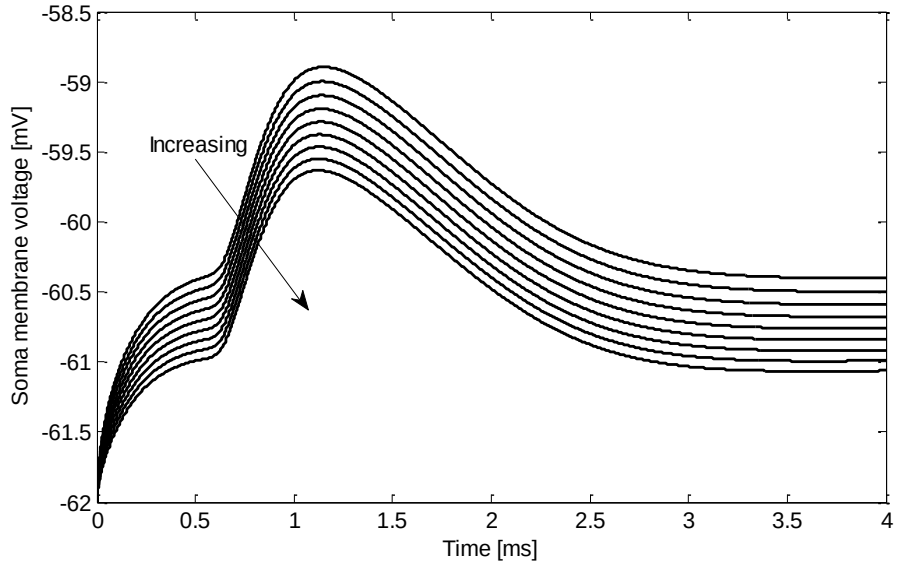

Figure 4.13. The membrane voltage at the soma for synaptic input at the most distal dendrite compartment with different values of the maximum K^+_{LT} conductance in the dendrites. The maximum K^+_{LT} conductance was changed from 0 mS/cm^2 to 80 mS/cm^2 in steps of 10 mS/cm^2. The arrow indicates an increase in the maximum soma K^+_{LT} conductance.

Blocking the K^+_{LT} channels with a channel blocker increased the membrane resistance threefold in some measurements (Bal and Baydas, 2009) while blocking K^+_{LT} in other measurements (Golding *et al.*, 1995) did not cause a measurable change in the input resistance. However the model membrane resistance was not as sensitive to blocking the K^+_{LT} channels since the blocking of these channels increased the membrane resistance by around 10%. The longer duration of the AP when K^+_{LT} is blocked was the same as in the measurements.

4.3.2.4 Simulation 4. Maximum I_h conductance

Dendrites

The soma membrane voltage for a distal synaptic input on a single dendrite with different values of the maximum I_h conductance in the dendrites is shown in Figure 4.14. The resting potential increases as the I_h conductance increases, leading to a higher voltage in the soma after the synapse. It has been measured that the resting potential decreases as the I_h channels are blocked, therefore the change in the model corresponds to measurements. As the I_h conductance is increased, the time to the maximum voltage in the soma decreases as the PSP rises faster. I_h channels are therefore also partially responsible for the speed of octopus cells. The I_h channels also contribute to the low membrane resistance of the octopus cell according to measurements (Cai *et al.*, 2000), while the membrane resistance decreases with increasing I_h conductance in the model as well.

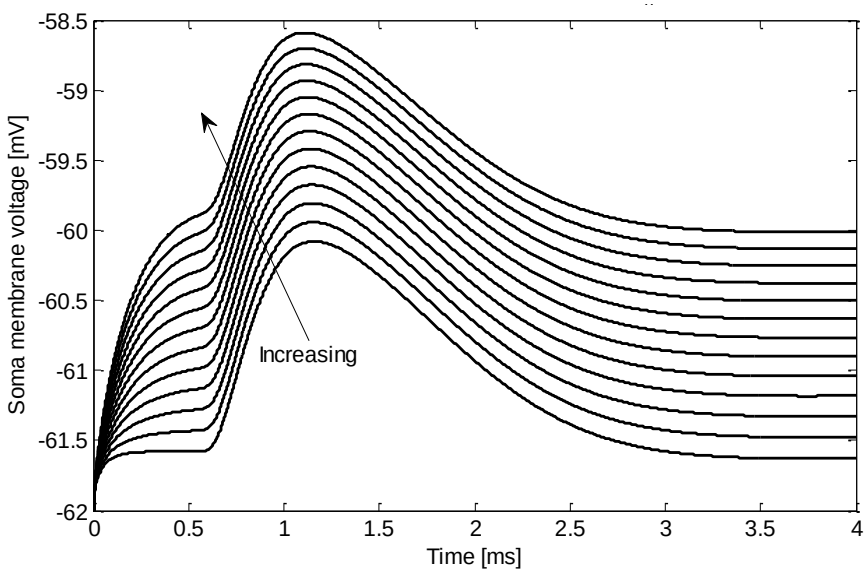

Figure 4.14. The membrane voltage at the soma for synaptic input at the most distal dendrite compartment with different values of the maximum I_h conductance in the dendrites. The maximum I_h conductance was changed from 0 mS/cm^2 to 1.2 mS/cm^2 in steps of 0.1 mS/cm^2. The arrow indicates an increase in the maximum I_h channel conductance.

Soma

The soma membrane voltage after a distal synaptic input for different values of the maximum I_h conductance in the soma is shown in Figure 4.15. Apart from the higher resting potential, changing the I_h conductance does not change the voltage in the octopus cell soma.

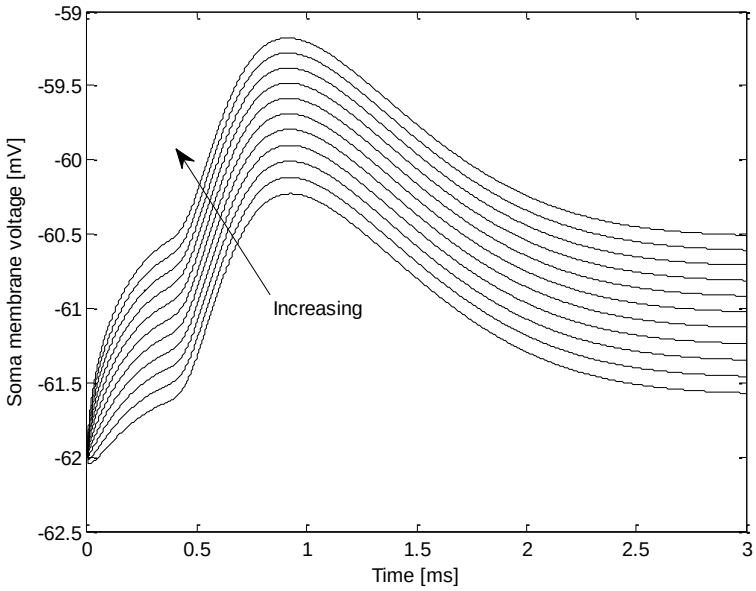

Figure 4.15. The membrane voltage at the soma for synaptic input at the most distal dendrite compartment with different values of the maximum I_h conductance in the soma. The maximum I_h conductance was changed from 1 mS/cm^2 to 11 mS/cm^2 in steps of 1 mS/cm^2. The arrow indicates an increase in the maximum I_h conductance.

Blocking the I_h channels has been shown to increase the membrane resistance tenfold (Bal and Baydas, 2009). Blocking the I_h channels in the model did increase the membrane resistance, but only by 3.87% when the dendrite channels were blocked and 6.37% with blocking of the soma channels. Blocking the channels also made APs slower, larger in amplitude and broader in measurements, which was the same in the model. Again the changes effected by blocking the channels in the model were not as large as in the measurements.

4.3.2.5 Simulation 5. Maximum Na^+ conductance in the axon initial segment

Changing the Na^+ conductance in the axon initial segment had no effect on the soma voltage for a distal synaptic input. For a maximum conductance smaller than 2000 mS/cm^2 no AP could be generated, therefore the Na^+ channels are crucial to the generation of APs.

The shape of the AP is greatly influenced by changes in Na^+ conductance as shown in Table 4.1. This shows that the Na^+ channels are mostly responsible for the generation of APs and their shape. Because the Na^+ is found in the axon initial segment, it does not have an effect on the dendritic delay of the octopus cell.

Of all the ion channels implemented in the model a change in the Na^+ channel conductance had the largest influence on the AP response of the model. Changing the Na^+ channel conductance had a larger effect on the rate of depolarisation threshold than changing the K^+_{LT} or the I_h channel conductances, while these channels are said to be responsible for the rate threshold. The model of the Na^+ channels used in an octopus cell model can therefore have a large effect on the response of the model and should be selected carefully. It was stated in Spencer *et al.* (2012) that the model results may depend on the particular model of sodium channel that was used, which seems to be the case after this investigation.

4.3.2.6 Summary of simulations 1-5

The results are summarised in Table 4.1. The axial resistance, membrane capacitance and the maximum channel conductances were all changed to half and double the original values of the model to investigate the effect of increasing and decreasing these parameters.

The results in the table are plotted for all the ion channel conductances in Figure 4.16. Increasing conductances of all the channels leads to a decrease in the membrane resistance, as would be expected. The K^+_{LT} channel conductance in the soma has the largest effect on the membrane resistance in the soma. The transmembrane current that needs to be injected in the soma to generate an AP increases for some conductances while it decreases for others.

Therefore the membrane resistance, which is decreased by increases in all the conductances, is not the only influence on the current that is needed for an AP. Changes in the Na^+ channel conductance has the largest effect on the current threshold. The conductance of the Na^+ channels is the only conductance that has a real effect on the amplitude of the AP. The AP duration is influenced mostly by the K^+_{LT} channel conductances and it decreases when the conductance is increased. This again shows that the K^+_{LT} channels are responsible for the speed of the response of octopus cells. The K^+_{LT} conductance in the dendrites has the largest influence on the latency of the AP. This, as well as the influence of the Na^+ and I_h channels, is however not linear and there is no clear relationship between any conductance and the latency. Unlike what was expected from literature, the K^+_{LT} and I_h channels did not have the largest influence on the rate of depolarisation threshold, but the Na^+ channel conductance had the largest influence. The dendritic delay decreases mostly with an increase in any ion channel conductance, which might be because of a decrease in the membrane resistance, which also decreases the time constant of the membrane. The K^+_{LT} channels in the dendrites have the largest effect on the dendritic delay by increasing the delay most when the channels are blocked.

For continued stimulation by a transmembrane current, the octopus cell had an onset response, which was the same as measurements (Bal and Baydas, 2009; Golding *et al.*, 1999). However when either or both the I_h channel or the K^+_{LT} channel conductance were set to zero, there was still an onset response and the cell did not discharge repetitively. In measurements the onset response was found to be caused by the presence of K^+_{LT} and I_h channels (Bal and Baydas, 2009; Cai *et al.*, 2000), since octopus cells fire repetitively when these channels are blocked. In this model however it may be more dependent on the Na^+ channel model that was used. In the article by Spencer *et al.* (2012) from which the model was adapted, it was stated that the behaviour of the model may be dependent on the Na^+ channel model.

Table 4.1. Results of changing the parameters. The measured values are from literature, as shown in Table 2.2. The original values are from the model with the parameters in Table 3.2. The values in brackets in the first column are the values used in the original model. AIS = Axon initial segment.

		Membrane resistance soma (kΩ)	Resting potential (mV)	Current for AP (nA)	Voltage threshold (mV)	AP peak (mV)	AP amplitude (mV)	AP duration (ms)	Latency (ms)	Depolarisation rate threshold (mV/ms)	Dendritic delay (ms)
Measured		3200 - 24000	-59 - -62	-	-	-	26 – 56.3	0.32 – 0.5	0.54 – 1.14	9.5 ± 3.6	-
Original		601.81	-60.72	40	-39.09	-12.81	47.91	0.46	0.19	12.07	0.38
R_i (0.3)	0.15	401.14	-61.08	69	-34.75	-20.16	40.92	0.44	0.20	18.30	0.23
	0.2	466.70	-61.01	54	-37.43	-18.59	42.42	0.48	0.23	14.72	0.29
	0.6	899.18	-60.41	24	-42.43	-12.63	47.78	0.52	0.25	9.12	0.57
Cm (0.9)	0.45	588.15	-60.65	31	-39.00	-6.70	53.95	0.37	0.18	11.87	0.18
	1.8	627.09	-61.01	55	-38.86	-19.67	41.34	0.62	0.22	13.14	0.73
K^+_{LT} dendrite (2.7)	0	618.89	-60.48	39	-39.44	-13.11	47.37	0.49	0.21	11.86	0.50
	1.35	590.56	-60.56	39	-39.75	-16.11	44.45	0.54	0.28	12.31	0.43
	5.4	576.91	-60.95	40	-39.70	-16.90	44.05	0.53	0.28	12.73	0.32
Ih dendrite (0.6)	0	625.09	-61.58	42	-38.86	-12.49	49.09	0.47	0.19	12.05	0.41
	0.3	610.40	-61.15	41	-38.95	-12.60	48.55	0.46	0.19	12.14	0.39
	1.2	574.50	-59.71	38	-39.47	-13.55	46.16	0.46	0.21	12.64	0.36
K^+_{LT} soma (40.7)	0	706.27	-60.44	38	-39.43	-11.58	48.86	0.52	0.21	10.18	0.39
	20.35	643.80	-60.57	39	-39.28	-12.22	48.35	0.50	0.20	11.25	0.39
	81.4	530.99	-61.00	42	-38.74	-13.97	47.03	0.42	0.19	14.38	0.38
Ih soma (7.6)	0	640.14	-61.59	41	-39.05	-12.00	49.59	0.47	0.19	12.05	0.39
	3.8	616.42	-61.15	40	-39.55	-13.42	47.73	0.49	0.22	11.91	0.39
	15.2	559.00	-59.94	39	-39.21	-13.82	46.12	0.45	0.20	12.85	0.37
K^+_{HT} soma (6.1)	0	592.86	-60.72	40	-39.09	-12.79	47.93	0.46	0.19	12.32	0.38
	3.05	598.32	-60.72	40	-39.09	-12.80	47.92	0.46	0.20	12.33	0.38
	12.2	600.77	-60.73	40	-39.09	-12.81	47.92	0.46	0.20	12.39	0.38
Na+ AIS (4244.1)	2122.05	601.36	-60.73	48	-34.49	-30.88	29.85	0.48	0.22	26.21	0.38
	8488.2	602.50	-60.72	34	-42.42	-1.15	59.57	0.47	0.20	7.53	0.38

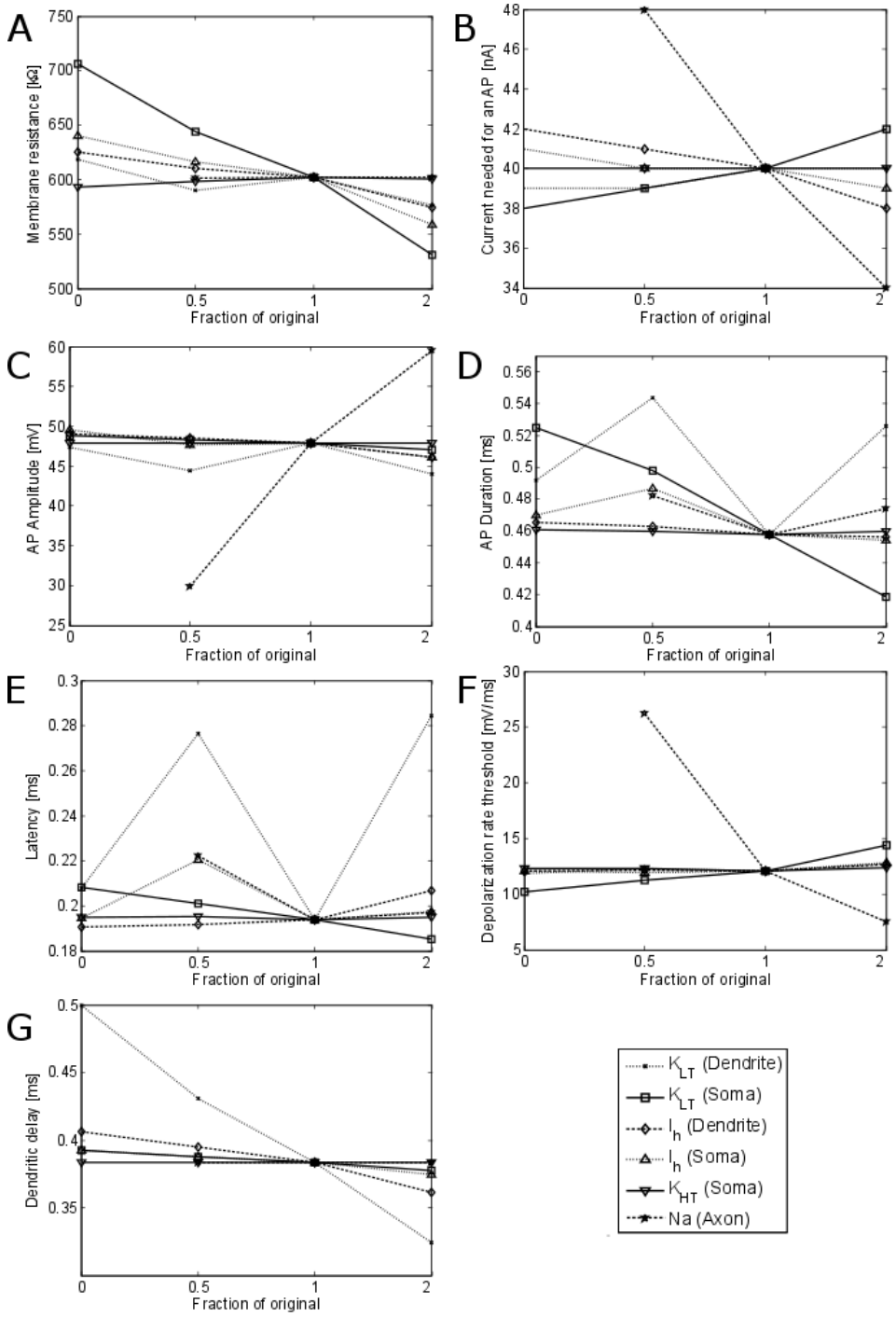

Figure 4.16. Sensitivity of octopus cell model response to changes in the ion channel conductances. It was simulated for all the conductances at 0, 0.5, 1 and 2 of the original model to test the effects of these changes. A. Membrane resistance in the soma. B. Transmembrane current needed in the soma to generate an AP. C. AP amplitude measured in the soma. D. AP duration measured in the soma. E. Latency of the AP measured in the soma. F. Rate of depolarisation threshold for a ramped transmembrane current in the soma. G. Dendritic delay measured between the peaks of the PSPs in the soma from the most distal and proximal dendrite compartments of a single dendrite.

4.4 DISCUSSION

The octopus cell model implemented here had a response in the range of measured values except for the membrane resistance, which was much lower than the measured values. In some measurements (Bal and Baydas, 2009) an AP was generated with much less injected current than that which was needed in the model. The higher current needed in the model is a result of the lower membrane resistance, since more current is needed to reach the voltage threshold when the resistance is lower. However, the aim of the model was not to predict an octopus cell's response to transmembrane electrical stimulation, but rather to stimulate via synapses where the model response was the same as measured data. The model can therefore be used to predict octopus cell responses to synaptic stimulation from ANF inputs.

The lower voltage at the soma for a synaptic input when the axial resistance or the membrane capacitance is increased will cause the octopus cell to need more coincident inputs to reach threshold. The rate of rise of each PSP also decreases, which may cause the cell never to reach the rate of depolarisation threshold. This threshold is larger when the membrane capacitance is increased, which may lead to the cell never reaching threshold. A C_m of around 1 µF/cm^2 is therefore suggested as a good value to use in an octopus cell model.

In previous studies it was determined that the axial resistance and membrane capacitance do not influence the maximum rate of depolarisation, or the dendritic delay/optimal sweep duration (Mcginley *et al.*, 2012), but the present investigation shows that the axial resistance has a large effect on the dendritic delay. It is proposed in McGinley et al. (2012) that animals with lower frequency hearing and therefore longer travelling wave delays might have octopus cells with higher input resistances to compensate for the longer delay. Therefore a larger axial resistance should influence the dendritic delay if it has an influence on the input resistance of the cell. For changing the dendritic delay of an octopus cell model the axial resistance of a model is suggested to be implemented between the values of 100 Ω·cm and 500 Ω·cm. Below 100 Ω·cm the model becomes unstable when it is solved with the Euler method used here and above 500 Ω·cm the resistance is so large that distal PSPs never reach the soma.

The calculated values for the axial resistance and membrane capacitance of 33 Ω·cm and 28000 µF/cm^2 from Wesselink *et al.* (1999) for myelinated sensory nerve fibres, could not be used with the solver used for the current model, but should be considered if the model is solved with a more stable solver. The much smaller axial resistance may result in a lower membrane resistance and a faster response, while the capacitance, which is much larger than

what was implemented, may result in a much slower response. The effect of using these values should be investigated in future research. The measurements from Wesselink *et al.* (1999) is for myelinated axons, while the implementation in the octopus cell model is for unmyelinated dendrites. This should be considered, especially for the capacitance which will be much larger for the myelinated fibre.

The K^+_{LT} channels in the dendrites are partly responsible for the speed of the response of octopus cells. When the K^+_{LT} conductance is increased the dendritic delay of the octopus cell decreases. This happens without a large change in the membrane resistance, which may slow down the response of the octopus cell. Therefore to achieve a faster response, the K^+_{LT} conductance can be increased. In the range over which the K^+_{LT} conductance was changed, there was no limit where the cell's behaviour changed from what was expected. The model is therefore robust against changes in the maximum K^+_{LT} conductance.

The I_h channels are also responsible for the speed of the octopus cell response and an increase in the I_h channel conductance in the dendrites decreases the dendritic delay. Therefore the I_h channel conductance can be increased for a faster response. The model response did not change to a great extent over the range were the I_h channel conductance was changed. The model is therefore also robust against changes in the maximum I_h channel conductance.

The Na^+ channels are primarily responsible for the generation of APs in the model, which is the same as measurements suggesting that APs are mediated by Na^+ (Bal and Baydas, 2009). When the maximum Na^+ channel conductance was decreased below 2 000 mS/cm^2, no AP could be generated by the octopus cell. Therefore the maximum conductance should be above this value. When the maximum Na^+ conductance was increased to 10 000 mS/cm^2, the AP amplitude became quite large and the duration was at the upper limit of measured values. Too high Na^+ conductance will therefore slow down the response of the octopus cell and generate APs with amplitudes and durations outside measurements. The maximum Na^+ conductance in the model is therefore suggested to remain in the range 2 000 mS/cm^2 to 10 000 mS/cm^2 for a valid response.

Changing the Na^+ channel conductance has the largest influence on the rate of depolarisation threshold of the octopus cell of all the channels. Therefore in this model the Na^+ channels are mostly responsible for the sensitivity to the rate of depolarisation, and not the K^+_{LT} and I_h channels as shown by measurements. Using another Na^+ channel model in an octopus cell model can have a large influence on the response of the model.

4.5 CONCLUSION

The compartmental Hodgkin-Huxley octopus cell model that was implemented in Matlab can accurately predict octopus cell behaviour in response to synaptic inputs from the AN. The model can therefore be used to study the behaviour of octopus cells in response to AN stimulation in the cochlea, either acoustically or electrically.

The axial resistance and the membrane capacitance in the model has a great influence on the membrane resistance and also the dendritic delay of the model.

The K^+_{LT} and I_h channels are responsible for the speed of the response of octopus cells. The model behaviour is highly dependent on the Na^+ channel model and less on the other channel models.

CHAPTER 5 DENDRITIC DELAY AND REDUCTION IN JITTER

5.1 INTRODUCTION

The travelling wave on the BM takes a finite time to propagate from the cochlear base to the apex. This causes a difference in the activation times of the apical neurons compared to the basal neurons. The travelling wave delay in ms to the position of a certain CF f_c can be approximated with the simple equation

$$d(f_c) = \frac{1000}{f_c} + k \quad , \tag{5.1}$$

where k is a delay constant of 0.2 ms (Greenberg, 1997). The travelling wave delay across the length of the human cochlea has been measured and calculated theoretically to be up to 10 ms (Goldstein *et al.*, 1971; Ruggero and Rich, 1987).

From manipulation of equation (5.1) the differential travelling wave delay between two points in the cochlea can be calculated with

$$t_{delay} = \frac{1000}{f_1} - \frac{1000}{f_2} \quad , \tag{5.2}$$

where f_1 is the higher frequency and f_2 the lower frequency of the range over which the delay is calculated. The frequencies can be calculated from position x in mm from the base of the cochlea by using the equation

$$f_c = s_0 \times 10^{-\gamma x} - apex\ correction\ constant \tag{5.3}$$
$$f_c = 20682 \times 10^{-60x} - 140.59 \quad ,$$

where f_c is the CF, s_0 is the upper limit frequency, modified from Greenwood (1990) to fit human data (Duifhuis, 2012) and γ is the stiffness decay constant (Duifhuis, 2012).

Because of the capacitance in the cell membrane, the PSPs from synaptic inputs on the dendrites of octopus cells take time to reach the soma. This time delay is longer for distal synapses than proximal synapses. The PSPs from many inputs on several dendrites are superimposed on the soma to generate an AP when the voltage reaches threshold. The

tonotopic arrangement of ANFs is preserved in the octopus cell area with the octopus cells' dendrites stretching across the ANFs in a way in which high-frequency ANFs from the cochlear base will terminate distally on the octopus cell dendrites and low-frequency ANFs from the apex will terminate proximally. This anatomical arrangement suggests that the dendritic delay of the octopus cells may compensate for the travelling wave delay in the ANF firing (Golding *et al.*, 1999; Mcginley *et al.*, 2012; Oertel, 1997). A computational model of an octopus cell showed that soma-directed sweeps of excitation with durations matching measurements result in the largest and sharpest PSPs in the soma, suggesting that the octopus cell compensated optimally for the travelling wave delay under these conditions (Mcginley *et al.*, 2012). Another model was also most sensitive to the input when the inputs were arranged such that the model's dendritic delay was the same as the theoretical travelling wave delay of the input (Spencer *et al.*, 2012).

Octopus cells have also been classified as coincidence detectors in literature, since they need the summation of many nearly coincident inputs to reach threshold (Oertel *et al.*, 2000; Mcginley and Oertel, 2006; Rhode and Smith, 1986). With this mechanism octopus cells convey with precision the average timing of firing of the ANFs that terminate on the cell (Golding *et al.*, 1995). In the study by Golding *et al.* (1995) the ANFs remaining in slices of the CN containing octopus cells were stimulated by an electrode. All the ANFs were stimulated at the same time and there was no travelling wave delay or sweep of excitation on the octopus cells, yet the octopus cells reached threshold and responded to the stimuli. This indicates that octopus cells might not be as sensitive to the sweep direction and delay as predicted by the models of Mcginley *et al.* (2012) and Spencer *et al.* (2012) and it appears less likely that their function is to compensate for the travelling wave delay and more likely that they act as coincident detectors to convey the average timing of many inputs precisely. The precise timing by the averaging of many scattered inputs will lead to a reduction in the noise or jitter in the temporal information contained in the spike timing (Bal and Baydas, 2009; Rhode and Smith, 1986). Using this mechanism octopus cells may potentially detect common ISIs in the ANF firing.

The range of ANFs from which octopus cells receive input is unclear from literature, since there are no measurements available that show from where the octopus cells receive input. Table 5.1 provides a summary of the available information found in literature regarding the range of input to octopus cells.

Table 5.1. Ranges of ANFs terminating on octopus cells suggested in literature and used in previous octopus cell models.

Model	**Range of ANF input used or range suggested to be optimal**	**ANFs tonotopically arranged on dendrites?**
Spencer *et al.* (2012)	ANFs with CFs higher than 2 kHz seemed optimal owing to a more realistic octopus cell response.	Yes
Mcginley *et al.* (2012)	Suggested range of 1/5 and 2/3 of the tonotopic array, with octopus cells receiving lower frequency inputs spanning smaller ranges.	Yes
Levy and Kipke (1997)	Suggested ANFs with intermediate to high CFs. Used ANFs with CFs ranging from 1.4 kHz to 4 kHz.	Unknown
Cai *et al.* (2000)	Used ANFs with CFs between 880 Hz and 2970 Hz.	No
Cai *et al.* (2001)	Used ANFs with CFs between 1050 Hz and 3250 Hz.	No

In this chapter two hypotheses of the function of octopus cells were tested with the model that was developed, i.e. the ability of octopus cells to compensate for the travelling wave delay and their ability to reduce jitter.

A possible optimal range of input to the individual cells in an octopus cell population was also investigated. The assumption was that the range where the population reduced jitter as well as compensated for the travelling wave delay would be optimal.

5.2 METHOD

To test the response of the octopus cell model to sweeps of synaptic inputs, the synapse times were manually generated and used as inputs to the octopus cell model. To simulate the response of the octopus cell model to acoustic stimulation, the inputs to the octopus cell

model were obtained from simulations with a travelling wave model of the auditory periphery with acoustic stimulation as input as described in Section 3.2.2.

Standard deviation in the spike times of the octopus cell population was used as a measure of the jitter in the discharge times of the octopus cell population. The jitter was calculated as the average of the standard deviations of the spike times for each octopus cell in the population at each period of the stimulus, for a periodic stimulus. This was termed *local jitter* because it is calculated locally at each discharge time and each cell for many simulations, and is given mathematically as

$$Jitter_{Local} = \frac{\sum_{n=1}^{cell}\sum_{m=1}^{periods}\sigma_{sim}\left(t_{spike}(n,m)\right)}{cell \times periods \times sim} \quad , \tag{5.4}$$

where $\sigma_{sim}\left(t_{spike}(n,m)\right)$ is the standard deviation of the spike times at cell n and period m for sim number of simulation repetitions. For the population of nine octopus cells, $cell = 9$. For a pure tone or periodic stimulation

$$periods = \frac{t_{sim}}{1/f_{stim}} \quad , \tag{5.5}$$

where t_{sim} is the duration of the simulation and f_{stim} the stimulation frequency.

A second measure of the jitter was termed the *total jitter*, which was the average of the standard deviation of the spike times of the whole population over all the periods of the stimulus. This can be written mathematically as

$$Jitter_{total} = \frac{\sum_{m=1}^{periods}\sigma_{sim}\left(t_{spike}(m)\right)}{periods \times sim} \quad , \tag{5.6}$$

where $\sigma_{sim}\left(t_{spike}(m)\right)$ is the standard deviation of the spike times of all the octopus cells at period m.

5.2.1 Simulation 1. Linear sweep of synaptic inputs

The synapses on a single dendrite were activated with a linear sweep of inputs with different delays and sweep directions. Not all the synapses on the dendrite were activated to prevent the octopus cell from reaching threshold and generating an AP. For each input sweep the membrane voltage as a result of the summed PSPs in the soma was measured to determine

the effect of the sweep direction and delay on the soma voltage. Sweep direction refers to a sweep of inputs from the distal tips of the dendrites toward the soma, which had a positive sweep delay, and a sweep from the soma toward the tips of the dendrites, which was implemented as a negative sweep delay.

5.2.2 Simulation 2. Different ranges of input to a single octopus cell

The same frequency ranges were used as input to the octopus cell model as those used in Spencer *et al.* (2012) to compare those results with the results from this model and also to determine the effect it has when the range of input to a single octopus cell from the cochlea is changed. The frequency ranges, the positions along the BM calculated with equation (5.3) and the theoretical differential travelling wave delay over this range calculated with equation (5.1) are given in Table 5.2.

For each simulation 80 ANFs spaced linearly in position between the two points given in the table were used as inputs to the octopus cell model. The synapses were arranged in the manner described in Section 3.2.2 and shown in Figure 3.9.

The ANF activity was simulated for acoustic pure tone stimulation at different frequencies. The octopus cell responses for each frequency were classified as “Entrain” where the octopus cell output entrained to the input frequency, “Onset” where the octopus cell had an onset response and “No AP” where the octopus cell did not generate an AP for the time of stimulation.

5.2.3 Simulation 3. Different ranges of input to a population of octopus cells

The population of octopus cells as described in Section 3.2.3 was implemented and the jitter at the output of the population was evaluated for pure tone acoustic stimulation. This was done to determine whether the range of the BM from which each octopus cell in a population receives input has an effect on the jitter at the output of the octopus cell population. The average delay between the octopus cells receiving input from the most basal and apical ANFs (octopus cells number 1 and 9) was also calculated. This was done to determine at which range the octopus cell population compensates best for the travelling wave delay by reducing the delay between high and low frequency neurons. Both a reduction in jitter and compensation for the travelling wave delay were used to determine a possible optimal range of the ANF that terminates on octopus cells.

Table 5.2. Frequency ranges over which activity from ANFs were used as input to the octopus cell model for simulation of acoustic stimulation. *The direction of the nerve inputs were reversed, i.e. low frequency neurons terminated distally and high frequency neurons terminated proximally. **The nerve termination was randomised, i.e. there was no relationship between the position of the neuron in the cochlea and the position of its termination on the octopus cell.

	Frequency range (kHz)	**ANF positions along the BM (mm)**	**Travelling wave delay (ms)**
i	2.5 - 5	10.08 – 14.9	0.2
ii	0.25 - 1	20.97 – 28.73	5
iii	0.645 – 0.8	22.37 – 23.76	0.3
iv	1-10	5.16 – 20.97	1.1
v	3 – 3.3	12.98 – 13.64	0.03
vi	2.5 – 5 *	10.08 – 14.9	-0.2
vii	2.5 – 5 **	10.08 – 14.9	--
viii	5.75 – 11	4.48 – 9.09	0.083

The population of nine octopus cells was arranged so that each octopus cell in the population received input from $\frac{1}{1}, \frac{1}{2}, \frac{1}{3}, \ldots, \frac{1}{9}$ of the cochlea which resulted in nine different populations. The octopus cells were arranged to be spaced linearly from the base to the apex as shown in Figure 3.10. The populations were named Population 1…Population 9, where for Population N, each octopus cell received input from 1/N of the BM. For each population the number of ANFs from the cochlea and their termination on the different cells were implemented in such a manner that no two octopus cells received input from the same ANF while each octopus cell received input from 80 ANFs. All the simulations were done for a 500 Hz acoustic pure tone input and repeated five times for each population. The ANF discharge times were obtained from simulations of the travelling wave and AN model, which provided input to the octopus cells as described in Section 3.2.2.

The ranges of input as positions along the BM to each octopus cell in each population are given in Table 5.3. A graphical representation of the ranges on the BM for the nine populations is given in Figure 5.1. The BM in the travelling wave model had a length of 35 mm, which was divided among the octopus cells so each cell received input from 35/N mm for population N. Eighty ANFs were arranged linearly between the two points

given in the table, terminating on the octopus cells with the high frequency ANF distally and lower frequency ANFs close to the soma, as shown in Figure 3.9.

At the output of each population the discharge times were extracted as the peaks of the APs, with an AP being classified as a peak voltage higher than -30 mV in the soma. The total jitter and local jitter from equations (5.4) and (5.6) of the spike times were calculated for each population.

5.2.4 Simulation 4. Travelling wave delay vs jitter

The jitter in the spike times of the ANFs from the travelling wave and neural model was calculated and compared to the theoretical travelling wave delay from equation (5.1). The jitter was calculated at a few selected ANFs from the model for 50 simulations for a 200 Hz pure tone stimulus to determine how the discharge times of each of these fibres varied compared to the travelling wave delay at the positions of these fibres. If the jitter was smaller than the travelling wave delay up to that point, the octopus cells could potentially make use of the travelling wave delay. However, if the variation in the discharge times was larger than the travelling wave delay, the octopus cells would probably have difficulty compensating for the travelling wave delay because of the variation in the discharge times of the neurons.

The simulations were done for 80 ANFs spaced linearly between the positions of 2.5 kHz and 5 kHz. This is the same range as for cell (i) determined to be optimal in Spencer *et al.* (2012) because the differential travelling wave delay between those frequencies is the same as the dendritic delay of the octopus cell model.

Table 5.3. Positions on the BM of the ANFs terminating on each octopus cell for the different populations. Octopus cell 1 received input from the most basal ANFs and octopus cell 9 received input from the most apical ANFs. Each octopus cell received input from 80 ANFs arranged linearly between the positions given in the table. OC = Octopus cell.

	Positions on BM of the ANFs terminating on each octopus cell (OC)								
	OC 1	**OC 2**	**OC 3**	**OC 4**	**OC 5**	**OC 6**	**OC 7**	**OC 8**	**OC 9**
Population									
1	0-35	0-35	0-35	0-35	0-35	0-35	0-35	0-35	0-35
2	0-17.5	2.19-19.69	4.38-21.88	6.56-24.06	8.75-26.25	10.94-28.44	13.13-30.63	15.31-32.81	17.5-35
3	0-11.67	2.91-14.58	5.83-17.5	8.73-20.4	11.67-23.33	14.58-26.25	17.5-29.17	20.4-32.07	23.33-35
4	0-8.75	3.28-12.03	6.56-15.31	9.84-18.59	13.13-21.88	16.41-25.16	19.69-28.44	22.97-31.72	26.25-35
5	0-7	3.5-10.5	7-14	10.5-17.5	14-21	17.5-24.5	21-28	24.5-31.5	31.5-35
6	0-5.83	3.65-9.5	7.29-13.14	10.94-16.79	14.58-20.43	18.23-24.08	21.88-27.73	25.52-31.37	26.17-35.02
7	0-5	3.75-8.75	7.5-12.5	11.25-16.25	15-20	18.75-23.75	22.5-27.5	26.25-31.25	30-35
8	0-4.38	3.83-8.21	7.66-12.04	11.49-15.87	15.32-19.7	19.15-23.53	22.98-27.36	26.81-31.19	30.64-35
9	0-3.88	3.88-7.78	7.78-11.67	11.67-15.55	15.55-19.44	19.44-23.33	23.33-27.22	27.22-31.11	31.11-35

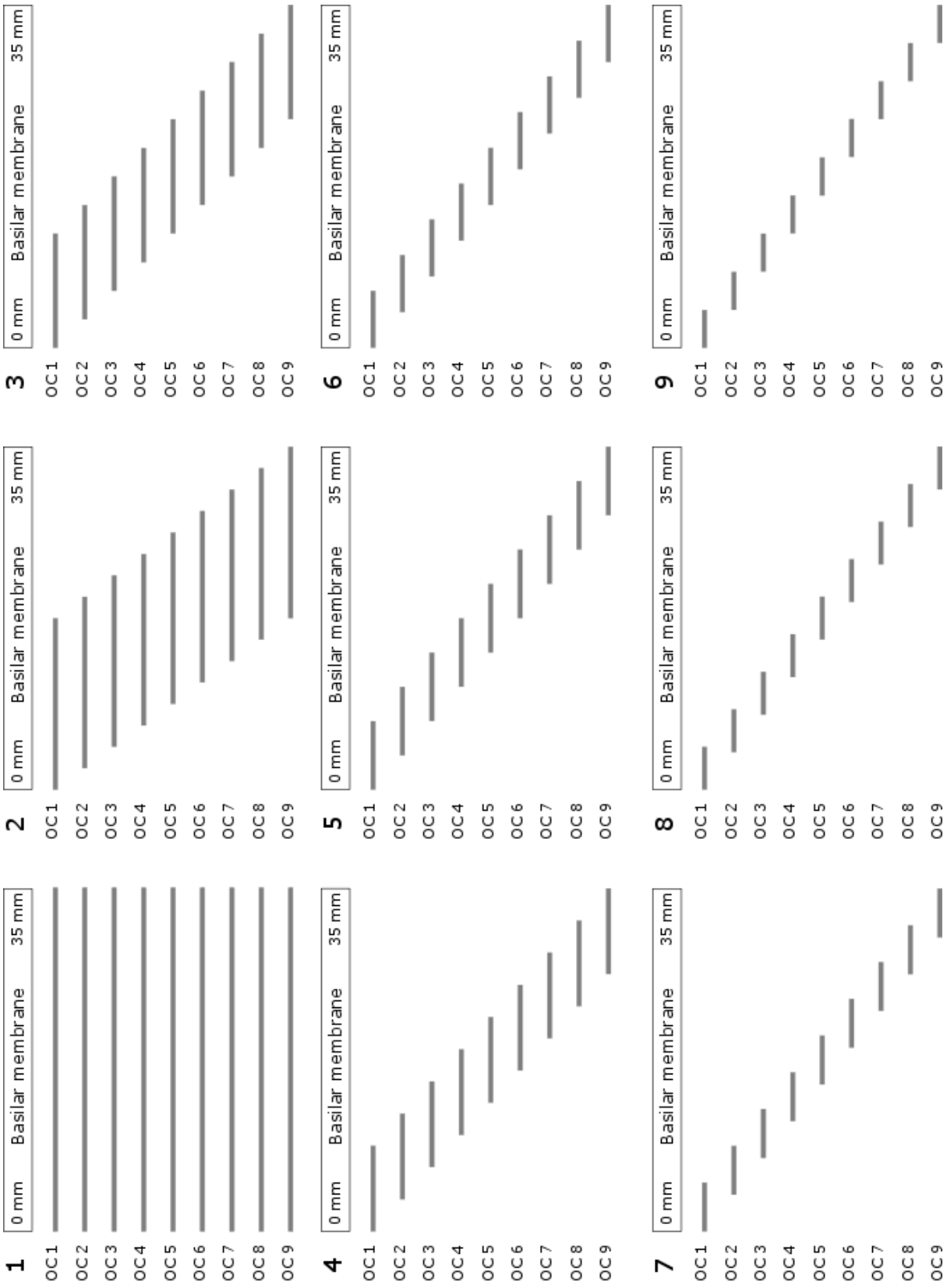

Figure 5.1. Ranges of the octopus cells in the nine populations. Each line represents the range of ANFs on the BM from the BM that terminates on each octopus cell. The population numbers are indicated in the top left corner of each figure.

5.3 RESULTS

5.3.1 Simulation 1. Linear sweep of synaptic inputs

The membrane voltage in the soma was measured for different dendritic input sweep delays. The resulting soma membrane voltages for different sweep delays are shown in Figure 5.2A. Negative sweep times as shown in the figure occured when the direction of the sweep was reversed, i.e. away from the soma toward the distal dendrite compartments. As the delay increased, the resultant PSP in the soma became broader as the individual PSPs from all the inputs were summed over a longer time. The soma membrane voltage reached a maximum when the input sweep duration was the same as the dendritic delay of the octopus cell, which was 0.38 ms as shown in Figure 5.2B. When the sweep delay is the same as the dendritic delay of the octopus cell, the peaks of the PSPs are summed optimally in the soma, producing a maximum summed PSP in the soma.

The maximum voltage in the soma decreased as the sweep time was changed from the optimal value, which is the same as the dendritic delay. However, the decrease was not so large that the octopus cell would never reach threshold and therefore it would still produce APs even when the input delay was not optimal. Even when the direction was reversed, the maximum voltage in the soma did not decrease to the extent that the octopus cell would not generate an AP when enough inputs were received. Octopus cells are therefore sensitive to the input sweep direction and delay but they will function over a wide range of sweep delays. For sweep delays up to 1 ms on either side of the dendritic delay, the octopus cell still reached threshold and was therefore broadly tuned to the input delay.

The dendritic delay of the octopus cell model used in the simulations is only 0.38 ms, which is really short compared to the travelling wave delay of the whole cochlea, which is up to 10 ms. If octopus cells receive input from a third of the cochlea, the delay between the inputs on their dendrites would be around 3 ms, which is much larger than 0.38 ms. The dendritic delay of the present octopus cell model could not be increased beyond 1.19 ms. To increase the delay beyond this point, the membrane resistance had to be made so large that the octopus cell would not reach threshold because of the small PSPs in the soma. The 1.19 ms dendritic delay was for the following conditions:

- C_m = 2 µF/cm^2
- G_{KLT} (dendrite) = 0.1 mS/cm^2
- G_{Ih} (dendrite) = 0.1 mS/cm^2

- G_{Ih} (soma) = 0.1 mS/cm^2
- R_i = 500 Ω·cm
- All the other parameters as in Table 3.2.

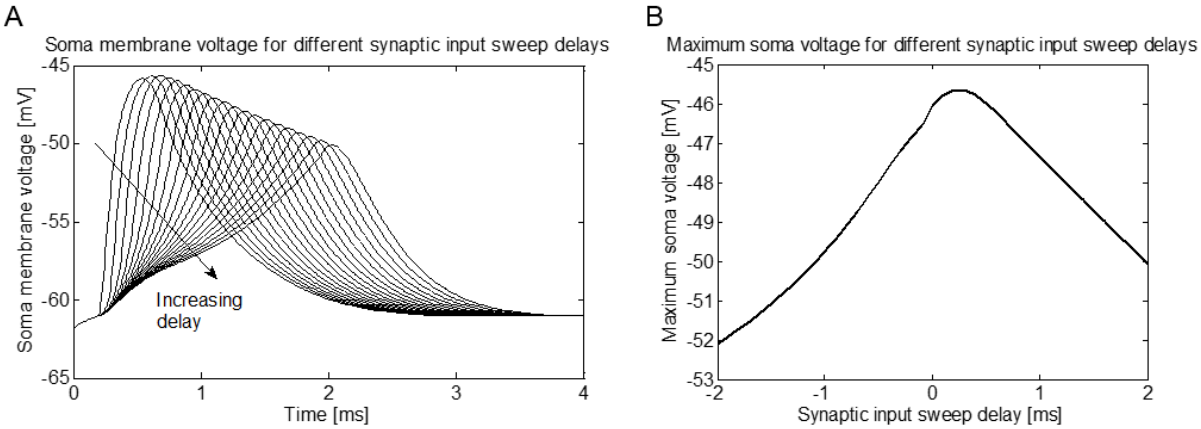

Figure 5.2. Membrane voltage in the soma for different input sweep delays. A. Soma membrane voltage for dendritic inputs with different positive delays, i.e. towards the soma. B. Maximum soma membrane voltage for different dendritic input sweep delays. A negative delay is for a sweep away from the soma while a positive delay is towards the soma. The membrane voltage in the soma reaches a maximum when the input sweep delay is the same as the dendritic delay of the octopus cell.

However at this point the PSP amplitudes in the soma decreased by an average of 1 mV each relative to the voltages at a 0.38 ms delay and more coincident inputs would be needed for the cell to reach threshold. The maximum dendritic delay of 1.19 ms in the model is still much smaller than this theoretical 3 ms that will be needed to compensate for the travelling wave delay. Therefore a model with a larger dendritic delay is needed to test whether octopus cells are sensitive to large travelling wave delays.

5.3.2 Simulation 2. Different ranges of input to a single octopus cell

The responses of the octopus cell receiving input from the ranges in Table 5.2 for different pure tone stimulation frequencies are summarised in Figure 5.3. For all the ranges except (iv) the octopus cell entrained at low frequencies up to around 500 Hz after which it had an onset response. At high frequencies the octopus cell did not generate an AP. Entrainment at low frequencies and an onset response at higher frequencies are characteristic of the response of octopus cells (Bal and Baydas, 2009; Rhode and Smith, 1986). All the ANF ranges therefore produced the desired output for an octopus cell regardless of the range in the cochlea from where the ANFs originated.

In the cases where the octopus cell response was different from what would be expected, it could not be explained by the travelling wave delay. For example, (v) had an onset response from a low frequency but the theoretical differential travelling wave delay was the same as the dendritic delay of the octopus cell model.

Range (iv) received input from a very broad frequency range which spans almost half of the BM length. Therefore it is possible that it is more optimal for octopus cells to receive input from a smaller range than what was used in (iv).

Reversing the direction of the ANF termination on the octopus cell dendrites to produce a reversed travelling wave delay and even randomising the input did not have a large effect on the response of the octopus cell. Therefore octopus cells are not as sensitive to the travelling wave delay and direction on the input sweep as was suggested by previous research (Spencer *et al.*, 2012).

From these simulations no optimal range of octopus cell input from the cochlea could be determined and octopus cells may receive input from ANFs anywhere in the ranges that were tested.

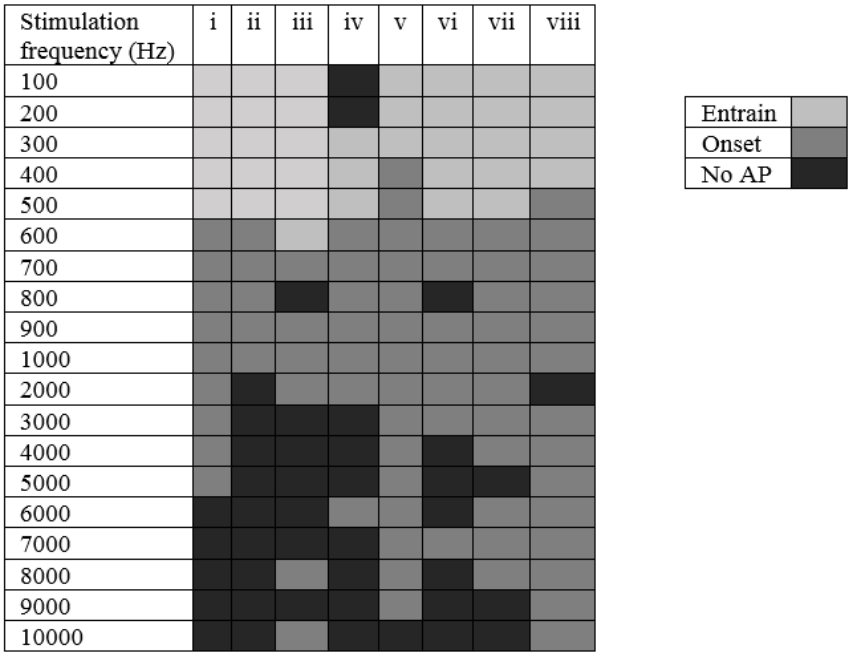

Figure 5.3. Responses of the octopus cell to different pure tone acoustic stimulation frequencies. "Entrain" is when the octopus cell discharges at the period of the input signal, "Onset" is when it generates an onset-response, that is, discharge only at the onset of the stimulation and not again and "No AP" is when no AP is generated by the octopus cell in the 50 ms simulation time. The numbers (i) to (viii) refer to the numbers in Table 5.2.

5.3.3 Simulation 3. Different ranges of input to a population of octopus cells

The discharge times for all the octopus cells in each population for ten simulations of 20 ms for 500 Hz acoustic pure tone stimulation are shown in Figure 5.4. The post-stimulus time histograms (PSTHs) for the same simulations are shown in Figure 5.5 and the corresponding ISI histograms in Figure 5.6.

Octopus cells entrain to low frequency stimuli and therefore it was expected that the octopus cells in the populations would entrain to the 500 Hz stimulus used in these simulations. The ranges of those populations of which the octopus cells entrained to the stimulus were therefore assumed to be more likely ranges of input to octopus cells.

Octopus cell 1 received input from the ANFs from the base of the cochlea with high CFs and octopus cell 9 received input from the ANFs from the apex with low CFs. The cells were arranged linearly to span the whole cochlea from the base to the apex.

The discharge times of Figure 5.4 show that the octopus cells in Populations 1 and 2 mostly have onset responses while the octopus cells in the rest of the populations entrain to the stimulus. The same is shown in the PSTHs in Figure 5.5, where Population 1 only has one peak and Population 2 has a very small second peak. The interspike interval histograms (ISIHs) in Figure 5.6 show that Populations 3 – 9 discharge with ISIs that are the same as the pure tone period.

The deviation around the peaks of the PSTHs in Figure 5.5 increase from Population 1 to Population 9. This indicates more jitter in the response of the octopus cell populations as the cells in the population receives input from smaller ranges of the BM.

Population 1 had an onset response and never entrained to the stimulation frequency. Because it was expected that the octopus cells would entrain to the stimulus, this result suggests that each single octopus cell does not receive input from the whole cochlea, but rather a part of the cochlea. In Population 2 most of the octopus cells also had an onset response, which suggests that octopus cells are unlikely to receive input from ANFs from half of the cochlea.

The responses of the octopus cell populations were not visibly different from Population 4 to Population 9, which suggests that octopus cells may receive input from 1/4 to 1/9 of the cochlea and still respond in the same manner as shown with experimental measurements for 500 Hz stimulation. In Population 3 fewer of the octopus cells in the population entrained to the stimulus but there was still some entrainment and octopus cells may receive input from

1/3 of the cochlea as suggested in literature, although the range may be somewhat smaller and 1/3 may be true only for octopus cells receiving input from basal ANFs.

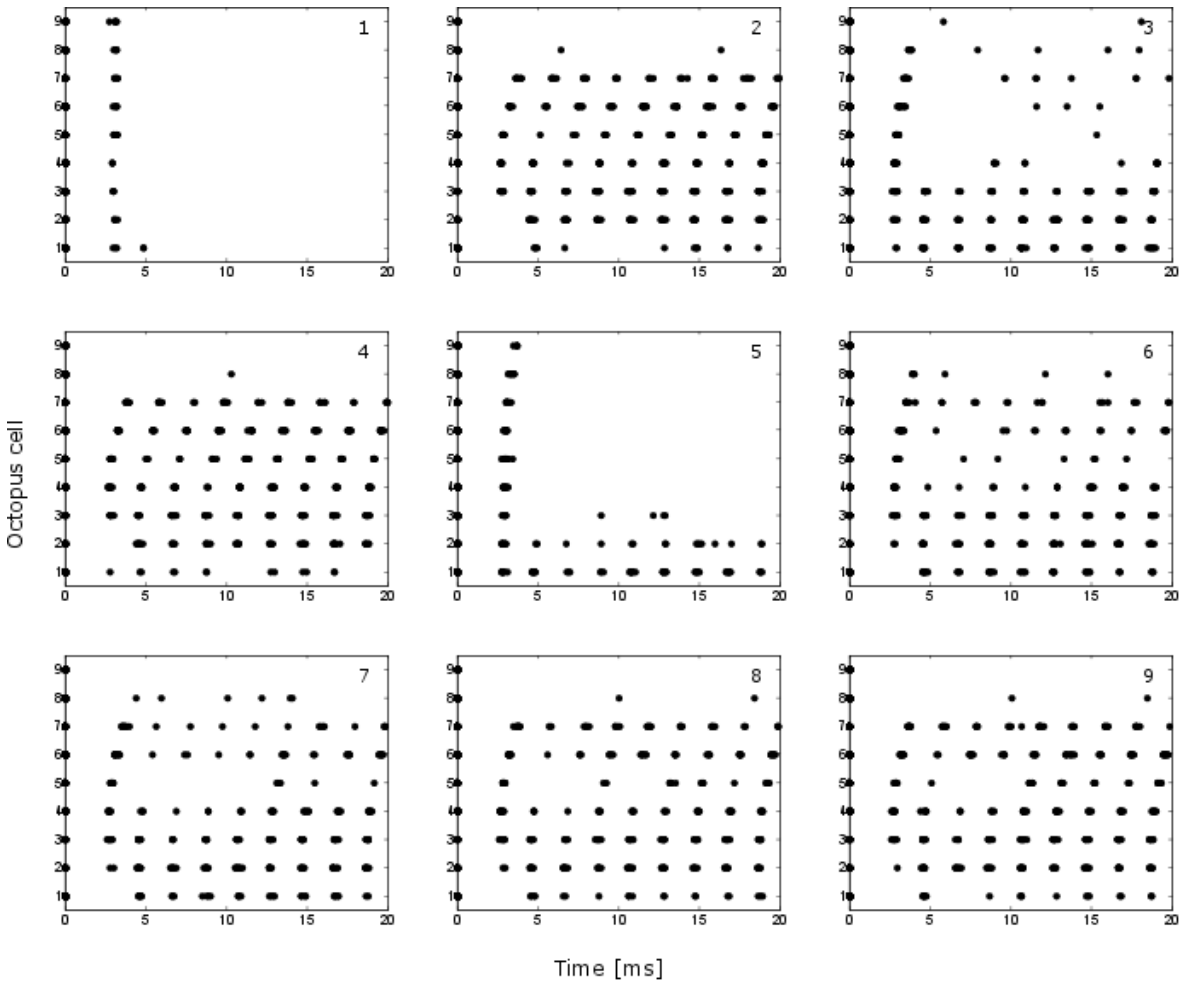

Figure 5.4. Discharge times of the nine octopus cells in the nine populations for a 500 Hz pure tone acoustic stimulus. Octopus cell number 1 receives input from the most basal ANFs while octopus cell number 9 receives input from the most apical ANFs. The population numbers are indicated in the top right corners of the graphs.

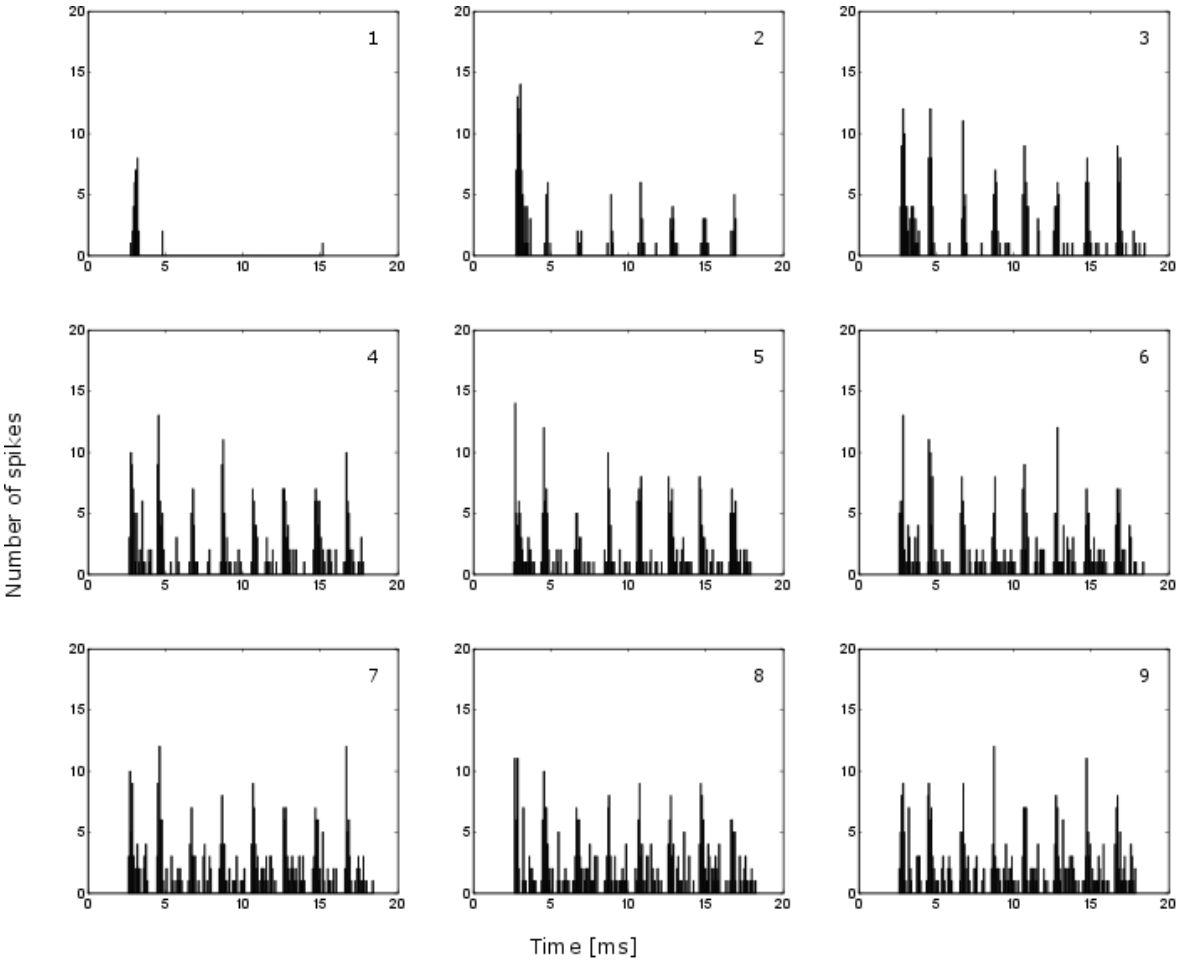

Figure 5.5. Post-stimulus time histograms of all the populations of nine octopus cells for a 500 Hz acoustic pure tone stimulus. The population numbers are indicated in the top right corners.

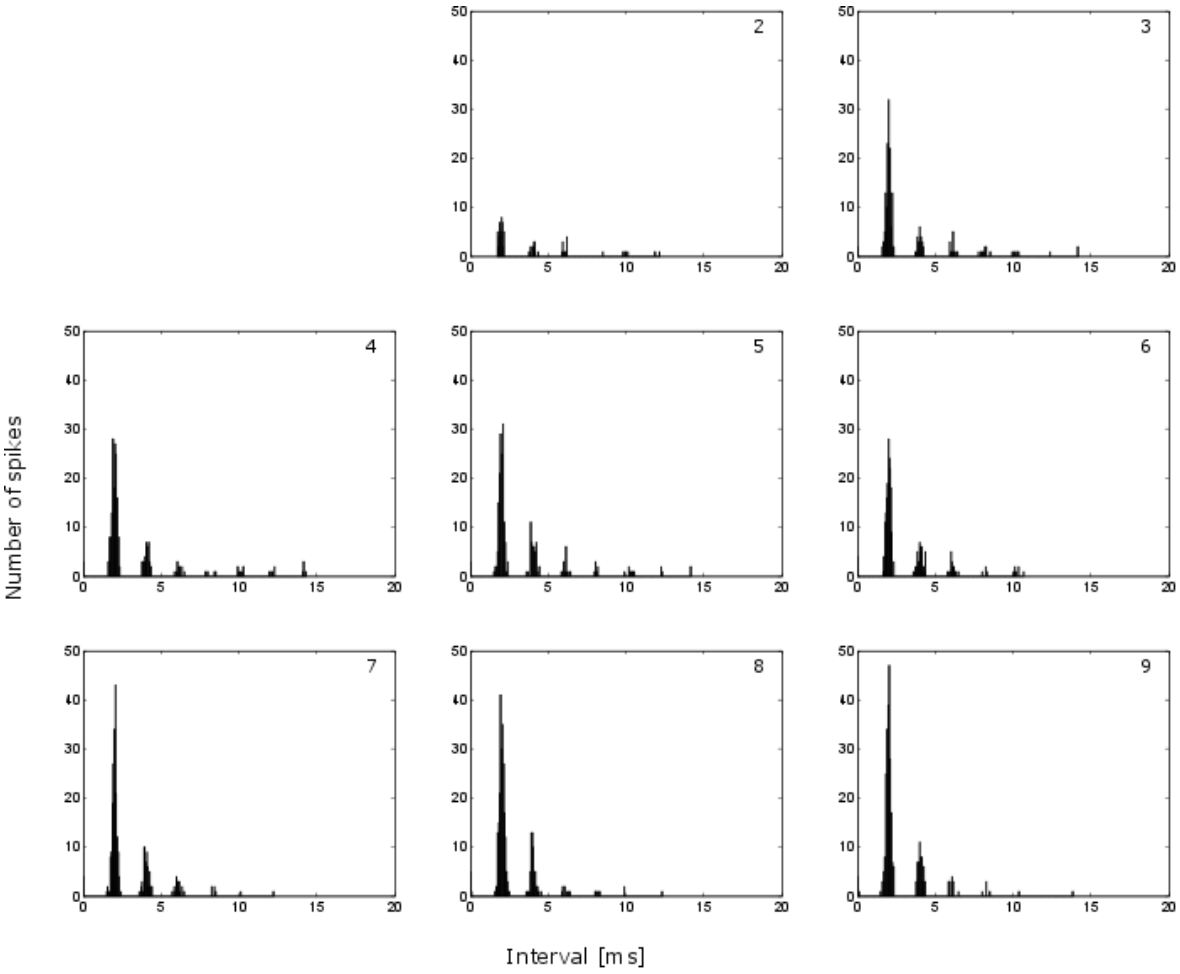

Figure 5.6. ISI histograms for the nine populations of octopus cells for a 500 Hz acoustic pure tone stimulus. Population 1 had an onset response with no ISIs and was therefore not included in the figure.

The total number of spikes generated by each octopus cell in each population is shown in Figure 5.7. The octopus cells receiving input from the ANFs from the apex, especially 8 and 9, do not discharge regularly for all the populations. Octopus cells 1-3, which receive input from the basal ANFs, generated most APs. This suggests that octopus cells do not receive input from low-frequency ANFs from the apex, but rather from high CF ANFs from the base. When the range of input to an octopus cell is small, like as populations 8 and 9, the most basal octopus cells also did not respond to the stimulus, which shows that octopus cells might not receive input from very high-frequency ANFs either, except when they receive wide input as in populations 2 and 3. Octopus cells 2-4 had a relative entrainment higher than 50% for populations 3-9. The range of these cells in all these populations is 2.91 – 20.4 mm, which corresponds to CFs of 13695 – 1094 Hz, which may therefore be the most likely range of ANFs for octopus cells to receive input from.

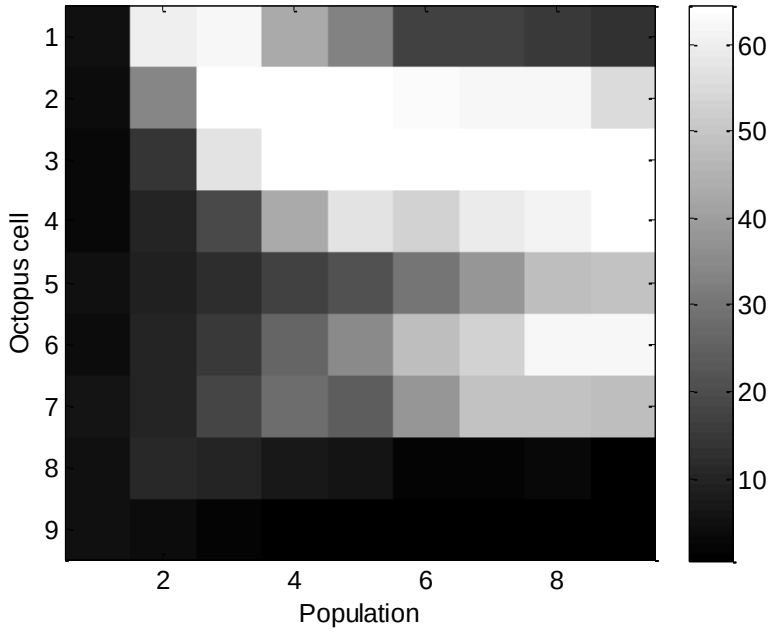

Figure 5.7. Total number of spikes on the nine octopus cells in the nine populations for ten simulations of a pure tone acoustic input of 500 Hz. Octopus cell 1 receives input from the most basal ANFs while octopus cell 9 receives input from the most apical ANFs. The total number of spikes is also an indication of the relative entrainment of the cells, since more spikes in the interval will mean that the cell entrained more to generate more APs.

The total jitter and the local jitter of all the populations are shown in Figure 5.8. The total jitter increased as the range of input to each octopus cell became smaller (Population 1 to Population 9). Therefore to reduce the jitter in the response of the whole population, the octopus cells should receive input from a wider range. The total jitter in Population 1 is the lowest because of its precise onset response and should not be counted as having the lowest jitter. The local jitter does not change significantly between the populations. The jitter on the response of a single octopus cell is therefore relatively independent from the range of ANFs from which the octopus cell receives input, while the jitter of the whole population is dependent on this range.

Because of the summation of many coincident inputs, octopus cells convey the average timing of the spike times of the many ANFs providing input to the octopus cell. Because of the travelling wave delay the apical ANF spike times are later than those of the basal ANFs. As can be seen in Figure 5.4, there is still some delay between the discharge times of the octopus cells receiving input from the apical ANFs and the cells receiving input from basal ANFs. The average delays between the discharge times of octopus cells 8 and 1 are shown in Figure 5.9. Here it is clear that the delay increases as octopus cells receive input from a

smaller range of ANFs. If the function of octopus cells is therefore to compensate for the travelling wave delay by discharging at the average time of many ANFs, they should receive input from a wider range of ANFs from the cochlea. Therefore, in order to compensate for the travelling wave delay by removing the delay between neural firing times, Population 3 is the optimal population from those that were evaluated. Population 3 receives input from a third of the cochlea, which is the same range as suggested by Mcginley *et al.* (2012).

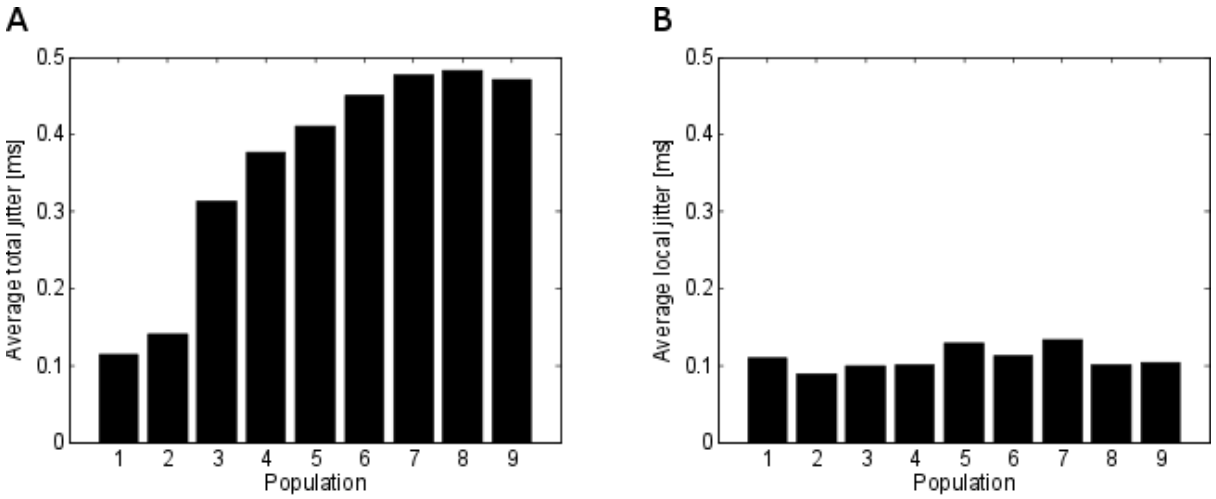

Figure 5.8. Two measures of jitter of the output of the octopus cell populations. A. Average total jitter for the nine populations. B. Average local jitter for the nine populations. The total jitter increases from Population 1 to Population 9 as the range of the cochlea from which the octopus cells receive input decreases. There is no trend in the local jitter and it stays in the same range for all the populations.

5.3.4 Simulation 4. Travelling wave delay vs jitter

The discharge times of 80 ANFs arranged between the positions of 5 kHz and 2.5 kHz for an acoustic pure tone stimulation of 200 Hz are shown in Figure 5.10. This result was generated by simulation of the travelling wave model for acoustic stimulation. From inspection of the spike times there is no clear delay between the times of the basal ANFs and the apical ANFs. The jitter on the AP times is larger than the delay, which causes the apical neurons to discharge randomly earlier or later than the basal neurons.

The jitter on some ANFs was calculated in terms of the standard deviation of the AP times for a 200 Hz stimulus over 50 ms. This was calculated from the averages of 50 runs of the travelling wave and ANF model. The average jitter calculated on the discharge times was 0.37 ms, which is larger than the calculated differential travelling wave delay of 0.22 ms over the range and almost the same as the dendritic delay of the octopus cell. With this large

variation in discharge times it would be difficult for an octopus cell to compensate for the travelling wave delay.

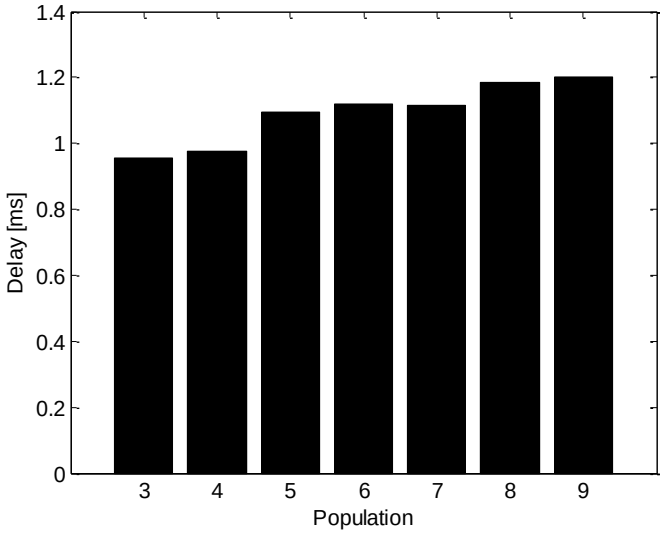

Figure 5.9. Average delay between the discharge times of octopus cell 1 and octopus cell 8 in the nine octopus cell populations for stimulation with a 500 Hz acoustic pure tone. Octopus cell 1 receives input from the most basal ANFs and octopus cell 9 from the most apical ANFs. Population 1 was not included in the figure because the octopus cells had an onset response and there were not enough discharge times from which to calculate an average delay. Population 2 was not included because only octopus cells 1 and 2 responded and a delay to octopus cell 8 could not be calculated. The average delay increased from population 3 to population 9**.**

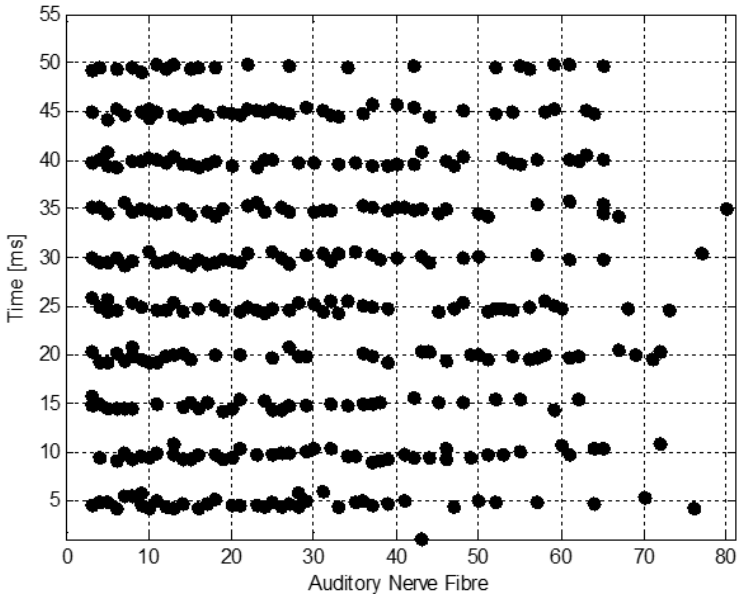

Figure 5.10. ANF firing times for a 200 Hz pure tone stimulus. The firing times were measured on 80 ANFs arranged linearly between the positions of 2.5 and 5 kHz, with fibre number 1 closest to the base at 5 kHz and fibre number 80 at 2.5 kHz.

The average delays and their standard deviations between the AP times at different positions and the position of the fifth ANF at 10.38 mm are shown in Figure 5.11 from simulations of the travelling wave model. The figure also shows the theoretical differential travelling wave delay calculated with equation (5.2). The average delays from the travelling wave model were larger than the calculated delays. The variation on the simulated delays was really large with an average standard deviation of 0.122 ms. These large variations in delay suggest that octopus cells may not be sufficiently sensitive to the delay to be able to function under the jitter present in the ANF activity. Because of the jitter octopus cells might rarely receive a valid sweep of inputs from the distal ends of the dendrites toward the soma.

Because the jitter on the ANF discharge times used as input to the octopus cell was higher than the travelling wave delay, the function of octopus cells may be as coincidence detectors to reduce jitter in the neural code rather than to compensate for the travelling wave delay.

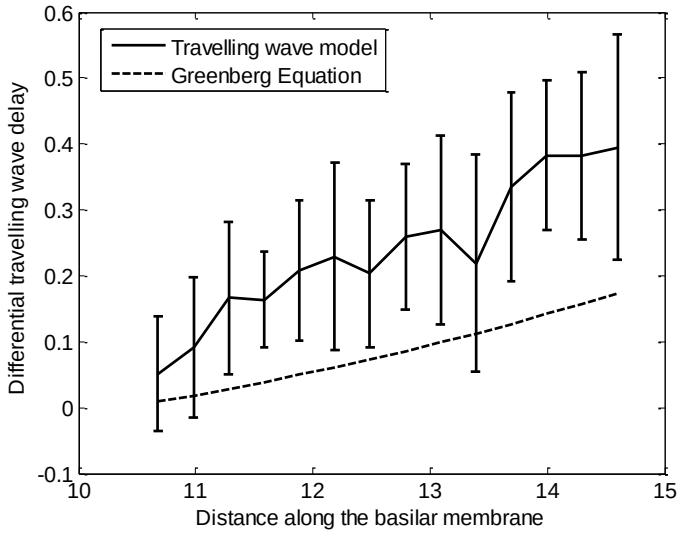

Figure 5.11. Average differential travelling wave delay to 10.38 mm from the other positions in the range measured from simulation of the travelling wave model compared to the theoretical values calculated with equation (5.2).

The jitter present in the ANF discharge times used in this simulation is from the noise implemented in the ANF model by Zilany *et al.* (2009). This was introduced as fractional Gaussian noise to generate the spontaneous rates of the ANFs. The spontaneous rates predicted from the model matched measured spontaneous rates in Liberman (1978) and the noise may therefore be assumed to be valid. The results of this section are still highly dependent on the noise from the ANF model and should be investigated for measured ANF data and with other models.

5.4 DISCUSSION

The octopus cell model is sensitive to the input delay and the sweep direction of synaptic inputs on its dendrites. The soma membrane voltage reaches a maximum when the delay of an input sweep in the direction of the soma is the same as the dendritic delay of the model. At this point the peaks of the individual PSPs from all the synapses are coincident and are summed most effectively to produce a maximum. The same behaviour with a peak in the soma voltage for a certain delay was observed in Mcginley *et al.* (2012). The travelling wave leads to a delay in the neural activity on the ANFs as it propagates from the base to the apex. Since an octopus cell receives inputs from neurons from different positions in the cochlea, with basal ANFs terminating most distal from the soma and apical ANFs most proximal, there will be a delay between the distal and proximal synapses of the octopus cell. The dendritic delay may compensate for this travelling wave delay by generating a maximum voltage in the soma when the dendritic delay matches the travelling wave delay.

When the sweep direction is reversed to be in the direction away from the soma toward the distal end of the dendrites, the voltage in the soma may still be high enough to reach threshold and the octopus cell may still generate an AP. Octopus cells are therefore sensitive to input sweep delay and direction, but can still function even when the sweep direction is reversed. This may imply that the many inputs on long dendrites are not only to compensate for the travelling wave delay, but there may be other functionality of the dendrites beyond the delay which may include reducing jitter.

As shown in Figure 5.3, the range of the cochlea from where the ANFs terminating on the octopus cell come does not have a large influence on the output behaviour of the octopus cell. The octopus cell model had the same type of response for the ranges that were tested. Even when the direction of input was reversed or randomised, the octopus cell model still yielded a valid response. Therefore, although the octopus cell is sensitive to the sweep direction, it still functions even when the sweep direction is reversed or when the inputs are randomised.

For the population of nine octopus cells the average total jitter for stimulation with a 500 Hz pure tone increased as the individual octopus cells received input from a smaller range of the cochlea. Therefore a larger range will ensure a larger reduction in jitter. However when the range becomes too large, as in populations 1 and 2, the octopus cells do not entrain to the low-frequency input. The delay between the discharge times of the octopus cells receiving input from the most basal and apical ANFs also increases as the individual octopus cells

receive input from a smaller range in the cochlea. The ability of the octopus cell population to compensate for the travelling wave delay therefore becomes poorer as the octopus cells receive input from a smaller range of the cochlea. Therefore the range of the cochlea from which the octopus cells receive input should again be large enough to remove the delay in the neural firing. Mcginley *et al.* (2012) suggested a range between 1/5 and 2/3 of the cochlea, which is in the same range found by these results. Because Population 3 was the population with the largest range that still produced the desired response (entrain at low frequency and produce onset response at high frequencies) this population was chosen for use in the rest of the investigations, which will be discussed in the next chapter.

It was assumed that there would be a delay between the distal and proximal inputs of the octopus cell and therefore the range of inputs to the model would influence the behaviour of the octopus cell. However, as can be seen in Figure 5.10, there is no clear delay between the neural spike times of the most basal and apical ANFs because of the noise present in the ANF discharge times. The average jitter of 0.38 ms on the ANF discharge times is more than the calculated differential travelling wave delay of 0.2 ms over the range of the cochlea that was investigated. Octopus cells therefore also have an important function in reducing jitter in neural firing (Bal and Baydas, 2009) and may be involved in more than compensating for the travelling wave delay.

Individual ANFs do not discharge exactly in phase with the input signal and in many cases they do not discharge on every cycle. However overall, across the population, the ANFs discharge on each cycle, known as the volley theory (Wever and Bray, 1930). The octopus cells seem to add these inputs from many individual ANFs over a range in the cochlea and extract the average period of the activity of the whole ANF population.

The ANF discharge times that were used to compare the travelling wave delay to the jitter was from a model that is only a representation of the real discharge times. Therefore measurements of ANF discharge times would provide a better measure of jitter and delay to be used in this comparison.

The dendritic delay of the octopus cell model could not be increased to the theoretical differential travelling wave delay of the inputs to octopus cells in humans. It is suggested that a model be developed of which the dendritic delay can be extended to test the effect of a longer dendritic delay on the response of an octopus cell model.

The range over which an octopus cell receives input from ANFs remains unknown and should be investigated to be able to determine the full functionality of octopus cells.

5.5 CONCLUSION

The octopus cell model is sensitive to the delay of synaptic inputs on its dendrites but seems to be only broadly tuned to this delay. The optimum delay where the voltage in the soma reaches a maximum is the same as the dendritic delay of the octopus cell model.

When the single octopus cell model received inputs from ANFs from different ranges of the BM, the response of the cell was not sensitive to the direction of the input or the differential travelling wave delay over the range.

Octopus cells may act as coincidence detectors to reduce jitter in addition to possibly compensating for the travelling wave delay to some extent.

Based on the ability of a population of nine octopus cells to reduce jitter and to remove delays in neural activity, it is suggested that the optimal range of input to octopus cells is around ⅓ – ¼ of the cochlea.

CHAPTER 6 RESPONSE TO ACOUSTIC AND ELECTRICAL STIMULATION OF THE AUDITORY NERVE

6.1 INTRODUCTION

In this chapter the response of the octopus cell population model was investigated for acoustic and electrical stimulation of the AN. The response to acoustic stimulation of the AN was simulated to investigate mainly the ability of octopus cells to extract rate pitch information in normal hearing. The response to electrical stimulation of the AN by a CI was also investigated to probe the differences between the response of octopus cells to acoustic and electrical stimulation. On the assumption that octopus cells play an important role in extraction of rate pitch information, this was especially to determine whether CIs generally encode temporal pitch in a way that can be extracted by octopus cells in the same way as in normal hearing. The ability of octopus cells to extract the pulse rate from single-electrode CI stimulation was also investigated. PRDLs were predicted from the ISIs of the octopus cell population response and compared to measured psychoacoustic data.

6.2 METHOD

The octopus cell population model as described in Section 3.2.3 was used for the simulations in this chapter. The individual octopus cells each received input from a third of the cochlea, as was proposed to be optimal in Section 5.3.3. For acoustic stimulation, the ANF discharge times from the travelling wave and neural model were used as input times to the synapses on the octopus cell. For CI stimulation, the discharge times of the ANF model connected to the CI model were used as input to the octopus cells. The models were connected as described in Section 3.2.2.

6.2.1 Simulation 1. Pure tone acoustic stimulation

The response of the octopus cell population to acoustic stimulation with pure tones of different frequencies was simulated.

6.2.2 Simulation 2. Acoustic stimulation with a vowel

An acoustic vowel from recorded speech was used as input to the travelling wave model. Speech was used because it is a complex signal of which the voice pitch changes over time. Speech is also the most important auditory signal for humans and understanding the processing thereof is therefore central in investigations of auditory processing.

The vowel /ɑː/ was from a recording made by Oosthuizen (2012) of the word “paat” by a female Afrikaans speaker. The vowel was recorded in an RE242 double-walled sound booth from Acoustic Systems. A Sennheiser ME62 microphone was connected to an M-Audio FastTrack PRO external sound card. A single channel was recorded and sampled at 44.1 kHz (Oosthuizen, 2012).

The ANF discharge times from the travelling wave model simulations were used as input to the octopus cell population model to simulate the response of octopus cells for acoustic speech stimulation. At the output of the octopus cell population model the maxima of the APs were measured as the discharge times of the octopus cell population, with an AP classified as a membrane voltage larger than -30 mV. The ISIs of the octopus cell population response were used to estimate of the pitch of the speech signal. The voice pitch extracted in this way from the ISIs was compared to the voice pitch extracted by the speech processing program Praat (Boersma and Weenink, 2016) using the same speech material as input.

6.2.3 Simulation 3. Cochlear implant stimulation for acoustic pure tone inputs

The same frequencies as used for the acoustic stimulation were used as input to the CI model to simulate the octopus cell response to CI stimulation at these pure tone frequencies.

6.2.4 Simulation 4. Single-electrode pulse rate

The pulse rate on electrode 15 in the CI model was varied and the ANF discharge times were simulated for this input. The octopus cell population response was simulated for the input from the ANFs stimulated with different single-electrode pulse rates. The relative entrainment of the active octopus cells in the population was calculated for the variation of the input pulse rate. The ISIs of the octopus cell population response was measured from the discharge times taken as the peak times of the APs. The standard deviation was calculated as a measure of the jitter in the ISIs. This was used to predict pulse rate difference limens, which were compared to measured data from literature.

6.3 RESULTS

6.3.1 Simulation 1. Pure tone acoustic stimulation

The discharge times of all the octopus cells in the population model for acoustic stimulation with pure tones of frequencies 200 – 700 Hz are shown in Figure 6.1. The frequencies of the pure tones are indicated above the blocks in the figure. Above around 500 Hz the octopus cells gradually lose synchronisation with the pure tone. At frequencies of 600 Hz and higher, only the octopus cells receiving input from basal ANFs show some entrainment to the stimulus, while the other octopus cells display an onset response.

The ISI histograms for the population of octopus cells for acoustic stimulation with pure tones of frequencies 200 – 700 Hz are shown in Figure 6.2. All the histograms were plotted to be on the same scale for easy comparison. For the 200 Hz input, the main peak of the ISIH is low because of the small number of 5 ms periods that fit into the 20 ms simulation time. At 300 Hz the main peak of the ISIH is much higher than the secondary peaks, indicating strong entrainment to the input. From 400 Hz to 600 Hz the secondary peaks increase relative to the primary peaks, showing that the octopus cells do not discharge on each stimulus cycle and do not fully entrain to the input as the frequency increases. At 700 Hz the ISIs are irregular and probably carry less information about the stimulus frequencies than lower frequencies. Octopus cells therefore seem to encode pure tone frequency, which is related to the pitch of a pure tone, in their ISIs.

The octopus cell population responses for stimulation of the AN with a 400 Hz pure tone acoustic signal are shown in Figure 6.3. In A the membrane voltage on each octopus cell is shown, showing the individual APs. B shows the times of the peaks of all the APs on the octopus cell population for 20 simulations. The PSTH and ISIH for the spike times over the 20 simulations of 20 ms are shown in C and D. The octopus cells entrain to the pure tone frequency. The mean ISI of the first peak on the ISIH is the same as the period of the pure tone, i.e. 2.5 ms in this case. The result in Figure 6.3 can be compared to Figure 6.8 and Figure 6.9 which were for CI stimulation and will be discussed later.

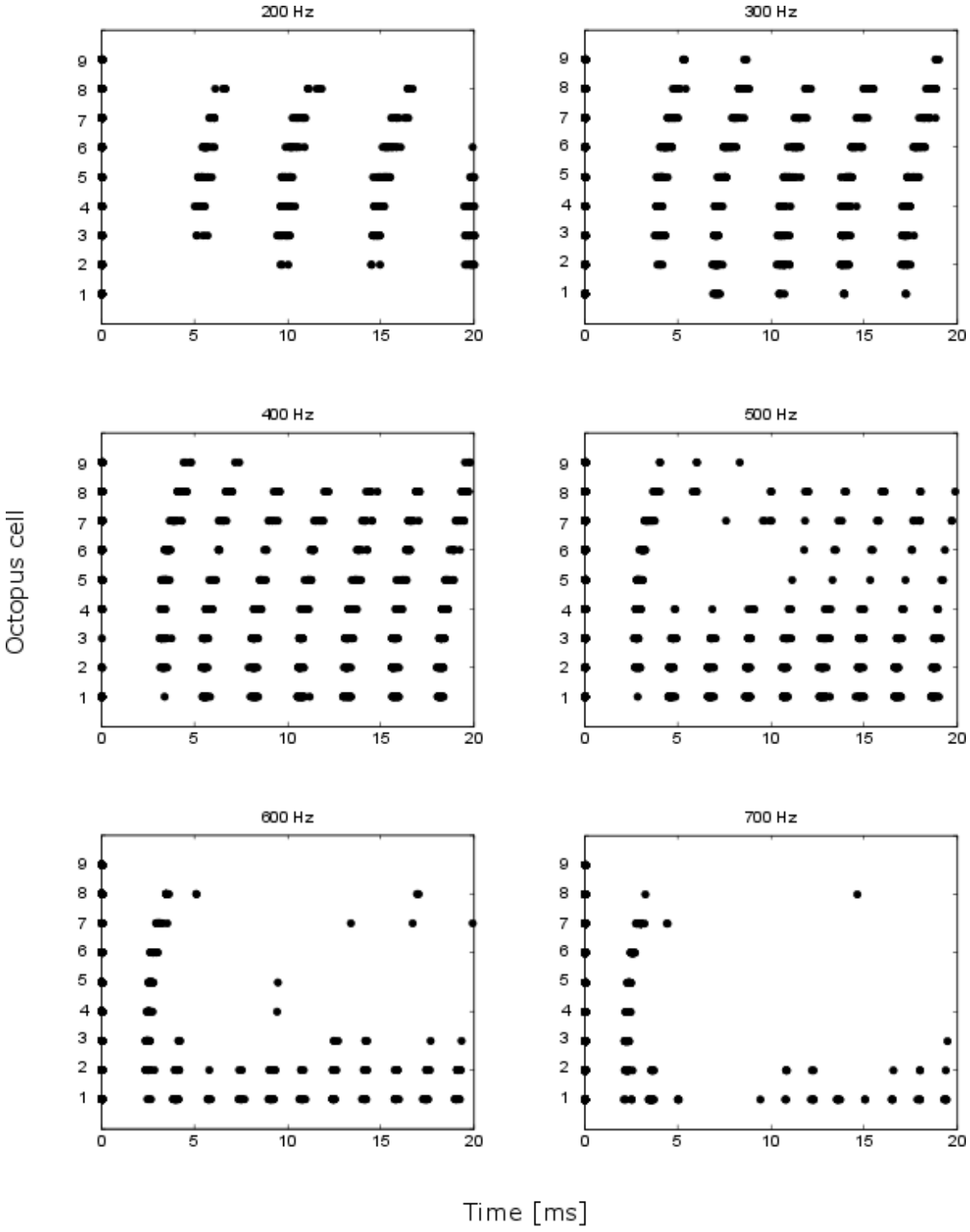

Figure 6.1. Discharge times of the population of octopus cells for acoustic pure tone stimulation at different frequencies. The results are shown for 20 simulations with a duration of 20 ms each.

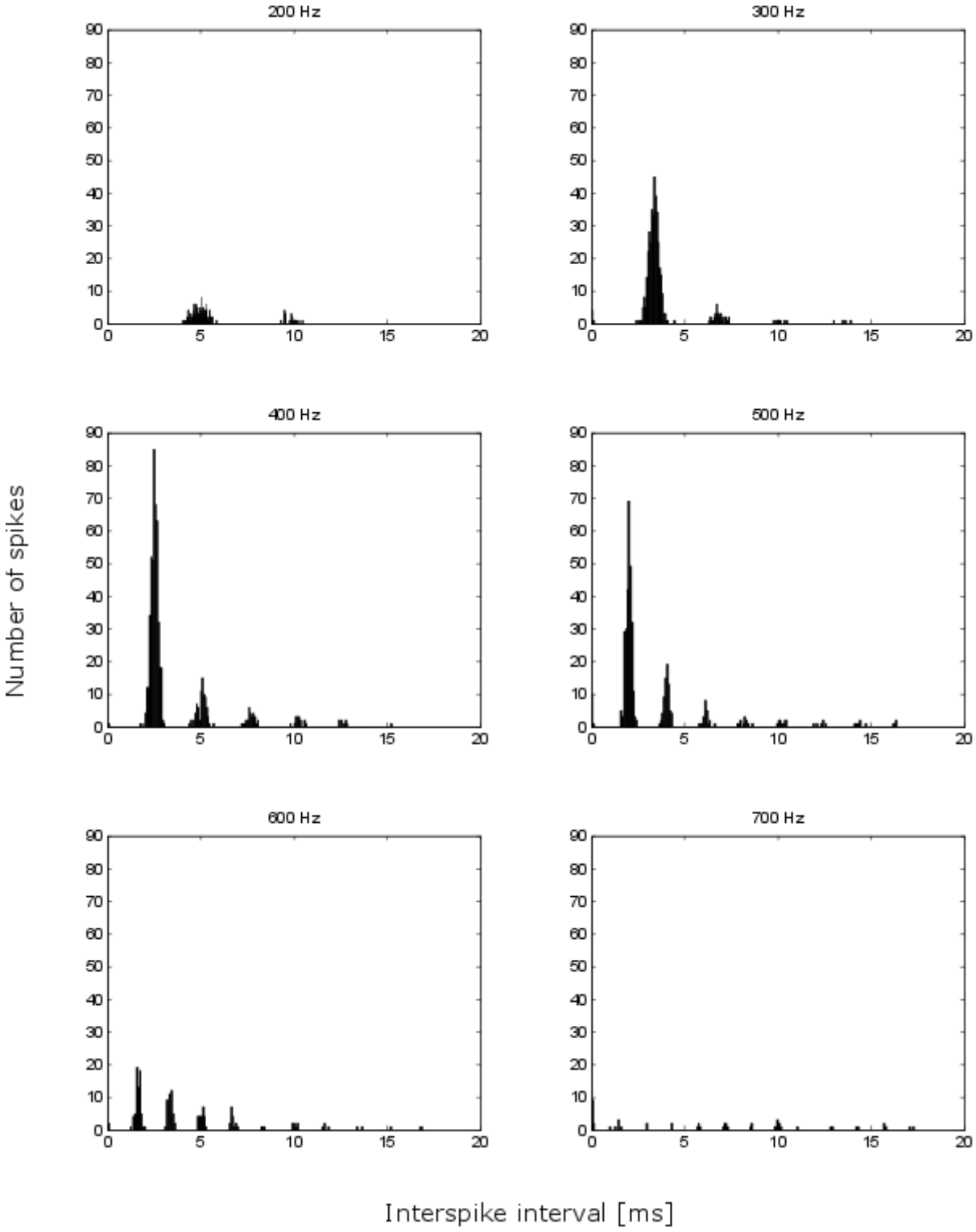

Figure 6.2. ISIHs for the population of octopus cells for 20 simulations at different frequencies of pure tone stimulation. The frequency of the pure tone is indicated at the top of each block.

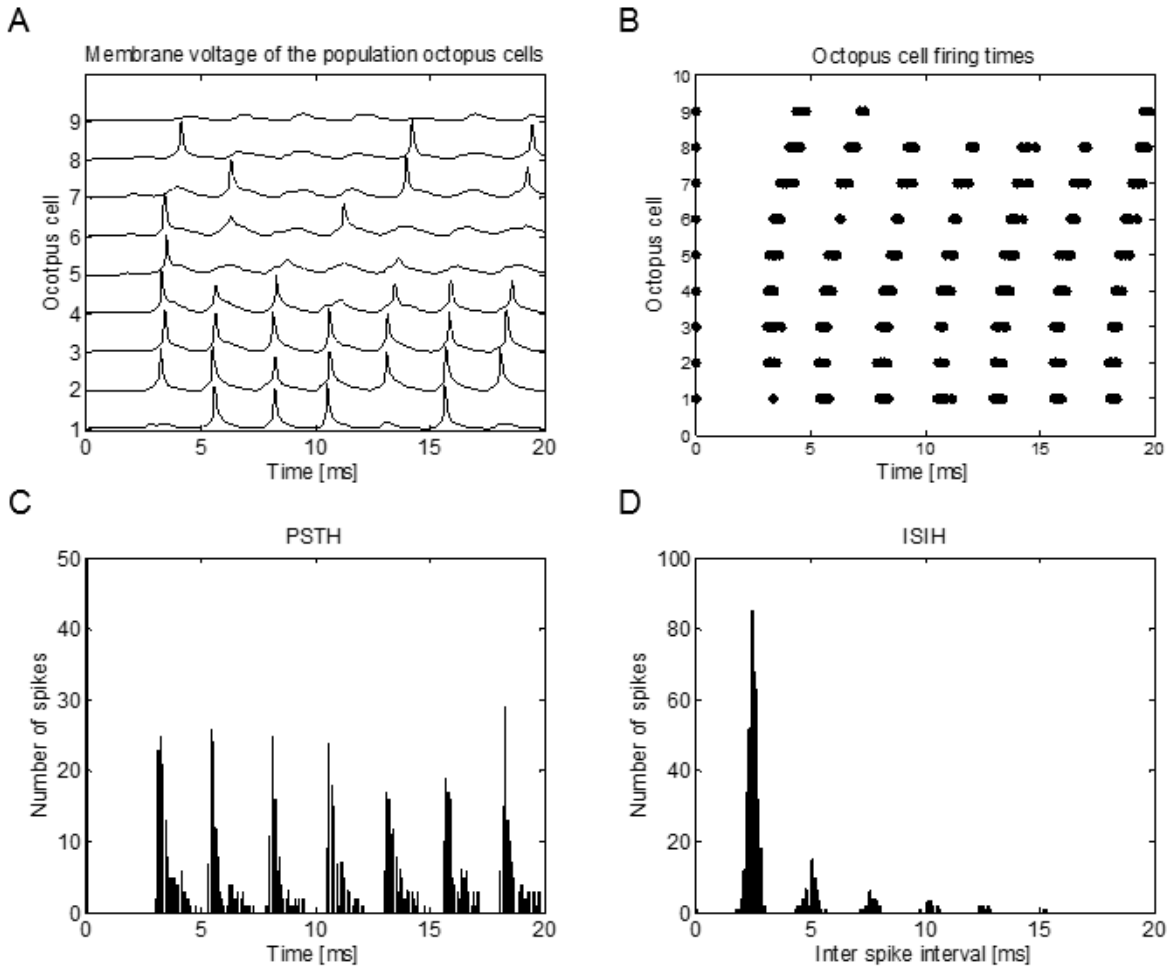

Figure 6.3. Response of the population of octopus cells to acoustic stimulation with a 400 Hz pure tone. A. Membrane voltage on each octopus cell in the population for one simulation. B. The octopus cell discharge times for 20 simulations of the population with pure tone acoustic stimulation. C. PSTH for the 20 simulations, showing the number of spikes over time. D. ISI histogram for all the spikes in the 20 simulations of the octopus cell population.

The relative entrainment at different pure tone stimulation frequencies was calculated. It was calculated as the number of APs observed in the simulation time divided by the number of periods of the pure tone input that fits in the simulation time. Only the octopus cells that generated APs were taken into account for the calculation. The average relative entrainment for all the simulated frequencies is shown in Figure 6.4. As the frequency increases the relative entrainment decreases. The octopus cells therefore lose synchronisation with the pure tone frequency as the frequency increases. The entrainment remains high up to 500 Hz, after which it decreases at a high rate for higher frequencies.

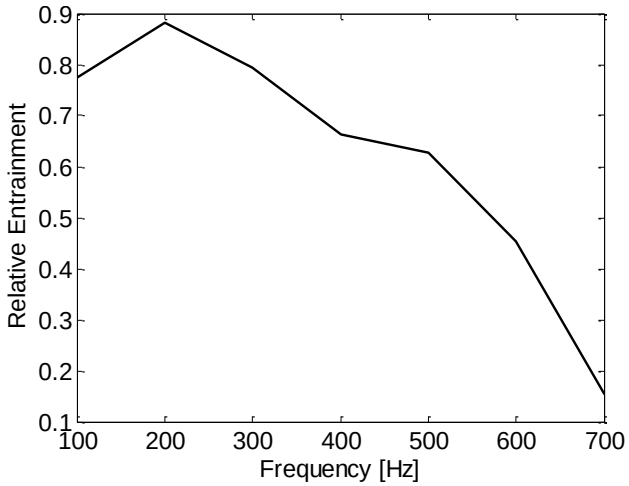

Figure 6.4. Relative entrainment of the octopus cells that discharge at each pure tone stimulation frequency as a function of frequency. The relative entrainment is high for low frequencies and decreases at high frequencies as the octopus cells do not discharge on each cycle of the stimulus. Only the octopus cells that generated action potentials during the simulation time were taken into account for the calculation.

6.3.2 Simulation 2. Acoustic stimulation with a vowel

A vowel was used as the input to the octopus cell population model for normal hearing to test the ability of octopus cells to extract voice pitch from speech.

The time signal and spectrograms of the speech recording are shown in Figure 6.5. Only the part of the word containing the vowel, i.e. 0.1 – 0.3 s, was used in the simulations since only the response to the vowel was evaluated.

The octopus cell population response for stimulation with the vowel is shown in Figure 6.6. In A the membrane voltages on the somas of the individual octopus cells are shown. All the octopus cells responded to the vowel stimulation. The vowel, which has a broad frequency spectrum as shown in the spectrogram, causes activation over the entire extent of the cochlea and therefore activation of all the octopus cells in the population. The PSTH of the whole population is shown in B in the figure. The ISI histogram for all the octopus cells for the whole time of stimulation is shown in C. The ISIs change with time but they remain in the same range. The discharge times of the octopus cells in Figure 6.6A can be related to the periodicity of the speech signal shown in Figure 6.5A. The modelled octopus cell discharges therefore tracked the periodicity of the speech signal.

The ISIs of the octopus cell population were extracted over time. The time difference between each successive pair of spikes on each octopus cell was calculated as the

instantaneous ISI and the average of the instantaneous ISIs for the whole population was calculated as an estimate of voice pitch. The fundamental frequency (F0) or voice pitch of the vowel was also extracted with Praat. A comparison between the average instantaneous ISIs of the octopus cell population and the pitch over time extracted by Praat is shown in Figure 6.7. The ISIs from the octopus cells follow the same trend as the pitch of the vowel. This suggests that the ISIs of octopus cells may be involved in the encoding of voice pitch in the vowel.

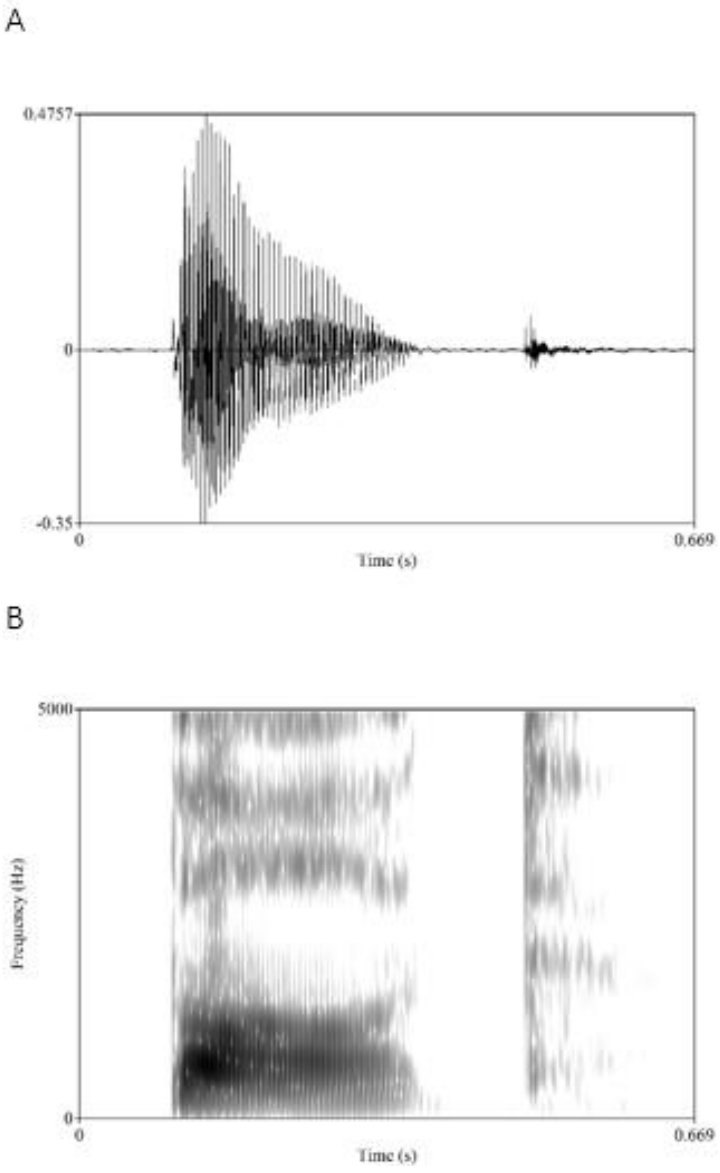

Figure 6.5. Voice recording of "paat" used to investigate the response of octopus cells to speech. A. Time signal of the word. B. Spectrogram of the word. These figures were generated by the use of Praat.

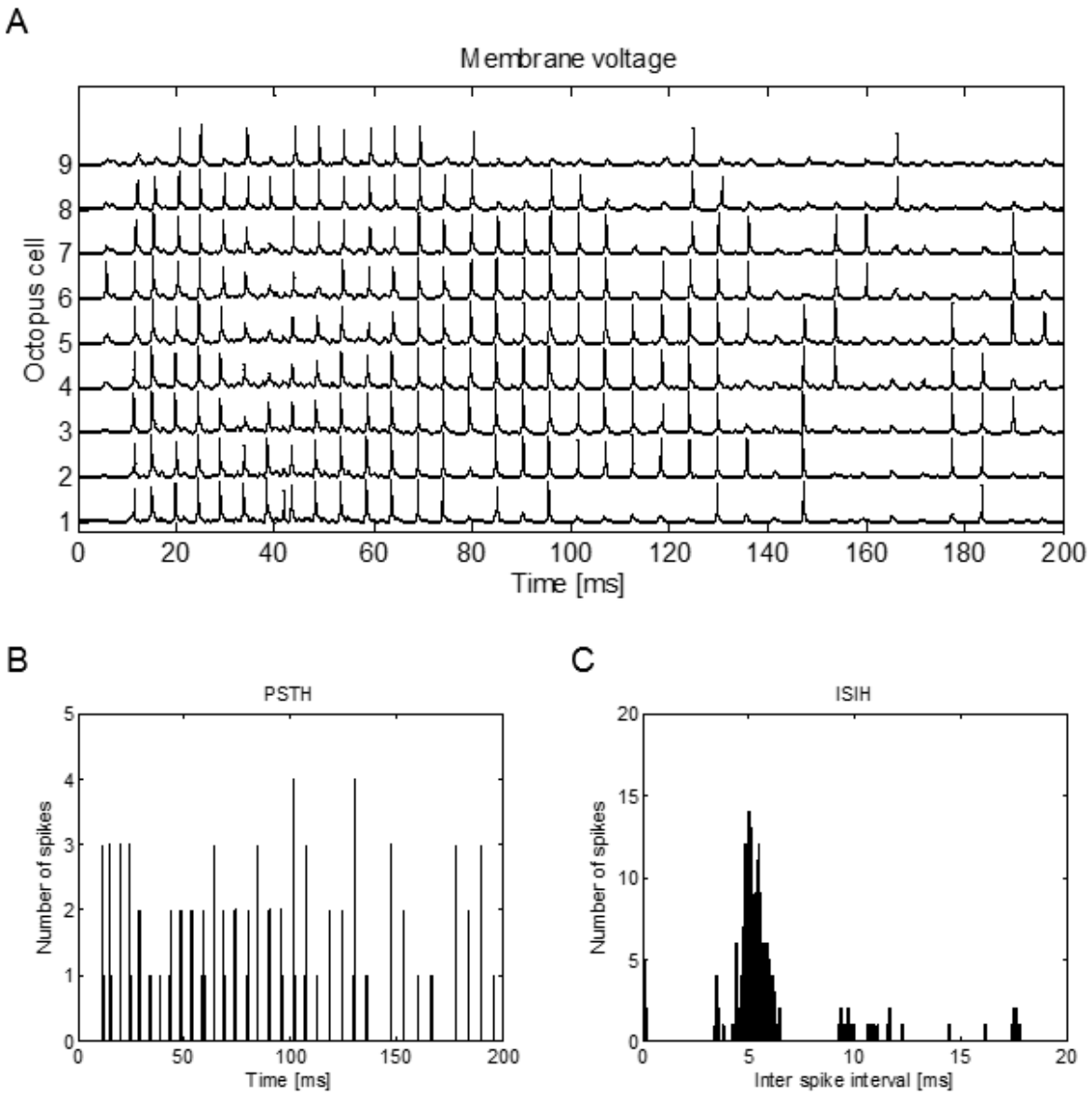

Figure 6.6. Octopus cell population response to acoustic stimulation with a vowel. A. The membrane voltage on the soma of each octopus cell for the duration of the vowel stimulation. B. PSTH for the population of octopus cells for stimulation with a vowel. C. ISIH for the population of octopus cells for acoustic stimulation with a vowel.

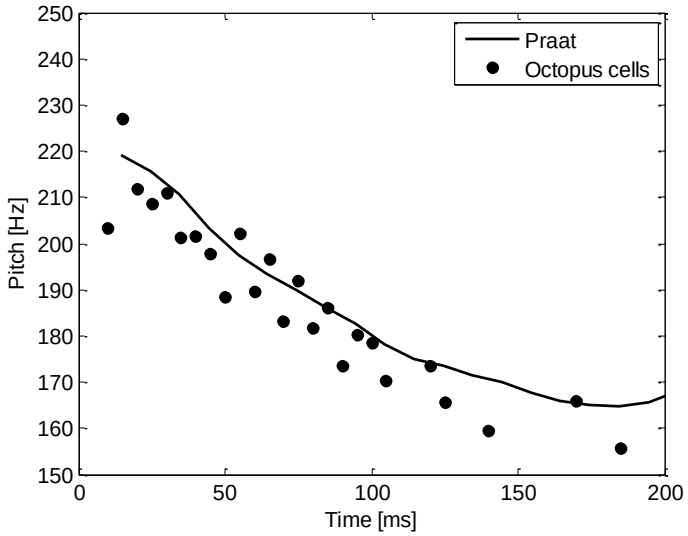

Figure 6.7. Comparison between the pitch extracted by the instantaneous ISIs of the octopus cell population and that extracted by Praat.

6.3.3 Simulation 3. Cochlear implant stimulation for acoustic pure tone inputs

The octopus cell population response for stimulation with a 400 Hz pure tone using a CI with the ACE strategy at 1200 pps is shown in Figure 6.8. Only some of the octopus cells show activity because of the focused stimulation of the CI, which activates only the most apical electrodes for this low-frequency input. The octopus cells also do not discharge at a rate that is the same as the pure tone frequency but they have an onset response, which is the same as for acoustic stimulation at high frequencies.

There is a large difference between the octopus cell population response to acoustic and electrical stimulation of the AN for the same pure tone input. This can be seen from a comparison between Figure 6.3A and Figure 6.8. For the acoustic stimulation the octopus cells discharge with ISIs, which is the same as the pure tone period. For CI stimulation, the octopus cells discharge only once at the onset of the stimulation, showing an onset response. For the CI stimulation there is therefore no information about the pure tone input available in the response of the octopus cells. This is because of the lack of temporal information encoded by the CI, which can be extracted by the octopus cells.

For acoustic stimulation of 400 Hz, octopus cells 1-4 showed most activity, while octopus cells 5-9 were the only cells activated for CI stimulation for a 400 Hz pure tone. This shows that even the little place information that is available in the octopus cell activity is not available when stimulating by CI.

The onset response observed for CI stimulation is because of the high pulse rate of 1200 pps which is used in the ACE strategy implemented in the CI model. Therefore the octopus cells detect the pulse rate of CI stimulation instead of the place of stimulation. The temporal pitch of a sound might be encoded in the ISIs of the octopus cells, as was shown in Sections 6.3.1 and 6.3.2. This encoding is probably lost in a CI that stimulates at a fixed high pulse rate. This may lead to difficulty in pitch discrimination for CI users.

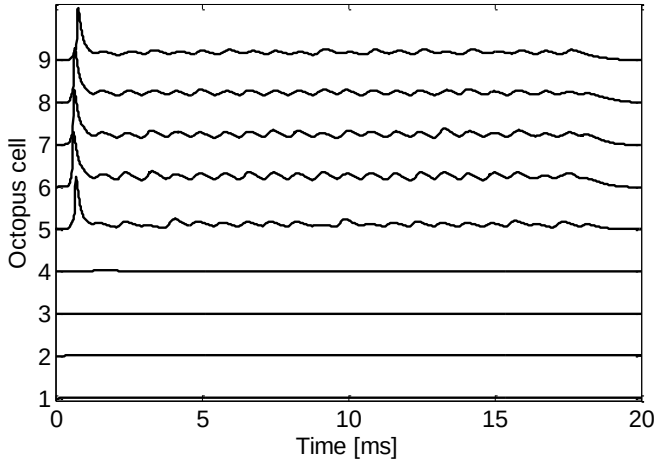

Figure 6.8. Octopus cell population response to a 400 Hz pure tone at 1200 pps using the ACE strategy.

6.3.4 Simulation 4. Single electrode pulse rate

The pulse rate on a single electrode, number 15 at 20.5 mm from the base, of the CI model was varied and the octopus cell population response to the stimulation was simulated. The octopus cell population response for a pulse rate of 400 pps is shown in Figure 6.9. The pulse rate of 400 pps was chosen for this figure to be able to compare the result with acoustic stimulation and CI stimulation for an acoustic pure tone of 400 Hz. The modelled octopus cells discharged with ISIs, which were the same as the pulse rate period of the CI electrode.

The relative entrainment of the octopus cells that were active (cells 4-8) is shown in Figure 6.10. The relative entrainment decreases as the pulse rate increases. This is the same trend as what was observed for acoustic pure tone stimulation shown in Figure 6.4.

The relative entrainment of the octopus cell population is 1 (100% entrainment) for low pulse rates up to 350 pps, after which it decreases. This may be related to the measured perceptual limit around 300 pps from where pulse rate discrimination limens for single-electrode pulse rate increase (Kong and Carlyon, 2010; Tong and Clark, 1985; Venter and Hanekom, 2014;

Zeng, 2002). This increase may be because of the reduction in the entrainment by octopus cells.

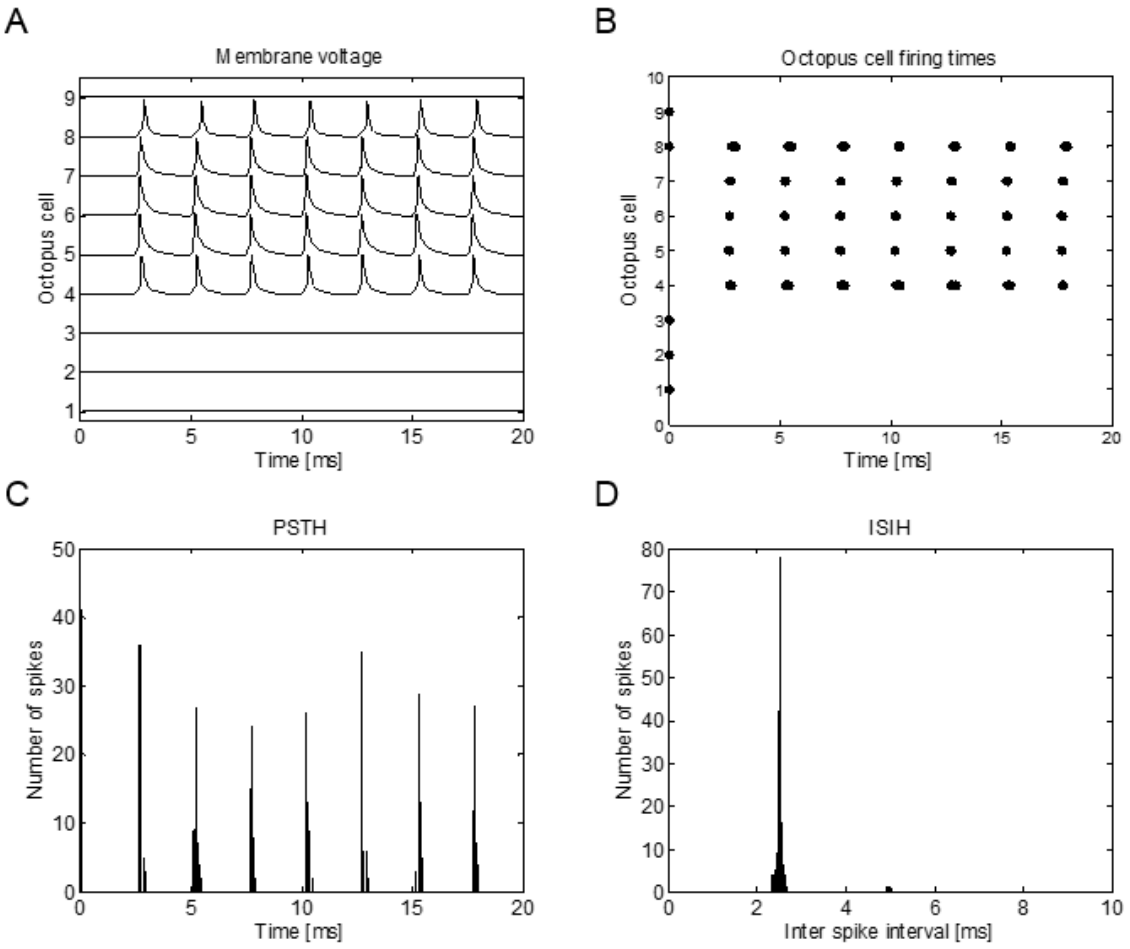

Figure 6.9. Octopus cell population response to stimulation on a single electrode at 400 pps. A. Membrane voltage in the somas of the octopus cells. B. Discharge times of the population over 10 simulations. C. PSTH of all the spike times of the population over 10 simulations. D. ISIH of all the spikes over 10 simulations.

Because it was shown that ISIs of the octopus cell population's response may encode pitch for acoustic stimulation, the perceived pitch of the single-electrode stimulation was predicted from the ISIs of the octopus cell population response. It was assumed that within one standard deviation from the peak in the ISIH a different pitch could not be perceived. A difference limen is the smallest change that is perceivable and therefore the standard deviation of the ISIs was used to estimate the pulse rate difference limens of the frequency discrimination. The PRDL was calculated with the equation

$$PRDL(f) = \frac{1}{1/f - \sigma} - \frac{1}{1/f + \sigma} \quad , \tag{6.1}$$

where f is the stimulation pulse rate and σ is the standard deviation of the ISIs of the octopus cell population response.

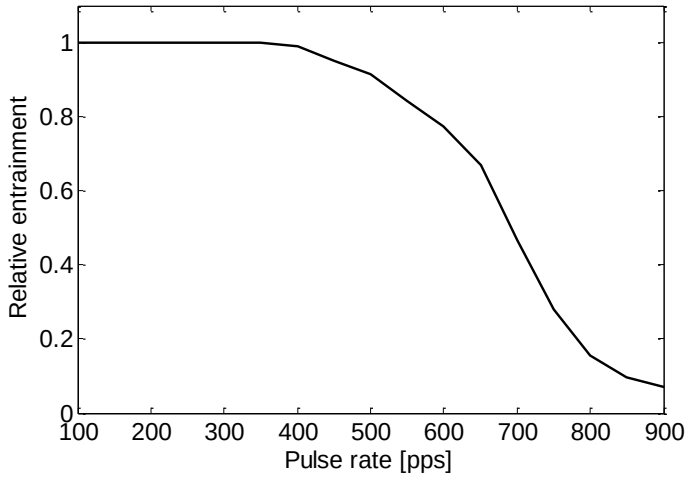

Figure 6.10. Average relative entrainment of the octopus cells that respond to the stimulus at different pulse rates on a single CI electrode.

The PRDLs was calculated with equation (6.1) for pulse rates of 150-700 pps. An exponential function, of the same form as used in Zeng (2002), was fit to the difference limens (DLs) as a function of frequency using the curve fitting tool in Matlab. The curve fitting tool is opened with the function `cftool`. This tool uses the nonlinear least squares method to fit the data. For this fit the input to the function `fittype` was '`exp1`' to fit a single exponential function to the data. The equation fitted to the data with this method was

$$DL(f) = 3.944e^{0.009301f} \tag{6.2}$$

with $R^2 = 0.9754$. A plot of the PRDLs from the equation derived from the standard deviations in ISIs is shown in Figure 6.11A together with data from Zeng (2002), as shown in his Figure 1. Equation (6.2) predicts frequency PRDLs in the same range as the experimentally measured PRDLs and can therefore be used to predict the PRDLs on a single electrode in a CI.

An equation for the pitch magnitude estimates on the scale in Zeng (2002) was also derived from the data. The measured pitch magnitude estimates were the subjective pitch on a scale of 0-100 measured with an absolute magnitude estimation procedure. The measurements in Zeng (2002) were done for pulse rates from 50 - 2000 pps while the simulations done here were only for 150 – 700 pps. Therefore the estimated pitch from the mean ISI in the range

150-700 Hz was scaled linearly to be in the range 50-80, which is the same as the magnitude estimates in the range between these frequencies in Zeng, Figure 2. The magnitude estimate for 150 pps was therefore equal to 50 and that of 700 pps was 80. An equation of the same form as Zeng's equation 3 was again fitted using the curve fitting tool in Matlab. In this case the `fittype` was a custom equation to fit the equation from Zeng (2002). The equation is given by

$$P(f) = 75.79 - \frac{4.569}{3.944 \times 0.009301 \times e^{0.009301f}} \quad , \tag{6.3}$$

with $R^2 = 0.8577$. The curve for equation (6.3) along with the curves from Zeng are shown in Figure 6.11B. The curve of pitch magnitude estimates from the octopus cell model is in the same range as those from the measurements. Pitch magnitude estimates for a single electrode can therefore be predicted from the standard deviation in ISI of the octopus cell population activity.

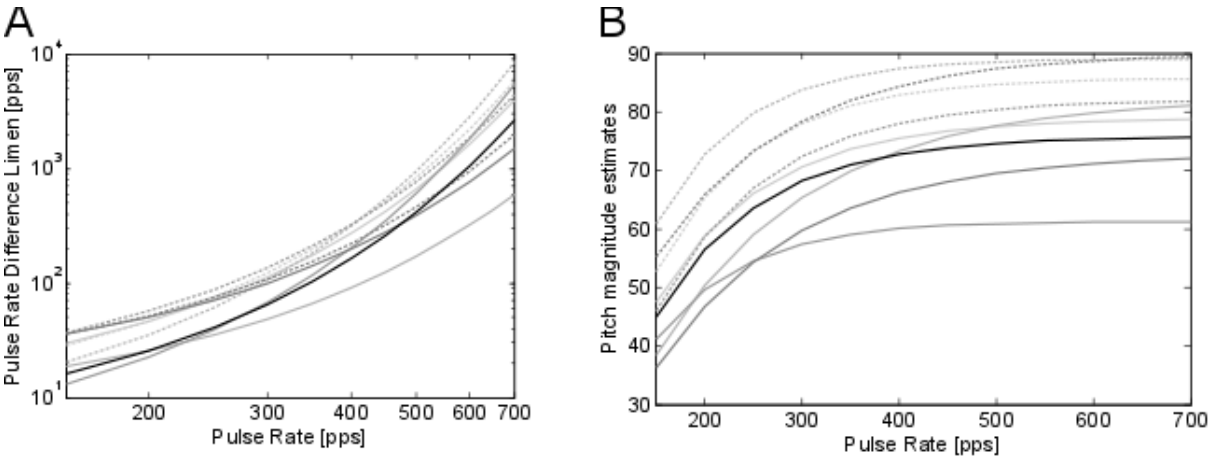

Figure 6.11. Frequency difference limens and pitch magnitude estimates predicted from the octopus cell model compared to the measured data in Zeng (2002). The black lines are the predictions from the octopus cell model and the grey lines are from the measurements. The dashed lines are for the basal electrodes and the solid lines for the apical electrodes. A. Frequency difference limens as a function of the pulse rate on a single electrode. B. Pitch magnitude estimates on a perceptual scale as a function of the pulse rate stimulation frequency on a single electrode.

The effect of the place of stimulation was not taken into account with the prediction of the perceived pitch from the octopus cell model results. The electrode that was stimulated was electrode 15, which is 20.5 mm from the base of the cochlea along the BM. If the place was to be taken into account, it can be assumed that the function will shift upward for more basal electrodes, having a higher pitch and downward for apical electrodes with lower pitch in the

same way as in the measured data. The analysis does however show that for low frequencies the temporal information in the pulse rate can be used to estimate temporal pitch regardless of the place of stimulation.

6.4 DISCUSSION

The ISIs of the APs of a population of octopus cells may encode the pitch of an acoustic stimulus. For pure tone acoustic stimulation the modelled octopus cell population discharged with ISIs the same as the period of the stimulus. For a vowel, which is a complex signal, the octopus cell population instantaneous ISIs followed the pitch extracted by a speech processing algorithm. The modelling results therefore suggest that octopus cells encode pitch in a temporal code in their ISIs as suggested by some models of pitch encoding (Rhode, 1995).

The octopus cell model responded to the rate of stimulation of the CI model rather than the input frequency. This result would be expected because of the high synchronisation of ANFs to electrical stimulation and the lack of temporal fine structure in the CI stimulation. The stimulation rate therefore carries most of the temporal information, which is then extracted by the octopus cells and encoded in their discharge times. This is an indication of the lack of temporal information available in CI stimulation.

Modelled octopus cells discharge in phase with the pulse rate of a CI model up to 350 pps, after which they lose synchronisation and have an onset response at about 700 pps and higher. Therefore high pulse rate CI stimulation such as the ACE, CIS and HiRes120 strategies (Kiefer *et al.*, 2001; Choi and Lee, 2012), are not expected to encode temporal pitch in the ANF firing patterns in a way that can be extracted by octopus cells. CI processing strategies such as SPEAK, Interleaved Processor and Spectral Maxima Sound Processor with fixed low stimulation rates (Loizou, 1999b) will most likely result in entrainment of the octopus cells to the pulse rate. This may also influence the pitch perception of the signal, which may be perceived as the stimulation rate. The pitch of the input acoustic signal should therefore be encoded in the periodicity of the activation of the electrodes in the CI to enable octopus cells to extract pitch from the periodicity of the AN activity.

The ISIs from the octopus cell population model used in the present study can be used to predict perceptual data of PRDLs as well as the pitch magnitude estimates for different single-electrode pulse rates. Even without taking the place of stimulation into account the pitch can be estimated from the model, suggesting that the encoding of low-frequency pitch

is more reliant on a temporal than a place code, which has also been suggested in literature (Hartmann, 1996; Cedolin and Delgutte, 2005; Larsen *et al.*, 2008; Clark, 1996; Moore, 2003; Zeng, 2002).

The octopus cell model, which loses synchronisation to the stimulation pulse rate around 300 Hz, may provide a basis for the measured perceptual limit of pulse rate discrimination on single electrodes at around 300 Hz (Kong and Carlyon, 2010; Tong and Clark, 1985; Zeng, 2002).

From these outcomes, to encode pitch in CIs in a way in which the pitch can be extracted by octopus cells, the pulse rate of the CI stimulation should follow the pitch or periodicity of the acoustic signal. Even if the pulse rate of each electrode cannot be the same as the pitch, there must be some periodicity in the electrode activation pattern that encodes the pitch. It has been shown that increasing the modulation depth at the fundamental frequency effects some improvement in pitch ranking experiments (Vandali *et al.*, 2005; Vandali and Van Hoesel, 2012; Vandali and Van Hoesel, 2011). These and similar methods should be investigated to provide temporal coding of pitch in CIs, which can be extracted in the CN.

6.5 CONCLUSION

The octopus cell model encodes pitch in a temporal code where the ISIs of the octopus cell response is the same as the period of the pitch of the input signal. The pitch information for this encoding is extracted from the periodicity in the ANF activity as encoded by the cochlear travelling wave.

The octopus cell model could not extract the frequency of pure tones from CI stimulation with the ACE strategy in the same way as for acoustic stimulation. The octopus cells responded to the pulse rate of the CI stimulation to generate an onset response.

PRDLs for single electrode CI stimulation can be predicted from the standard deviation of the discharge times of a population of octopus cells. Octopus cells may therefore provide a basis for the 300 pps limit that has been observed in single-electrode CI experiments (Kong and Carlyon, 2010; Tong and Clark, 1985; Venter and Hanekom, 2014; Zeng, 2002).

CHAPTER 7 DISCUSSION

7.1 CHAPTER OBJECTIVES

This chapter builds on the discussions from the previous chapters and considers the study as a whole. First the development and testing of the octopus cell model is discussed highlighting the main findings from this part of the study, which were described in detail in Chapters 3, 4 and 5. Then the findings regarding temporal processing performed by octopus cells are discussed, building on Chapters 5 and 6. Finally the application of the findings to CIs are discussed with regard to the results in Chapter 6.

The research questions, a short description of the results of the present study, the section in this document where the results are given and the sections where they will be discussed in this chapter are summarised in

Table 7.1.

7.2 OCTOPUS CELL MODEL

A compartmental Hodgkin-Huxley model of an octopus cell was developed. This model was based on the model in Spencer *et al.* (2012). The anatomy of the model is a good representation of anatomic and physiological measurements on octopus cells in cats, mice, dogs and guinea pigs (Bal and Baydas, 2009; Bal *et al.*, 2009; Ferragamo and Oertel, 2002; Golding *et al.*, 1995; Golding *et al.*, 1999; Hackney *et al.*, 1990). The ion channels that have been shown to be present in octopus cells (Golding *et al.*, 1995; Bal and Oertel, 2000) were included in the model.

The octopus cell model entrained to low frequency stimuli and had an onset response for high frequencies for both transmembrane electrical stimulation on the octopus cell and acoustic pure tone stimulation of the AN. This is the same type of response as measured in octopus cells (Bal and Baydas, 2009; Britt and Starr, 1975; Ostapoff *et al.*, 1994; Rhode and Smith, 1986), therefore the model is assumed valid to be used to simulate the response of octopus cells.

Table 7.1. Research questions, the results and the Discussion sections where they will be discussed.

Research question	**Result**	**Results Section**	**Discussion Section**
Are octopus cells sensitive to the delay of a sweep of synaptic inputs from ANFs terminating on their dendrites?	They seem to be sensitive but appears to be broadly tuned.	5.3.1 5.3.2	7.3
What is the optimal range of input from the cochlea to octopus cells?	1/3 – 1/4 of the cochlea	5.3.3	7.3
How do octopus cells respond to acoustic stimulation of the AN?	They entrain to the stimulus at low frequencies encoding the pitch in their ISIs.	6.3.1 6.3.2	7.4
What is the function of octopus cells in the processing of information from ANFs?	They seem to encode pitch in their ISIs.	6.4	7.4
How do octopus cells respond to electrical stimulation of the AN by a CI?	They respond to the pulse rate of the CI	6.3.3 6.3.4	7.5
What are the differences between the octopus cell response to acoustic and electrical stimulation of the AN?	For acoustic stimulation they entrain to the stimulus for acoustic stimulation while displaying an onset response to CI stimulation	6.4	7.5
Can pulse rate difference limens be predicted from the octopus cell model?	PRDLs were predicted from the standard deviations in the ISIs of the octopus cell population response	6.3.4	7.5

The input membrane resistance of the modelled octopus cell differed from measured membrane resistances (Bal and Baydas, 2009, Bal et al., 2009, Ferragamo and Oertel, 2002, Golding et al., 1995, Golding et al., 1999), which were several megaohms in magnitude, while the membrane resistance in the model was only around 600 kΩ. This resulted in a higher transmembrane stimulus current needed for the octopus cell model to reach threshold compared to measured data. A reason for this difference may be the method of measuring the membrane resistance, namely with instruments in experiments and under ideal conditions in the model, which may not represent the real-life situation. In spite of this difference, measurements on the APs generated by the single octopus cell model were the same as published measurements and therefore the model can be used to simulate the generation of APs by octopus cells especially for synaptic input. In future the reason for the small membrane resistance in the model and ways to change this resistance to a value closer to reality measurements should be investigated.

Models of the auditory periphery for both acoustic and electrical stimulation were successfully used as inputs to the octopus cell model. These models were integrate-and-fire type models, which only determined discharge times in the ANFs that had to be used in the octopus cell model. Therefore integrate-and-fire models such as the ANF models and a Hodgkin-Huxley model such as the octopus cell model had to be integrated in the simulations. This was only possible because of the method of implementing synapses on the octopus cell model where the membrane resistance changed upon the arrival of an AP at the synapse as a single spike from the integrate-and-fire model. The octopus cell model together with the models of the auditory periphery could therefore be used successfully to simulate the response of octopus cells to both acoustic and electrical stimulation of the AN. Only the response to acoustic stimulation was simulated in previous modelling studies (Cai *et al.*, 2000; Cai *et al.*, 2001; Cai *et al.*, 1997a; Levy and Kipke, 1997; Mcginley *et al.*, 2012; Spencer *et al.*, 2012) and simulation of CI stimulation was most likely performed for the first time in this study.

7.3 DENDRITIC DELAY AND COINCIDENCE DETECTION

In Section 5.3.1 it was found that the membrane voltage in the soma of the octopus cell because of the summed PSPs reached a maximum when the delay of an input sweep on the synapses was the same as the dendritic delay of the model. At this point the summation of the individual PSPs from all the synapses is optimal. The octopus cell model is therefore

sensitive to the delay of a sweep of inputs. However the model responded with an AP when enough synapses were activated for delays up to 1 ms on either side of the optimal, including reversed sweeps. The functionality of the octopus cell model is therefore not completely dependent on the delay of the inputs on the dendrites as long as the inputs are in a time window with a maximum around 1.4 ms, which is 1 ms larger than the dendritic delay of the model. The inputs may even be randomised in this same time window and the octopus cell will still reach threshold. Octopus cells may therefore be sensitive to the delay of inputs on their dendrites but they still function for delays that are not optimal and are broadly tuned to the delay.

Measurements on 2/3 layer pyramidal cells (Branco *et al.*, 2010) showed directional sensitivity of neurons where the PSP in the soma depended on the direction (towards or away from the soma) of the inputs. However the PSP amplitude in the soma was a maximum for the highest input velocities that were measured. Therefore the soma voltage was highest for the shortest sweep delay. It thus seems as if these pyramidal cells are not as sensitive to the time duration of the sweep as to the direction of the sweep. It was only measured for a small number of different delays and therefore it cannot be said whether there is an optimal forward sweep delay as seems to be the case for the octopus cell.

From a theoretical analysis of the signal delay in passive dendrites (Agmon-Snir and Segev, 1993; Agmon-Snir, 1995) it was found that the positions and timing of inputs on dendrites are not as important for signal integration in the soma, but the inputs need to be activated synchronously in a small time window for optimal operation. This also suggests that although a dendritic delay exists, it may not be as important in the signal processing of octopus cells, but that the integration of many inputs during a small time window is more important.

PSPs are broad, with a duration of about 1 ms when they reach the soma, as shown in Figure 3.4 for the present model and as measured in Gardner *et al.* (1999) and Mcginley and Oertel (2006). Therefore the summed PSP in the soma because of many synaptic inputs will still be large enough for the cell to reach threshold even when the peaks of the PSPs do not arrive at the soma at exactly the same time. This means that without the dendrites delaying the PSPs, asynchronous inputs can still be summed in the soma to generate an AP.

The simulations of the present study as well as the literature discussed above therefore do not exclude the possibility that there is some compensation for the travelling wave delay by the dendritic delay, but they also suggest that the dendrites play a large role in coincidence

detection. A review by Stuart and Spruston (2015) does not discuss the possibility of dendrites acting as a delay line for synaptic inputs, but emphasises that there are many active processes in dendrites involved in synaptic integration by coincidence detection. The function of octopus cells to compensate for the travelling wave delay is therefore proposed not to be as important as previously suggested by McGinley et al. (2012) and Spencer *et al.* (2012).

In Section 5.3.4 the local jitter present on the ANF output from the travelling wave and ANF model was calculated to be 0.37 ms, while the local jitter at the output of the octopus cell model in Section 5.3.3 was around 0.1 ms. Therefore it is suggested that the octopus cells reduce the noise in the neural firing by coincidence detection, as suggested by (Golding *et al.*, 1995). Octopus cells may generate APs when enough synapses are activated in a short enough time to depolarise the soma at a rate above threshold, regardless of the order of the activation of the inputs.

There have been attempts at encoding the travelling wave delay in CIs by delaying the filter bank outputs for an ACE processor before selecting the channels with maximum energy to be stimulated (Taft *et al.*, 2009; Taft *et al.*, 2010). If it is assumed that octopus cells behave optimally for an input delay corresponding to the travelling wave delay, it is expected that these speech-processing strategies would lead to better speech perception. It was found in Taft *et al.* (2009) that the strategy with the group delays resulted in better recognition of City University of New York sentences, as well as lower noise thresholds, while there was no significant improvement in pitch ranking. It was also found that the speech perception scores reached a maximum for a group delay of 6 ms, which may be the same as the travelling wave delay over the range of the CI. However, Taft et al. (2010) determined that there were improvements in performance for both forward and reverse delays and for most subjects also for a random delay. The hypothesis that there is a physiological mechanism that exploits travelling wave phase delays was also rejected by Taft et al. (2010) and it was suggested that the differences relied more on the delivery of information by the speech-processing strategy. The finding that it is not a physiological mechanism is in direct contrast to what would be expected if octopus cells were dependent on delays on their inputs. The results from Taft et al. (2010) together with the results from the octopus cell model of the present study, may indicate that it is possible that octopus cells are not as sensitive to the delay of their input, but rather to coincident inputs in a small time window, regardless of their order of arrival.

However many hypotheses exist about processing of synaptic inputs in dendrites, which go far beyond mere summation of many inputs (Stuart and Spruston, 2015; Williams and Stuart, 2003; Mel, 1995). A better understanding of these mechanisms, especially in octopus cells, may provide more insight into the functionality of their dendrites.

Apart from the suggested 1/5 – 2/3 of the travelling wave delay of Mcginley *et al.* (2012), no indication could be found in literature of exactly how long the dendritic delay of octopus cells really is. The suggestion by McGinley et al. (2012) is also not based on measurements but on the length of the dendrites, which seems to extend across that range of the ANFs in the CN that is assumed to represent the whole of the cochlea. Therefore it cannot be said whether the dendritic delay of the present octopus cell model is accurate, although this delay may have had a large influence on the results of the simulations of the present model. However, compared to parameters that have been measured experimentally, the octopus cell model was reasonably accurate. It is suggested that dendritic delays in octopus cells are measured experimentally for a better understanding of the proposed functionality of this delay.

In octopus cell model simulations the range of ANFs from which the cells received input varied greatly (Cai *et al.*, 2000; Cai *et al.*, 2001; Levy and Kipke, 1997; Mcginley *et al.*, 2012; Spencer *et al.*, 2012). The range of ANFs from which the nine octopus cells in the population each received input was changed to determine a possible optimal range. It was assumed that octopus cells both reduce jitter (Golding *et al.*, 1995; Rhode and Smith, 1986) and compensate for the travelling wave delay (Mcginley *et al.*, 2012; Spencer *et al.*, 2012) and the optimal input range was taken as the range where both these functions are performed. When the octopus cells receive input from larger ranges of the cochlea, they compensate better for the travelling wave delay, while the total jitter is also reduced more effectively. The possible optimal range from those that were evaluated was 1/3 – 1/4 of the cochlea, which is the same as suggested by Mcginley *et al.* (2012).

7.4 PROCESSING OF ACOUSTIC STIMULATION BY OCTOPUS CELLS

Pure tones

The single octopus cell model was simulated with synaptic inputs from the ANFs for acoustic stimulation, which were simulated with the travelling wave model. For pure tone stimulation the octopus cell model entrained to the stimulus frequency up to 500 Hz, after which it had an onset response. The type of response of the octopus cell was the same as

what is found in literature (Bal and Baydas, 2009; Britt and Starr, 1975; Ostapoff *et al.*, 1994; Rhode and Smith, 1986).

The octopus cell population model was also simulated for pure tone acoustic stimuli at various frequencies. The octopus cells receiving input from the basal ANFs showed most activity, while those receiving from the apex rarely discharged. It has been suggested previously that octopus cells may receive input from higher frequency ANFs (Spencer *et al.*, 2012), which seems to be the case from the results of the present study. However there are no anatomical measurements available to support this finding. Moreover, the octopus cells that responded to a stimulus were dependent on the activity of the ANFs terminating on the octopus cells. The ANF activity is in turn dependent on the ANF model as well as the travelling wave model used to simulate ANF responses to acoustic stimulation. These models are believed to provide a true representation of ANF activity for acoustic stimulation and therefore the results obtained from the present study should be true. The cells in the population that responded to the stimulation received input from ANFs with CFs of 1094 – 13695 Hz at positions 2.91 – 20.4 mm. Therefore ANFs originating from this range and spanning 1/3 – 1/4 of the cochlea are suggested to be most likely to terminate on octopus cells.

The octopus cells that responded to pure tone acoustic stimulation did not change significantly with a change in frequency to encode the frequency as a place code. The octopus cells that responded entrained to the stimulation frequency up to around 600 Hz, encoding the frequency in their ISIs. This shows encoding of pure tone frequency independent of the place of maximum displacement of the BM. This result confirms that octopus cells are involved in processing temporal information (Bal and Oertel, 2000; Clark, 2003; Ferragamo and Oertel, 2002; Gelfand, 2010; Golding *et al.*, 1995; Greenberg, 1997; Levy and Kipke, 1997; Oertel, 1997; Oertel, 1999; Oertel, 2005). For these pure tones the pitch of the stimulus is therefore encoded in the ISIs of the octopus cell population response, as suggested by Rhode (1995) for the cat CN.

For high-frequency pure tones the octopus cell model produced an onset response, in the same way as measured. The functionality of this response and the possible information encoding in the onset response were not investigated in the present study, only the encoding of low-frequency pitch information. Therefore no suggestions can be made about the processing of high-frequency information by octopus cells.

Speech

The octopus cell population response to the vowel /ɑː/ from a recording was simulated. The octopus cell population encoded the pitch of the vowel in the ISIs of their response. The average instantaneous ISIs of the population followed the trend of pitch extracted by the algorithm used in Praat (Boersma and Weenink, 2016). Therefore octopus cells may extract voice pitch from acoustic stimulation and encode the pitch in the ISIs of their response. The encoding of pitch in the ISIs of octopus cells (Rhode, 1995) is therefore not only valid for pure tones but also for complex signals such as human speech.

The pitch encoded in the ISIs of the octopus cell population model changed over time as the pitch of the vowel changed. Therefore it seems as if octopus cells can extract and encode pitch that changes over time. This may be useful in the perception of tonal languages and music.

7.5 OCTOPUS CELLS AND COCHLEAR IMPLANTS

The response of the octopus cell population was simulated for electrical stimulation of the AN by a CI using the ACE strategy. For pure tone inputs the octopus cell population response did not change with a change in the pure tone frequency. At a pulse rate of 1200 pps the octopus cells had an onset response that was the same as for acoustic pure tone stimulation at high frequencies. For lower CI stimulation pulse rates the octopus cell population encoded the pulse rate of the stimulation in their response by discharging with ISIs, which were the same as the pulse period. Instead of the frequency of the pure tone input being encoded by the octopus cells, as in normal hearing, they encoded the pulse rate used by the CI. This may be a reason why CI users experience difficulty in pitch and speech perception in noise (Gfeller *et al.*, 2007). This result is therefore a demonstration of the lack of temporal encoding of pitch in CIs.

The ability of octopus cells to extract CI pulse rate was then further investigated by changing the pulse rate of a single CI electrode and measuring the octopus cell response. The octopus cells entrained to the pulse rate up to around 350 Hz, after which they lost synchronisation with the pulse rate. The pulse rate DLs were predicted from the variance in the ISIs of the octopus cell population response. The predicted DLs were in the same range as measured pulse rate DLs (Zeng, 2002; Venter and Hanekom, 2014). The frequency of the input on a perceptual scale was predicted from the same data and was the same as measured values. The entrainment of octopus cells to low frequencies may therefore be a reason for the

measured perceptual limit of single-electrode pulse rate near 300 pps (Kong and Carlyon, 2010; Tong and Clark, 1985; Zeng, 2002).

At pulse rates above 300 pps, the CI listener still perceives a pitch but loses the ability to discriminate between different pulse rates. At these high pulse rates the octopus cell model responds with an onset response, which is the same as for high frequency acoustic pure tones. It is suggested that the listener perceives the pitch from the place coding of the placement of the electrode, rather than from the temporal encoding in the pulse rate. This corresponds to the idea that low frequencies are encoded with a temporal code and high frequencies with a place code (Hartmann, 1996; Cedolin and Delgutte, 2005; Larsen *et al.*, 2008; Clark, 1996; Moore, 2003; Zeng, 2002). This may also explain why the pitch magnitude estimates in Figure 1 from Zeng (2002) remains constant at high pulse rates with the pitch for basal electrodes being higher than that of apical electrodes.

The extraction of rate pitch by octopus cells was only investigated for single-electrode stimulation. It has been suggested that the perceptual limit observed at 300 Hz may be extended to higher frequencies for multielectrode stimulation where the electrode activation is spread over time (Venter and Hanekom, 2014). Stimulating more electrodes also improved the PRDLs, conceivably because there is wider activation providing more coincident inputs to octopus cells, which possibly receive input from a wide range of the cochlea. It is suggested that the ability of octopus cells to extract pitch from such stimuli be investigated in future.

If CIs encode the pitch of their input in such a way that it produces periodicity in the ANF activity that can be extracted by octopus cells, the pitch perception of CI users may improve. Old feature extraction strategies such as F0/F2, F0/F1/F2 and MPEAK proved to have poor performance in noise (Loizou, 1999b) compared to the newer strategies that present the whole frequency spectrum with many electrodes. Therefore, although the feature extraction strategies encoded pitch in the pulse rate of the stimulation, they may not be optimal for encoding pitch in periodicity. The experimental stimulation strategies developed (Vandali *et al.*, 2005; Vandali and Van Hoesel, 2011; Vandali and Van Hoesel, 2012), which are based on the ACE strategy but encode F0, did however show some improvement in pitch perception. This might be because these strategies encode pitch in the periodicity that could be extracted by octopus cells. The response of octopus cells to these strategies should be investigated in the future to test this hypothesis. Other strategies, such as the Spike-based Temporal Auditory Representation processing strategy suggested in Grayden *et al.* (2004),

which encodes periodicity with varying pulse rates in the CI stimulation, should also be considered, since the results of the present study suggest that octopus cells may extract periodicity encoded in this manner.

CHAPTER 8 CONCLUSION

8.1 FINDINGS AND CONTRIBUTION

The main findings from the present study are:

- Octopus cells are sensitive to the delay of a sweep of synaptic inputs but they are broadly tuned to this delay.
- The optimal range of input to octopus cells seems to be between 1/4 and 1/3 of the cochlea.
- Octopus cells are involved in the temporal processing of acoustic information, especially temporal pitch.
- Octopus cells encode the pitch of acoustic stimuli in their ISIs.
- For low-frequency pure tone stimulation octopus cells encode the frequency of the pure tone in their ISIs while they encode the pulse rate of CI stimulation for the same input regardless of the pure tone frequency.
- PRDLs for single-electrode CI stimulation can be predicted from the standard deviation of the ISIs of the octopus cell population response.
- Octopus cells may be partly responsible for the perceptual limit in pulse rate discrimination around 300 pps.

The new work involved in the present study is:

- A model of a population of octopus cells was developed whereas only single octopus cell models had been used before.
- A possible optimal range on the BM of ANFs terminating on octopus cells was determined, which seems to be between 1/3 and 1/4 of the BM.
- The response of octopus cells to acoustic speech stimulation was simulated.
- The response of octopus cells to CI stimulation with the ACE strategy was simulated.
- A model to predict PRDLs from the response of octopus cells was developed and compared to measured data.

8.2 FUTURE WORK

8.2.1 Octopus cell model

Dendritic delay

The dendritic delay of the octopus cell seems to be important in the processing of input sweeps of excitation. The dendritic delay of the model could not be adjusted over a large range and the effect of dendritic delay could not be investigated fully. The octopus cell model that was implemented in this study had a very short dendritic delay of 0.38 ms, while the travelling wave delay over the whole cochlea can be up to 10 ms. The differential travelling wave delay of the ANFs terminating on each octopus cell is therefore much larger than the dendritic delay of the cell if each octopus cell receives input from a third of the cochlea. The dendritic delay of the model could not be increased to values that would be the same as the travelling wave delays. A model with a longer, preferably adjustable dendritic delay should be developed to be able to investigate the ability of octopus cells to compensate for long travelling wave delays. This might also aid in finding a possible optimal dendritic delay and in testing whether octopus cells respond optimally when their dendritic delays match the differential travelling wave delay over the range of their inputs.

It may be possible that cats use temporal coding up to higher frequencies than humans (Javel and Mott, 1988). Therefore studying temporal coding, as was done in this study, should be done with a human model instead of a cat model. However no data are available on human octopus cells and they should be measured experimentally first before they can be implemented in a model.

The real dendritic delay of octopus cells has not been measured experimentally and therefore it is not known whether the short delay of 0.38 ms of the present model is accurate. The assumption that it should be longer, around a third of the travelling wave delay, is based on more assumptions, which are that octopus cells receive input from a third of the cochlea and that they compensate for the travelling wave delay with their dendritic delay. Therefore it is suggested that the exact dendritic delay of octopus cells as well as the ANFs from which octopus cells receive input be measured experimentally.

Solver

The octopus cell model was solved using the Euler method. This method requires a very small time step, which causes log simulation times. Using such small time steps also requires a large amount of computer memory to execute because of the large number of points where

calculations are performed. Implementing another solver for the octopus cell model would make it possible for the model to execute faster and also enable simulations for longer simulation times. Therefore it is suggested that the octopus cell model should be implemented with a faster solver.

Matlab has several built-in ordinary differential equation (ODE) solvers. The `ode45` solver is the simplest and is based on an explicit Runge-Kutta formula and is usually the best solver for a first attempt. The `ode15s` solver is suggested to be used when `ode45` fails or if the problem is stiff, which is likely for the octopus cell model. `ode15s` is a variable order solver based on the numerical differentiation formulas (NDFs). These or other Matlab ODE solvers should be investigated for possible solvers for the octopus cell in the future.

8.2.2 Cochlear implants and octopus cells

The investigation of the response of octopus cells to CI stimulation was limited to pulse trains on a single electrode. Although this shows that octopus cells seem to respond to the periodicity of the stimulus, it does not predict how octopus cells will respond to temporally fluctuating stimuli, as would be present in CI stimulation. It is therefore suggested that the response of octopus cells to temporally fluctuating stimuli from a CI be investigated in the future to determine whether they respond to the periodicity of that stimuli in the same way as to pulse trains.

The only CI speech processing strategy that was used in this study was the ACE strategy. More CI strategies, for example CIS, should be modelled in such a way that they can provide ANF firing patterns, which can be used in the octopus cell model. When more CI stimulation strategies are tested in the same way as the ACE strategy in this study, the encoding of information that is useful to octopus cells by CIs should be more clearly understood. It may also be determined which strategies are more suitable for temporal encoding of pitch in CIs, which may be extracted by octopus cells. Only the response to pure tone inputs was tested with the simulations of CI stimulation. This should be extended to stimulation with complex sounds, especially speech, over a longer period of time.

The development of a new CI stimulation strategy, which produces the same response in octopus cells as in normal hearing, should be investigated. This strategy should first be modelled and the response of the octopus cell model for this strategy should be evaluated and compared to the response to acoustic stimulation and other CI strategies such as ACE.

It has been shown that the cells in the CN, especially the anteroventral CN, have larger somas after sensorineural deafening of kittens when the AN is stimulated by a CI (Matsushima *et al.*, 1991). The stimulation of the AN therefore prevents the degeneration of CN cells after deafness and may negate the effects of deafness on the cells. If a person receives a CI a long time after onset of deafness the octopus cells in the CN may therefore not respond in the same way to the CI as when the implantation immediately follows the onset of deafness. This should be kept in mind when stimulation strategies are tested that are especially designed to stimulate the CN, since the degeneration of CN cells may have an effect on the response. However the plasticity of the auditory system (Fallon *et al.*, 2008) may compensate for these effects, especially a long time after receiving a CI. All of these should be investigated in future, together with the development of new CI stimulation strategies.

REFERENCES

Agmon-Snir, H. (1995). A Novel Theoretical Approach to the Analysis of Dendritic Transients. *Biophysical Journal*, **69**(5):1633-1656.

Agmon-Snir, H. & Segev, I. (1993). Signal Delay and Input Synchronization in Passive Dendritic Structures. *Journal of Neurophysiology*, **70**(5):2066-2085.

Babalian, A. L., Ryugo, D. K. & Rouiller, E. M. (2003). Discharge Properties of Identified Cochlear Nucleus Neurons and Auditory Nerve Fibers in Response to Repetetive Electrical Stimulation of the Auditory Nerve. *Hearing Research*, **153**(4):452-460.

Bal, R. & Baydas, G. (2009). Electrophysiological Properties of Octopus Neurons of the Cat Cochlear Nucleus: An in Vitro Study. *Journal of the Association for Research in Otolaryngology*, **10**(2):281-293.

Bal, R., Baydas, G. & Naziroglu, M. (2009). Electrophysiological Properties of Ventral Cochlear Nucleus Neurons of the Dog. *Hearing Research*, **256**(1-2):93-103.

Bal, R. & Oertel, D. (2000). Hyperpolarization-Activated, Mixed-Cation Current (Ih) in Octopus Cells of the Mammalian Cochlear Nucleus. *Journal of Neurophysiology*, **84**(2):806-814.

Bal, R. & Oertel, D. (2001). Potassium Currents in Octopus Cells of the Mammalian Cochlear Nucleus. *Journal of Neurophysiology*, **86**(5):2299-2311.

Bell, A. (2012). A Resonance Approach to Cochlear Mechanics. *PLOS*, **7**(11):1-21.

Boersma, P. & Weenink, D. 2016. Praat: Doing Phonetics by Computer.

Branco, T., Clark, B. A. & Häusser, M. (2010). Dendritic Discrimination of Temporal Input Sequences in Cortical Neurons. *Science*, **329**(5999):1671-1675.

Britt, R. & Starr, A. (1975). Synaptic Events and Discharge Patterns of Cochlear Nucleus Cells. I. Steady-Frequency Tone Bursts. *Journal of Neurophysiology*, **39**(1):162-178.

Bruce, I. C., Irlicht, L. S., White, M. W., O'leary, S. J., Dynes, S., Javel, E. & Clark, G. M. (1999). A Stochastic Model of the Electrically Stimulated Auditory Nerve: Pulse-Train Response. *IEEE Transactions on Biomedical Engineering*, **46**(6):630-637.

Burns, E. M. & Viemeister, N. F. (1976). Nonspectral Pitch. *Journal of the Acoustical Society of America*, **60**(4):863-869.

Cai, Y., Mcgee, J. & Walsh, E. J. (2000). Contributions of Ion Conductances to the Onset Responses of Octopus Cells in the Ventral Cochlear Nucleus: Simulation Results. *Journal of Neurophysiology*, **83**(1):301-314.

Cai, Y., Mcgee, J. & Walsh, E. J. 2001. Processing of Pitch Information in Complex Stimuli by a Model of Octopus Cells in the Cochlear Nucleus. *In:* Greenberg, S. & Slaney, M. (eds.) *Computational Models of Auditory Function.* Amsterdam: IOS Press.

Cai, Y., Walsh, E. J. & Mcgee, J. (1997a). Mechanisms of Onset Responses in Octopus Cells of the Cochlear Nucleus: Implications of a Model. *Journal of Neurophysiology,* **78**(2):872-883.

Cai, Y., Walsh, E. J. & Mcgee, J. (1997b). A Simple Program for Simulating the Responses of Neurons with Arbitrarily Structured and Active Dendritic Trees. *Journal of Neuroscience Methods,* **74**(1):27-35.

Carlyon, R. P. & Deeks, J. M. (2010). The Upper Limit for Temporal Pitch for Cochlear-Implant Listeners: Stimulus Duration, Conditioner Pulses, and the Number of Electrodes Stimulated. *Journal of the Acoustical Society of America,* **127**(3):1469-1478.

Carney, L. H. (1993). A Model for the Response of Low-Frequency Auditory-Nerve Fibers in Cat. *Journal of the Acoustical Society of America,* **93**(1):401-417.

Cedolin, L. & Delgutte, B. (2005). Pitch of Complex Tones: Rate-Place and Interspike Interval Representations in the Auditory Nerve. *Journal of Neurophysiology,* **94**(1):347-362.

Choi, C. T. M. & Lee, Y.-H. 2012. A Review of Stimulating Strategies for Cochlear Implants. *In:* Umat, C. (ed.) *Cochlear Implant Research Updates.* 27 April 2012 ed.: InTech.

Clark, B. D., Goldberg, E. M. & Rudy, B. (2009). Electrogenic Tuning of the Axon Initial Segment. *The Neuroscientist,* **15**(6):651-668.

Clark, G. (2003). *Cochlear Implants. Fundamentals and Applications,* New York, Springer-Verlag.

Clark, G. M. (1996). Electrical Stimulation of the Auditory Nerve: The Coding of Frequency, the Perception of Pitch and the Development of Cochlear Implant Speech Processing Strategies for Profoundly Deaf People. *Clinical and Experimental Pharmacology and Physiology,* **23**(9):766-776.

Clopton, B. M. & Glass, I. (1984). Unit Responses at Cochlear Nucleus to Electrical Stimulation through a Cochlear Prosthesis. *Hearing Research,* **14**(1):1-11.

Duifhuis, H. (2012). *Cochlear Mechanics. Introduciton to a Time Domain Analysis of the Nonlinear Cochlea,* New York, Springer.

Duifhuis, H., Hoogstraten, H. W., Van Netten, S. M., Diependaal, R. J. & Bialek, W. 1985. Modelling the Cochlear Partition with Coupled Van Der Pol Oscillators. *In:* Allen, J. B., Hall, J. L., Hubbard, A. E., Neely, S. T. & Tubis, A. (eds.) *Peripheral Auditory Mechanisms.* New York: Springer.

Eddington, D. K., Dobelle, W. H., Brackmann, D. E., Mladejovsky, M. G. & Parkin, J. (1978). Place and Periodicity Pitch by Stimulation of Multiple Scala Tympani Electrodes in Deaf Volunteers. *Transactions - American Society for Artificial Internal Organs*, **24**(1):1-5.

Elberling, C., Don, M., Cebulla, M. & Stürzebecher, E. (2007). Auditory Steady-State Responses to Chirp Stimuli Based on Cochlear Traveling Wave Delay. *Journal of the Acoustical Society of America*, **122**(5):2772-2785.

Fallon, J. B., Dexter, R. F. I. & Shepherd, R. K. (2008). Cochlear Implants and Brain Plasticity. *Hearing Research,* **238**(1-2):110-117.

Ferragamo, M. J. & Oertel, D. (2002). Octopus Cells of the Mammalian Ventral Cochlear Nucleus Sense the Rate of Depolarization. *Journal of Neurophysiology*, **87**(5):2262-2270.

Francart, T., Osses, A. & Wouters, J. (2015). Speech Perception with F0mod, a Cochlear Implant Pitch Coding Strategy. *International Journal of Audiology,* **54**(6):424-432.

Friesen, L. M., Shannon, R. V., Baskent, D. & Wang, X. (2001). Speech Recognition in Noise as a Function of the Number of Spectral Channels: Comparison of Acoustic Hearing and Cochlear Implants. *Journal of the Acoustical Society of America,* **110**(2):1150-1163.

Gardner, S. M., Trussel, L. O. & Oertel, D. (1999). Time Course Permeation of Synaptic Ampa Receptors in Cochlear Nuclear Neurons Correlate with Input. *The Journal of Neuroscience,* **19**(20):8721.

Gelfand, S. A. (2010). *Hearing. An Introduction to Psychological and Physiological Acoustics*, London, informa healthcare.

Gfeller, K., Turner, C., Oleson, J., Zhang, X., Gantz, B., Froman, R. & Olszewski, C. (2007). Accuracy of Cochlear Implant Recipients on Pitch Perception, Melody Recognition, and Speech Reception in Noise. *Ear & Hearing,* **28**(3):412-423.

Godfrey, D. A., Kiang, N. Y. S. & Norris, B. E. (1975). Single Unit Activity in the Dorsal Cochlear Nucleus of the Cat. *Journal of Comparative Neurology,* **162**(2):269-284.

Golding, N. L., Ferragamo, M. J. & Oertel, D. (1999). Role of Intrinsic Conductances Underlying Responses to Transients in Octopus Cells of the Cochlear Nucleus. *The Journal of Neuroscience,* **19**(8):2897-2905.

Golding, N. L., Robertson, D. & Oertel, D. (1995). Recordings from Slices Indicate That Octopus Cells of the Cochlear Nucleus Detect Coincident Firing of Auditory Nerve Fibers with Temporal Precision. *The Journal of Neuroscience,* **15**(4):3138-3153.

Goldstein, J. L., Baer, T. & Kiang, N. Y. S. 1971. A Theoretical Treatment of Latency, Group Delay, and Tuning Characteristics for Auditory-Nerve Responses to Clicks and Tones. *In:* Sachs, M. B. (ed.) *Physiology of the Auditory System.* Baltimore, Maryland: National Educational Consulants, Inc.

Grayden, D. B., Burkitt, A. N., Kenny, O. P., Clarey, J. C., Paolini, A. G. & Clark, G. M. A Cochlear Implant Speech Processing Strategy Based on an Auditory Model. Intelligent Sensors, Sensor Networks and Information Processing Conference, 2004., 14-17 Dec 2004. 491-496.

Green, T., Faulkner, A. & Rosen, S. (2004). Enhancing Temporal Cues to Voice Pitch in Continuous Interleaved Sampling Cochlear Implants. *Journal of the Acoustical Society of America,* **116**(4):2298-2310.

Greenberg, S. 1997. The Significance of the Cochlear Travelling Wave for Theories of Frequency Analysis and Pitch. *In:* Lewis, E. R., Steele, C. & Lyom, R. F. (eds.) *Diversity in Auditory Mechanics.* World Scientific Publishing.

Greenwood, D. D. (1990). A Cochlear Frequency-Position Function for Several Species - 29 Years Later. *Journal of the Acoustical Society of America,* **87**(6):2592-2605.

Gulledge, A. T., Kampa, B. M. & Stuart, G. J. (2005). Synaptic Integration in Dendritic Trees. *Journal of neurobiology,* **64**(1):75-90.

Hackney, C. M., Osen, K. K. & Kolston, J. (1990). Anatomy of the Cochlear Nucleus Complex of Guinea Pig. *Anatomy and Embryology,* **182**(2):123-149.

Hartmann, W. M. (1996). Pitch, Periodicity, and Auditory Organization. *Journal of the Acoustical Society of America,* **100**(6):3491-3502.

Hodgkin, A. L. & Huxley, A. F. (1952). A Quantitative Description of Membrane Current and Its Application to Conduction and Excitation in Nerve. *Journal of Physiology,* **117**(4):500-544.

Horst, J. W., Javel, E. & Farley, G. R. (1986). Coding of Spectral Fine Structure in the Auditory Nerve. I. Fourier Analysis of Period and Interspike Interval Histograms. *Journal of the Acoustical Society of America,* **79**(2):398-416.

Javel, E. & Mott, J. B. (1988). Physiological and Psychophysical Correlates of Temporal Processes in Hearing. *Hearing Research,* **34**(3):275-294.

Kalluri, S. & Delgutte, B. (2003). Mathematical Models of Cochlear Nucleus Onset Neurons: I. Point Neuron with Many Weak Synaptic Inputs. *Journal of Computational Neuroscience,* **14**(1):71-90.

Kane, E. S. (1977). Descending Inputs to the Octopus Cell Area of the Cat Cochlear Nucleus: An Electron Microscopic Study. *Journal of Comparative Neurology,* **173**(2):337-354.

Kiefer, J., Hohl, S., Pfenningdorff, T. & Gstöettner, W. (2001). Comparison of Speech Recognition with Different Speech Coding Strategies (Speak, Cis, and Ace) and Their Relationship to Telemetric Measures of Compound Action Potentials in the Nucleus Ci 24m Cochlear Implant System. *Audiology,* **40**(1):32-42.

Kole, M. H. P., Ilschner, S. U., Kampa, B. M., Williams, S. R., Ruben, P. C. & Stuart, G. J. (2008). Action Potential Generation Requires a High Sodium Channel Density in the Axon Initial Segment. *Nature Neuroscience,* **11**(2):178-186.

Kole, M. H. P. & Stuart, G. J. (2012). Signal Processing in the Axon Initial Segment. *Neuron,* **73**(2):235-247.

Kong, Y.-Y. & Carlyon, R. P. (2010). Temporal Pitch Perception at High Rates in Cochlear Implants. *Journal of the Acoustical Society of America,* **127**(5):3114-3123.

Kuba, H. (2012). Structural Tuning and Plasticity of the Axon Initial Segment in Auditory Neurons. *Journal of Neurophysiology,* **590**(22):5571-5579.

Laneau, J. & Wouters, J. (2004). Relative Contributions of Temporal and Place Pitch Cues to Fundamental Frequency Discrimination in Cochlear Implantees. *Journal of the Acoustical Society of America,* **116**(6):3606-3619.

Larsen, E., Cedolin, L. & Delgutte, B. (2008). Pitch Representation in the Auditory Nerve: Two Concurrent Complex Tones. *Journal of Neurophysiology,* **100**(3):1301-1319.

Levy, K. L. & Kipke, D. R. (1997). A Computational Model of the Cochlear Nucleus Octopus Cell. *Journal of the Acoustical Society of America,* **102**(1):391-402.

Liberman, M. C. (1978). Auditory-Nerve Response from Cats Raised in a Low-Noise Chamber. *Journal of the Acoustical Society of America,* **63**(2):442-455.

Loizou, P. C. (1999a). Introduction to Cochlear Implants. *IEEE Engineering in Medicine and Biology,* **18**(1):32-42.

Loizou, P. C. (1999b). Signal-Processing Techniques for Cochlear Implants: A Review of Progress in Deriving Electrical Stimuli from the Speech Signal. *IEEE Engineering in Medicine and Biology,* **18**(3):34-46.

Macherey, O., Deeks, J. M. & Carlyon, R. P. (2011). Extending the Limits of Place and Temporal Pitch Perception in Cochlear Implant Users. *Journal of the Association for Research in Otolaryngology,* **12**(2):233-251.

Manrique, M., Huarte, A., Morera, C., Caballé, L., Ramos, A., Castillo, C., García-Ibáñez, L., Estrada, E. & Juan, E. (2005). Speech Perception with the Ace and Speak Speech Coding Strategies for Children Implanted with the Nucleus Cochlear Implant. *International Journal of Pediatric Otorhinolaryngology,* **69**(12):1667-1674.

Matsushima, J.-I., Shepherd, R. K., Seldon, H. L., Xu, S.-A. & Clark, G. M. (1991). Electrical Stimulation of the Auditory Nerve in Deaf Kittens: Effects on Cochlear Nucleus Morphology. *Hearing Research,* **56**(1-2):133-142.

Mcginley, M. J., Liberman, M. C., Bal, R. & Oertel, D. (2012). Generating Synchrony from the Asynchronous: Compensating for Cochlear Travelling Wave Delays by the Dendrites of Individual Brainstem Neurons. *The Journal of Neuroscience,* **32**(27):9301-9311.

Mcginley, M. J. & Oertel, D. (2006). Rate Thresholds Determine the Precision of Temporal Integration in Principal Cells of the Ventral Cochlear Nucleus. *Hearing Research,* **216-217**(1-2):52-63.

Mckay, C. M., Mcdermott, H. J. & Clark, G. M. (1995). Pitch Matching of Amplitude-Modulated Current Pulse Trains by Cochlear Implantees: The Effect of Modulation Depth. *Journal of the Acoustical Society of America,* **97**(3):1777-1785.

Mel, B. W. (1995). Synaptic Integration in an Excitable Dendritic Tree. *Journal of Neurophysiology,* **70**(3):1086-1101.

Moore, B. C. J. (2003). Coding of Sounds in the Auditory System and Its Relevance to Signal Processing and Coding in Cochlear Implants. *Otology & Neurotology,* **24**(2):243-254.

Oertel, D. (1997). Encoding of Timing in the Brain Stem Auditory Nuclei of Vertebrates. *Neuron,* **19**(5):959-962.

Oertel, D. 1999. The Role of Timing in the Brain Stem Auditory Nuclei of Vertebrates. *Annual review on Physiology.*

Oertel, D. (2005). Importance of Timing for Understanding Speech. Focus on "Perceptual Consequences of Disrupted Auditory Nerve Activity". *Journal of Neurophysiology,* **93**(6):3044-3045.

Oertel, D., Bal, R., Gardner, S. M., Smith, P. H. & Joris, P. X. (2000). Detection of Synchrony in the Activity of Auditory Nerve Fibers by Octopus Cells of the Mammalian Cochlear Nucleus. *PNAS,* **97**(22):11773-11779.

Olson, E. S., Duifhuis, H. & Steele, C. R. (2012). Von Békésy and Cochlear Mechanics. *Hearing Research,* **293**(1-2):31-43.

Oosthuizen, D. J. J. 2012. *Acoustic Cues for Vowel Identification in Noise: Modelling and Measurement.* Master of Engineering (Bioengineering), University of Pretoria.

Osen, K. K. (1969). Cytoarchitecture of the Cochlear Nuclei in the Cat. *Journal of Comparative Neurology*, **136**(4):453-484.

Ostapoff, E. M., Feng, J. J. & Morest, D. K. (1994). A Physiological and Structural Study of Neuron Types in the Cochlear Nucleus. Ii. Neuron Types and Their Structural Correlation with Response Properties. *The Journal of Comparative Neurology,* **346**(1):19-42.

Plonsey, R. & Barr, R. C. (2007). *Bioelectricity. A Quantitative Approach,* New York, Springer.

Rattay, F. (1990). *Electrical Nerve Stimulation. Theory, Experiments and Applications,* New York, Springer-Verlag.

Reichenbach, T. & Hudspeth, A. J. (2014). The Physics of Hearing: Fluid Mechanics and the Active Process of the Inner Ear. *Reports on Progress in Physics,* **77**(7):1-45.

Ren, L.-J., Hua, C. & Ding, G.-H. (2013). Hydrodynamic Modelling of Cochlea and Numerical Simulation for Cochlear Traveling Wave with Consideration of Fluid-Structure Interaction. *Journal of Hydrodynamics,* **25**(2):167-173.

Rhode, W. S. (1995). Interspike Intervals as a Correlate of Periodicity Pitch in Cat Cohlear Nucleus. *Journal of the Acoustical Society of America,* **97**(4):2414-2429.

Rhode, W. S., Roth, G. L. & Recio-Spinoso, A. (2010). Response Properties of Cochlear Nucleus Neurons in Monkeys. *Hearing Research,* **259**(1-2):1-15.

Rhode, W. S. & Smith, P. H. (1986). Encoding Timing and Intensity in the Ventral Cochlear Nucleus of the Cat. *Journal of Neurophysiology,* **56**(2):261-286.

Rothman, J. S., Young, E. D. & Manis, P. B. (1993). Convergence of Auditory Nerve Fibers onto Bushy Cells in the Ventral Cochlear Nucleus: Implications of a Computational Model. *Journal of Neurophysiology,* **70**(6):2562-2583.

Rubinstein, J. T. (2004). How Cochlear Implants Encode Speech. *Current Opinion in Otolaryngology & Head and Neck Surgery,* **12**(5):444-448.

Ruggero, M. A. & Rich, N. C. (1987). Timing of Spike Initiation in Cochlear Afferents: Dependence on Site of Innervation. *Journal of Neurophysiology,* **58**(2):379-403.

Schmidt, L. 2016. *Viability of Cochlear Travelling Wave Signal Processing for Cochlear Implants.* Master of Engineering (Bioengineering) Dissertation, University of Pretoria.

Schwartz, A. M. & Kane, E. S. (1977). Development of the Octopus Cell Area in the Cat Ventral Cochlear Nucleus. *American Journal of Anatomy,* **148**(1):1-18.

Skinner, M. W., Clark, G. M., Whitford, L. A., Seligman, P. M., Staller, S. J., Shipp, D. B., Shallop, J. K., Everingham, C., Menapace, C. M., Arndt, P., Antogenelli, T., Brimacombe, J., Pijl, S., Daniels, P., George, C. R., Mcdermott, H. J. & Beiter, A. L. (1994). Evaluation of a New Spectral Peak Coding Strategy for the Nucleus 22 Channel Cochlear Implant System. *American Journal of Otology,* **15**(2):15-27.

Spencer, M. J., Grayden, D. B., Bruce, I. C., Meffin, H. & Burkitt, A. N. (2012). An Investigation of Dendritic Delay in Octopus Cells of the Mammalian Cochlear Nucleus. *Frontiers in Computational Neuroscience,* **6**(September):1-19.

Strydom, T. & Hanekom, J. J. (2011). An Analysis of the Effects of Electrical Field Interaction with an Acoustic Model of Cochlear Implants. *Journal of the Acoustical Society of America,* **129**(4):2213-2226.

Stuart, G. J. & Spruston, N. (2015). Dendritic Integration: 60 Years of Progress. *Nature Neuroscience,* **18**(12):1713-1721.

Sucher, C. M. & Mcdermott, H. J. (2007). Pitch Ranking of Complex Tones by Normally Hearing Subjects and Cochlear Implant Users. *Hearing Research,* **230**(1-2):80-87.

Taft, D. A., Grayden, D. B. & Burkitt, A. N. (2009). Speech Coding with Travelling Wave Delays: Desynchronizing Cochlear Implant Frequency Bands with Cochlea-Like Group Delays. *Speech Communication,* **51**(11):1114-1123.

Taft, D. A., Grayden, D. B. & Burkitt, A. N. (2010). Across-Frequency Delays Based on the Cochlear Traveling Wave: Enhanced Speech Presentation for Cochlear Implants. *IEEE Transactions on Biomedical Engineering,* **57**(3):596-606.

Tong, Y. C. & Clark, G. M. (1985). Absolute Identification of Electric Pulse Rates and Electrode Positions by Cochlear Implant Patients. *Journal of the Acoustical Society of America,* **77**(5):1881-1888.

Townshend, B., Cotter, N., Van Compernolle, D. & White, R. L. (1987). Pitch Perception by Cochlear Implant Subjects. *Journal of the Acoustical Society of America,* **82**(1):106-115.

Vandali, A. E., Sucher, C., Tsang, D. J., Mckay, C. M., Chew, J. W. D. & Mcdermott, H. J. (2005). Pitch Ranking Ability of Cochlear Implant Recipients: A Comparison of Sound-Processing Strategies. *Journal of the Acoustical Society of America,* **117**(5):3126-3138.

Vandali, A. E. & Van Hoesel, R. J. M. (2011). Development of a Temporal Fundamental Frequency Coding Strategy for Cochlear Implants. *Journal of the Acoustical Society of America,* **129**(6):4023-4036.

Vandali, A. E. & Van Hoesel, R. J. M. (2012). Enhancement of Temporal Cues to Pitch in Cochlear Implants: Effects on Pitch Ranking. *Journal of the Acoustical Society of America*, **132**(1):392-402.

Venter, P. J. & Hanekom, J. J. (2014). Is There a Fundamental 300 Hz Limit to Pulse Rate Discrimination in Cochlear Implants? *Journal of the Association for Research in Otolaryngology*, **15**(5):849-866.

Von Békésy, G. (1956). Current Status of Theories of Hearing. *Science,* **123**(3201):779-783.

Wesselink, W. A., Holsheimer, J. & Boom, H. B. K. (1999). A Model of the Electrical Behaviour of Myelinated Sensory Nerve Fibres Based on Human Data. *Medical & Biological Engineering & Computing*, **37**(2):228-235.

Wever, E. G. & Bray, C. W. (1930). Auditory Nerve Impulses. *Science,* **71**(1834):215.

Williams, S. R. & Stuart, G. J. (2003). Role of Dendritic Synapse Location in the Control of Action Potential Output. *Trends in Neurosciences,* **26**(3):147-154.

Wilson, B. S. & Dorman, M. F. (2008). Cochlear Implants: Current Designs and Future Possibilities. *Journal of Rehabilitation Research & Development,* **45**(5):695-730.

Xu, L. & Pfingst, B. E. (2003). Relative Importance of Temporal Envelope and Fine Structure in Lexical-Tone Perception (L). *Journal of the Acoustical Society of America*, **114**(6):3024-3027.

Zeng, F.-G. (2002). Temporal Pitch in Electric Hearing. *Hearing Research*, **174**(1-2):101-106.

Zilany, M. S. A., Bruce, I. C., Nelson, P. C. & Carney, L. H. (2009). A Phenomenological Model of the Synapse between the Inner Hair Cell and Auditory Nerve: Long-Term Adaptation with Power-Law Dynamics. *Journal of the Acoustical Society of America*, **126**(5):2390-2412.